



HAL
open science

Cellular evaluation of superoxide dismutase mimics as catalytic drugs: Challenges and opportunities

Gabrielle Schanne, Sylvie Demignot, Clotilde Policar, Nicolas Delsuc

► To cite this version:

Gabrielle Schanne, Sylvie Demignot, Clotilde Policar, Nicolas Delsuc. Cellular evaluation of superoxide dismutase mimics as catalytic drugs: Challenges and opportunities. *Coordination Chemistry Reviews*, 2024, 514, pp.215906. 10.1016/j.ccr.2024.215906 . hal-04573377

HAL Id: hal-04573377

<https://hal.science/hal-04573377>

Submitted on 13 May 2024

HAL is a multi-disciplinary open access archive for the deposit and dissemination of scientific research documents, whether they are published or not. The documents may come from teaching and research institutions in France or abroad, or from public or private research centers.

L'archive ouverte pluridisciplinaire **HAL**, est destinée au dépôt et à la diffusion de documents scientifiques de niveau recherche, publiés ou non, émanant des établissements d'enseignement et de recherche français ou étrangers, des laboratoires publics ou privés.

Cellular evaluation of superoxide dismutase mimics as catalytic drugs: challenges and opportunities

Gabrielle Schanne,^{a,b} Sylvie Demignot,^b Clotilde Policar^a and Nicolas Delsuc^{a*}

^aLaboratoire des Biomolécules, LBM, Département de chimie, Ecole Normale Supérieure, PSL University, Sorbonne Université, CNRS, 75005 Paris, France

^bCentre de Recherche Saint Antoine, INSERM, UMR S 938, INSERM, Sorbonne Université, EPHE, PSL University, 27 rue de Chaligny, 75012 Paris, France

*Corresponding author: nicolas.delsuc@ens.psl.eu

Highlights

- Superoxide dismutases mimics (SOD mimics) are catalytic drugs that decrease oxidative stress
- Cellular models for evaluation of SOD mimics are comprehensively reviewed
- Assays to decipher SOD mimics bioactivity in cells are presented

Abstract

Oxidative stress is known to be associated with many pathologies including inflammation, cancer, diabetes, etc. However, oxidative stress resulting from the imbalance between reactive oxygen species flows and antioxidant defenses has been largely overlooked so far as a therapeutic target. Among antioxidant defenses, superoxide dismutases (SOD) are metalloenzymes that catalyze efficiently the dismutation of superoxide, the first reactive oxygen species resulting from the monoelectronic reduction of dioxygen. Superoxide, as a quite reactive chemical species, is a transient species. So, the cellular evaluation of metal complexes mimicking SOD (SOD mimics) in cellular models can be particularly tedious and calls for multiple direct and indirect strategies including probes and biochemical assays. This review highlights methods and assays to evaluate in cells SOD mimics, a new class of catalytic antioxidants.

Keywords

Superoxide dismutase mimics; antioxidants; cellular evaluation; superoxide; catalytic drug

Highlights	1
Abstract	1
Keywords	1
Abbreviations	3
1. Introduction	4
2. Cellular models of oxidative stress for SODm evaluation	9
2.1. SOD-deficient microorganisms and cells	9
2.2. Other cellular models of oxidative stress	19
2.2.1. Class 1: cells exposed to exogenous ROS, added directly in the culture medium or generated enzymatically or cells naturally rich in endogenous H ₂ O ₂	20
2.2.2. Class 2: cellular models involving anticancer drugs or treatments whose primary mode of action is ROS production	24
2.2.3. Class 3: cellular models exposed to drugs whose adverse effects generate ROS	26
2.2.4. Class 4: cellular models closely mimicking physiopathological situations: ROS production upon activation of native cellular pathways	28
2.2.4.1. Cellular model of oxidative stress based on immune response activation	30
2.2.4.2. Cellular model of OS related to diabetes context	32
2.2.4.3. Cellular model of OS mediated by inflammation	33
2.2.4.4. Cellular model of OS related to excitotoxicity	35
3. Assays to evaluate SODm activity in cells	36
3.1. Evaluation of the direct effects of SODm on ROS scavenging in cells	36
3.1.1. Cell permeant fluorescent probes	36
3.1.1.1. Hydroethidine (HE) / dihydroethidium (DHE)	36
3.1.1.2. MitoSOX	39
3.1.1.3. 2',7'-Dichlorodihydrofluorescein diacetate (DCFH-DA)	40
3.1.1.4. Lucigenin	42
3.1.2. Colorimetric non-cell-permeant probes	43
3.1.3. Aconitase activity assay	46
3.1.4. Electrochemical detection of ROS	47
3.2. Evaluation of the protective effects of SODm in cells	50
3.2.1. Observation of the cell morphology by optical microscopy	51
3.2.2. Assays based on cell growth determination	53
3.2.3. Assays based on the evaluation of the overall metabolic activity	54
3.2.4. Assays based on cell death evaluation	58
3.2.4.1. Necrosis: assays based on loss of cell membrane integrity	58
3.2.4.2. Assays relying on apoptosis evaluation	61
3.2.5. Assays focused on the analysis of specific organelles known to be altered by oxidative stress	63
3.2.5.1. Morphological analysis of cellular organelles	63
3.2.5.2. Examination of mitochondrial dysfunctions	64
3.2.5.3. Measure of cytosolic calcium fluctuations	67
3.3. Indirect effects of SODm on ROS-induced cellular damages	68
3.3.1. Effect of SODm on cellular constituents	68
3.3.1.1. Effects on abundance and activities of endogenous antioxidant enzymes	68
3.3.1.2. Effects on lipid peroxidation	72
3.3.1.3. Effect on ROS-induced DNA damages	75
3.3.2. Effect of SODm in a pathological context: focus on inflammation	79
3.3.2.1. Inhibition of NFκB and MAPK activation and signaling by SODm	79
3.3.2.2. Impact on inflammation-related up-regulation of pro-inflammatory cytokines, iNOS and FAS	83
3.3.3. Opening remarks: SODm use in cancer and diabetes	86

4. Conclusion	88
Acknowledgments	89
Funding sources	89
References	90

Abbreviations

A-T: Ataxia-Telangiectasia	mRNA: messenger RNA
ATP: adenosine triphosphate	NADPH: nicotinamide adenine dinucleotide phosphate
BAECs: Bovine aortic endothelial cells	NBT: nitroblue tetrazolium
CAT: catalase	NFκB: nuclear factor-kappa B
COX2: cyclooxygenase 2	NMDA: N-methyl-D-aspartate
CRISPR: Clustered Regularly Interspaced Short Palindromic Repeats	NOX: NADPH oxidase
d4T: stavudine	nPG: n-propyl gallate
DCF: dichlorofluorescein	NRTI: nucleoside reverse transcriptase inhibitors
DCFH-DA: Dichlorodihydrofluorescein diacetate	OS: oxidative stress
DHE: Dihydroethidium	PAMPs: pathogen-associated molecular patterns
DMSO: dimethylsulfoxide	PCR: polymerase Chain reaction
DNA: Deoxyribonucleic acid	PMA: phorbol-12-myristate-13-acetate
EGF: epidermal growth factor	PMS: phenazine methosulfate
EGFR: epidermal growth factor receptor	PQ: paraquat
EMSA: electrophoretic mobility shift assay	PRRs: pathogen recognition receptors
ER: Endoplasmic reticulum	RASM: Rat aorta smooth muscle cells
ERK: Extracellular signal-regulated kinase	RNA: ribonucleic acid
EthD-1: Ethidium homodimer-1 probe	ROS: Reactive oxygen species
Exc/em: excitation/emission	RNS: reactive nitrogen species
FAS: First apoptosis signal receptor	RT-qPCR: Reverse Transcriptase-quantitative Polymerase Chain Reaction
fMLP: N-formyl- Met-Leu-Phe peptide	shRNA: short hairpin RNA
Gpx: glutathione peroxidase;	SIN-1: 3-morpholino-sydnonimine
HE: Hydroethidine	SOD: Superoxide dismutase
HEK: 293 Human embryonic kidney 293	SODm: superoxide dismutase mimic
IFN-γ: Interferon-γ	TBARS: thiobarbituric acid reactive substances
IKK: IκB kinases	TGF-β: transforming growth factor β
IL: interleukin	TLRs: toll-like receptors
iNOS: inducible nitric oxide synthase	TNF-α: Tumor necrosis factor α;
INS: Insulin-secreting cells	TPP: triphenylphosphonium cation
JNK: c-Jun N-terminal kinase	TRx: Thioredoxins
KO: knock out	VEGF: Vascular endothelial growth factor
LDH: lactate dehydrogenase	WB: western blot
LPS: lipopolysaccharides	WT: wild-type
MAPK: mitogen-activated protein kinase	XO: xanthine oxidase
MDA: malondialdehyde	
MnPAM = Pentaazamacrocyclic Mn	
MnPs: Mn-porphyrins	

1. Introduction

Reactive oxygen species (ROS) are defined as byproducts of the dioxygen reduction. Indeed, molecular dioxygen can undergo either a single-step four-electron reduction leading directly to the formation of water or partial and consecutive one-electron reductions, then producing a series of ROS [1]. The first monoelectronic reduction of dioxygen results in the formation of superoxide radical anion $O_2^{\bullet-}$, abbreviated as superoxide thereafter. It can act as precursor of other ROS and the further addition of electrons, one after another, generates stepwise hydrogen peroxide (H_2O_2) and hydroxyl radical (HO^{\bullet}) (Figure 1). $O_2^{\bullet-}$, H_2O_2 and HO^{\bullet} can then react with other cellular components to form other ROS such as alkoxyl RO^{\bullet} , peroxy radical ROO^{\bullet} or hydroperoxyl radical HOO^{\bullet} .

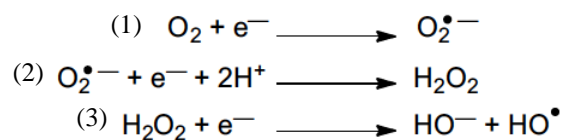
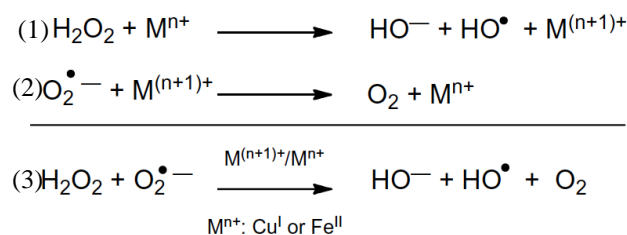


Figure 1. Reduction cascade of dioxygen resulting in the sequential formation of (1) superoxide, (2) hydrogen peroxide and (3) hydroxyl radical.

ROS are generated by multiple endogenous processes [2], including the mitochondrial respiration [3] and the nicotinamide adenine dinucleotide phosphate (NADPH) oxidase enzymes [4] that are considered to be the two major producers of ROS. First, mitochondrial respiration, that is part of all normal aerobic life, plays a key role in oxidative adenosine triphosphate (ATP) production *via* a reverse process of photosynthesis in which dioxygen is converted into water. However, a decoupling in the four-electron transfer occurring along the electron transport chain is known to affect about 3% of processed dioxygen. This is responsible for the aforementioned incomplete reduction of dioxygen into superoxide [1,3]. Consequently, high amounts of superoxide are released in the mitochondrial matrix and into the intermembrane mitochondrial space. Many others enzymes were shown to induce ROS

generation in the mitochondria, including cytochrome P450 enzymes, NADH-cytochrome b5 reductase, various dehydrogenases, monoamine oxidases (MAO) and mitochondrial aconitase [5]. Secondly, while multiple enzymes produce ROS as secondary effects, NADPH oxidases (NOXs) constitute the rare enzymes for which ROS production is the primary action. NOXs enzymes are located in the plasma membrane and in the phagosomes (created after bacteria phagocytosis) and catalyze the reduction of dioxygen into superoxide and hydrogen peroxide via NADPH oxidation [6]. Lastly, Haber-Weiss chemistry is strongly involved in the production of hydroxyl radical in living cells. As illustrated in Figure 2, reduced metal cations such as iron Fe(II) can induce the reduction of hydrogen peroxide into hydroxide and hydroxyl radical (Fenton reaction) *via* metal oxidation into Fe(III) [7]. In turn, Fe(III) can be reduced back to Fe(II) by superoxide: this renders the process catalytic (Haber-Weiss reaction) (Figure 2). To limit this phenomenon, cells have developed multiple storage components (ferritin, lipocalin-2, siderophores, etc.) to tightly regulate the cellular ferrous



availability.

Figure 2. (3) Haber Weiss reaction: (1) oxidation of low-oxidation state metal ion by hydrogen peroxide (Fenton reaction) and (2) cycling back to low-oxidation state with superoxide.

All ROS possess inherent chemical properties that confer them not only different reactivities but also different biological targets. For instance, the reactivity of aforementioned ROS can be ranked with the following order: $\text{H}_2\text{O}_2 < \text{O}_2^{\bullet-} < \text{HO}^\bullet$ [8]. On one hand, HO^\bullet indiscriminately attacks every bio-molecules around it with a kinetic rate limited

by diffusion. HO^\bullet consequently has a very short half-life (10^{-9} s) and reacts at its formation site. Its extreme reactivity is related to its very high one-electron redox potential ($E^\circ(\text{HO}^\bullet/\text{H}_2\text{O}) = 2.33$ V/NHE). HO^\bullet can cause important damages through the oxidation of lipids, DNA (attack of the guanine residues mostly) [9] or proteins and is considered as the most dangerous and toxic ROS. $\text{O}_2^{\bullet-}$ possesses a lower but still high one-electron redox potential ($E^\circ(\text{O}_2^{\bullet-}/\text{H}_2\text{O}_2) = 0.93$ V/NHE) than hydroxyl radical one. Consistently, its half-life is longer (10^{-5} s) which allows superoxide to migrate and reach further targets. However, superoxide is also confined close to its production site since its negative charge prevents any diffusion through membranes. Superoxide is involved in DNA nicking, in lipid peroxidation and in the inactivation of enzymes containing iron-sulfur clusters [10]. For its part, H_2O_2 is the most stable ROS with a half-life around 10^{-2} - 10^{-3} s and has the ability to cross membranes thanks to its neutral charge, H_2O_2 is notably responsible for the oxidation of cysteines but its oxidizing power mostly results from its conversion to hydroxyl radical by the Haber-Weiss reactions.

ROS exhibit two faces: they are indeed key actors of both redox biology and oxidative stress. ROS can hence induce opposite effects, depending not only on their concentration but also on their cellular location which itself depends on their site of production and their stability (type of ROS). On one hand, excessive intracellular levels of ROS induce oxidative stress. Oxidative stress indeed refers to an overproduction of ROS that damage lipids, proteins and DNA and subsequently alter cell homeostasis, structures, and functions [10,11]. As a result, high intracellular ROS levels were shown to contribute to the development of various human pathologies including cardiovascular, neurodegenerative and metabolic disorders as well as cancer and inflammation [12]. On the other hand, appropriate levels of ROS were shown to dictate redox biology. At controlled concentrations, ROS maintain the

redox balance of the cells that is essential for the proper course of physiological processes. In this way, ROS are strongly implicated in the redox signaling of various pathways initiating for instance cellular differentiation, cell adhesion and growth, tissue regeneration and prevention of aging [13]. Moreover, small increases of ROS can be useful when considering that they do not always cause toxicity to the host but rather to invading pathogens. Indeed, macrophages, white blood cells and other immune cells are known to generate oxidative burst to eliminate exogenous microorganisms [14].

To fight against oxidative stress while ensuring redox homeostasis, ROS concentration is tightly regulated by an arsenal of endogenous antioxidant defenses. These defenses gather redox enzymes whose mode of action are based on catalysis, and stoichiometric scavengers [15,16] such as ascorbic acid and the tripeptide glutathione (GSH) which is present in cells at millimolar concentrations [17,18]. Antioxidant enzymes are specific to one type of ROS. First, superoxide dismutase enzymes specifically catalyze the dismutation of superoxide into dioxygen and hydrogen peroxide [10]. Alternatively to SODs, a superoxide reductase (SOR) enzyme was shown to reduce superoxide into H_2O_2 without releasing dioxygen in an air-sensitive bacteria [19,20]. In turn, H_2O_2 is mostly converted to water by peroxiredoxin/thioredoxin reductase systems. Under increased amount of H_2O_2 , the glutathione peroxidase/glutathione reductase systems and catalase provide additional support to catabolize H_2O_2 [16,17]. The activity of these enzymes is continuously regulated to finely tune the concentration of each ROS.

Among the arsenal of antioxidant defenses, SOD enzymes constitute the first line of defense against oxidative stress since superoxide is the primary ROS generated from the cascade of dioxygen monoelectronic reduction. Related to their key protective role, SODs are found in many organisms: almost all aerobic ones and some of the anaerobic [20]. These

metalloenzymes catalyze very efficiently the dismutation of superoxide at a rate close to the diffusion limit. To this end, SODs require a metallic center that is successively oxidized and reduced via a ping-pong mechanism. All SODs, whatever their difference in structure, possess a high catalytic rate ($\approx 10^9 \text{ M}^{-1} \cdot \text{s}^{-1}$) that can be correlated to their favorable standard redox potential ($\approx 0.36 \text{ V/NHE}$) [21]. As a matter of fact, whatever the metal involved in the active site of SODs, the redox potentials are all positioned in a narrow potential range around the optimal value, i.e., at the midpoint potential between superoxide oxidation (-0.18 V/NHE) and reduction (0.91 V/NHE pH 7) [22]. Moreover, the presence of positively charged residues arranged as a funnel in SODs structure facilitates the approach of negative-charged superoxide toward the active site and hence contributes to the high catalytic activity. Owing to these advantageous parameters, SODs are very efficient in maintaining a low and steady-state level of superoxide inside cells (superoxide content was evaluated to be 0.2 pM and 30 pM in *E. coli* and mammalian cells, respectively) [23,24].

In a therapeutic perspective, the use of compounds mimicking SOD activity (SOD mimic, SODm) is a strategy that has been widely investigated to reduce oxidative stress [25]. Multiple redox-active metal-based compounds were described in the literature for their ability to catalyze superoxide dismutation. A number of reviews from Salvemini *et. al* [26], Iranzo *et. al* [27], Miriyala *et. al* [28], Batinic *et. al* [25], Policar *et. al* [1,29] or Signorella *et. al* [30] provide a comprehensive overview of the state of the art of SODm and report the major knowledges on the understanding of their SOD activity. Some of these SODm have been successfully tested on cells and even *in vivo* on models of ischemia-reperfusion [31–34], colitis [35,36], radiation protection [37–39], diabetes [40], neuronal oxidative stress [41] and others [25,26,42–47]. However, establishing the link between the SOD activity of the SODm and the bioactivity observed remains highly challenging since superoxide is a transient

species that has a short lifetime in cells and cannot be easily detected. In addition, to be efficient, a SODm has to fulfil a certain number of criteria: (i) it must be non-toxic, (ii) it must be stable in the biological environment and thus be thermodynamically stable (to prevent decoordination) and kinetically inert (to prevent metal and/or ligand exchanges), (iii) it must penetrate cells and (iv) must reach the site of superoxide production (mainly mitochondria). Biological environments and cells display specific physico-chemical characteristics [48], including high viscosity, molecular crowding, with compartments separated by membranes, and high content of Lewis bases and metal ions. All that can impact the bioactivity of the complexes. For these reasons, this is important to evaluate metal-based drugs such as SOD mimics in a biological context. In this review, we will focus on cells studies as a bridge between studies of their intrinsic activity (kinetics of the reaction with superoxide out of any cellular context) and *in vivo* evaluation. We will describe different cellular models and assays that have been developed to specifically decipher the SOD activity of SODm in cells either using direct methods or by using assays measuring the protective effects of anti-superoxide treatments. The review is organized so that information on SOD mimic evaluation can be found by searching for either the type of cellular model (section 2) or by the methods (section 3).

2. Cellular models of oxidative stress for SODm evaluation

2.1. SOD-deficient microorganisms and cells

Genetically engineered SOD-deficient *Escherichia coli* (*E. coli*) and *Saccharomyces cerevisiae* (*S. cerevisiae*) were the first widely used tools for investigating the SODm effects in biological systems [49]. The genetics of the bacteria *E. coli* and of the unicellular eukaryote *S. cerevisiae* are very well known and efficient tools are available to manipulate their

genome and produce mutants lacking SOD enzymes. Moreover, these unicellular organisms constitute relatively simple testing systems while retaining the complexity of a living cell context, thus with the majority of the barriers that may limit action of SODm, with even more challenges than eukaryotic cells in terms of penetration [50,51]. Finally, the metabolic pathways sensitive to ROS in *E. coli* have been well described in literature and were recently summarized in a review by M. Fasnacht and N. Polacek [52].

The SOD-deficient *E. coli* strain mutant JI132, lacking both the cytosolic MnSOD (SOD-A) and FeSOD (SOD-B) is commonly used and compared to the wild-type AB1157 as a control [53–59]. Carlioz *et al.* observed that the double mutant was unable to grow aerobically in minimal glucose medium but the growth could be restored in anaerobic conditions [59]. SOD-A and B deficiency was also associated with a slow aerobic growth of the mutant in media containing all the required nutrients and with the inability to grow in the same medium depleted with sulfur-containing amino acids (cysteine) [53].

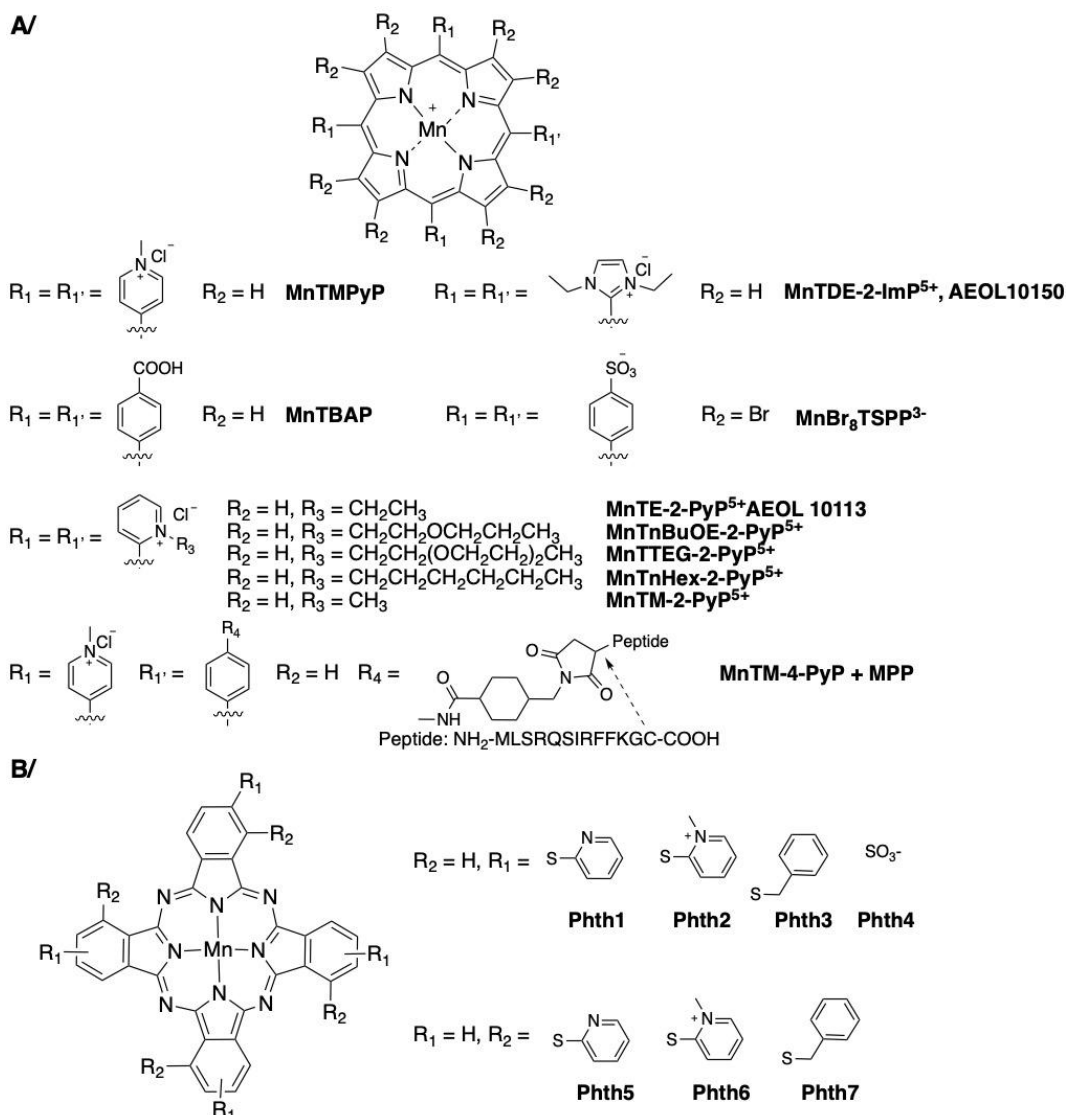


Figure 3. Structures of SODm based on porphyrin ligand (MnP) (A) or phthalocyanines (B).

SOD-deficient *E. coli* also exhibits a high sensitivity to hydrogen peroxide and paraquat, that clearly impacts the bacterial growth and survival [53].

A SOD-deficient *S. cerevisiae* yeast strain constructed by Gralla *et al.* is based on deletion-replacement mutations in the cytoplasmic CuZnSOD gene, which is the most abundant SOD in eukaryotes [60]. Similarly to SOD-deficient *E. coli*, SOD deficiency in this model resulted in multiple phenotypic defects attributable to the damages caused to important cellular components by superoxide ($O_2^{\bullet-}$): reduced growth rate in aerobic conditions with higher mutation rates; decreased stationary phase survival [61] and onset of amino-acid auxotrophies, such as lysine [60] and methionine [62] auxotrophies.

Interestingly, for both *E. coli* and *S. cerevisiae* mutants suffering from growth deficiencies, the impaired growth rate in aerobic conditions can be partially restored in the presence of a compound mimicking and thus substituting the SOD activity (Figure 3 and Figure 4) [57,63]. Overall, both mutants constitute very useful oxidative stress models for a quick screening of the activity of SODm by determining whether they restore the growth rate of the mutants to that of the SOD-proficient parents (Figure 4).

Faulkner *et al.* were the first to use SOD-deficient *E. coli* JI132 cultured in complete medium to demonstrate the positive effect of several Mn-porphyrins (MnPs) SODm, including MnTMPyP and MnTBAP, on the mutants growth rate (Figure 3 and Figure 4) [63]. The activity of MnTBAP was surprising: this negatively charged porphyrin should neither be strongly active against superoxide, nor cross negatively charged membranes. However, in a subsequent paper, Batinic *et al.* showed that a pure MnTBAP sample was unable to substitute for SOD enzyme in SOD-deficient *E. coli* JI132 cultured in a medium lacking essential amino acids (i.e. without leucine, threonine, proline, arginine and histidine) and they suggested an impurity from the commercially available MnTBAP could have been responsible for this positive result [54]. Note that JI132 cells were shown to suffer from superoxide toxicity when grown aerobically in the same 5-amino acid restricted medium. Indeed, in the absence of a compound substituting for SOD enzyme, the bacteria can not compensate for the lack of these amino-acids in the culture medium via their synthesis since they require enzymes that are superoxide sensitive [53,64]. This shows the importance of considering the nature of the medium when assessing the activity of a SODm, with the possibility that a restricted medium for the growth of SOD deficient *E. coli* be optimal, if not required, to avoid any side rescuing pathway.

For more than 20 years, SOD-deficient *E. coli* model has been very useful to determine the impact of the structure of MnPs complexes on SOD activity in a cellular context. The effect of charge, shape and size have been investigated and demonstrated the requirement of a positive charge for cellular and mitochondrial uptake and for attractive interaction with the anionic superoxide. Moreover, bulky substituents were shown to hinder the diffusion across the membranes and prevent a sufficient cellular uptake [56]. Studies of relationship between MnPs lipophilicity and protective effect in the *E. coli* J1132 strain established the improved efficacy of lipophilic mimics due to their higher cellular accumulation (Figure 4) [55,57]. In addition, manganese complexes made of scorpion-like ligands (Figure 5) were able, in the presence of dioxygen and in restrictive culture medium, to sustain the growth of J1132 to wild type levels [65,66]. Recent studies explored the SOD-like activity of these complexes [65,67] and of other metal-based biomimetic compounds [68] using a *S. cerevisiae* strain lacking the cytoplasmic Cu/Zn-SOD enzyme. These complexes were shown to respectively support the aerobic growth of the SOD-deficient strains and extend SOD-deficient yeast chronological life-span (Figure 4). Chronological life-span is defined as the length of time for which cells survive in stationary phase.

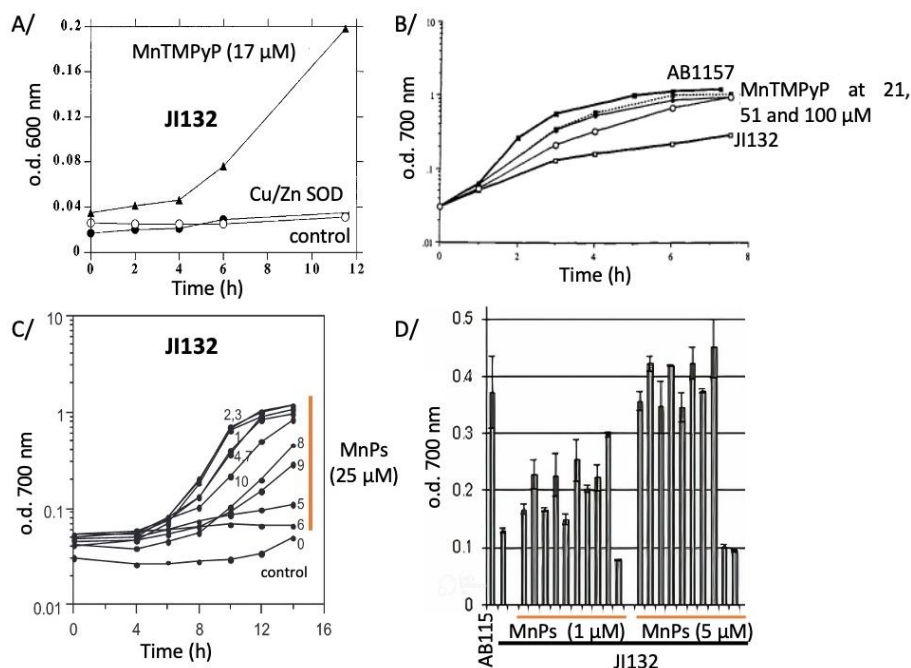


Figure 4. Effect of SODm on the growth of SOD-deficient *E. coli* mutant JI132, assessed by OD measurement at 600 to 700 nm of the cell culture, in comparison with the SOD-replete wild-type strain AB1157. A/ Figure from [53], aerobic growth curves in medium without cysteine and methionine and in presence of MnTMPyP, native Cu/Zn-SOD or none. B/ Figure from [63], aerobic growth curves in complete medium in presence or not of MnTMPyP. C/ Figure from ref [57], aerobic growth curve in 5 amino acids minimal medium in presence of various Mn(III) porphyrins, which are identified by numbers (1 – 10). Copyright © 2004 Elsevier Inc. All rights reserved. D/ Aerobic growth at 18 h in 5 amino acids minimal medium in presence of ten different Mn(III) porphyrins at 1 μ M and 5 μ M), adapted with permission from [55]. Copyright 2009 American Chemical Society.

To sum-up, genetically engineered SOD-deficient *E. coli* and *S. cerevisiae* offer numerous advantages for investigating the efficacy and the mechanisms of biological actions of SODm. Most importantly, they allow to distinguish SODm from non-SODm. Indeed, as mentioned above, these SOD-deficient organisms can discriminate efficient SODm from compounds that stimulates their growth by an action other than catalytic scavenging of $O_2^{\bullet-}$ when cultured in amino acids restricted medium [54]. For instance, the protection often described using pure MnTBAP (Figure 3) in cell/animal models of oxidative stress was suggested to be actually related to its ability to scavenge peroxynitrite and carbonate radical and not to its ability to dismute $O_2^{\bullet-}$ [69].

Moreover, combination of experiments on *E. coli* and *S. cerevisiae* mutants provides complementary information on mimics mechanism and their localization, as shown in a study carried out by Munroe *et al.* [58]. More precisely, they showed that manganese

complexes (salen derivatives EUK-8 and EUK-134 and M40403, Figure 5 and Figure 6), while exhibiting a SOD activity *in vitro*, were actually not able to rescue the slow aerobic growth phenotypes of SOD-deficient *E. coli* and *S. cerevisiae* strains. These results point out the importance of the mimics accumulation into cells and an appropriate intracellular localization for a proper cellular SOD activity. Indeed, the catalytic anti-superoxide agents should reach their target to be active.

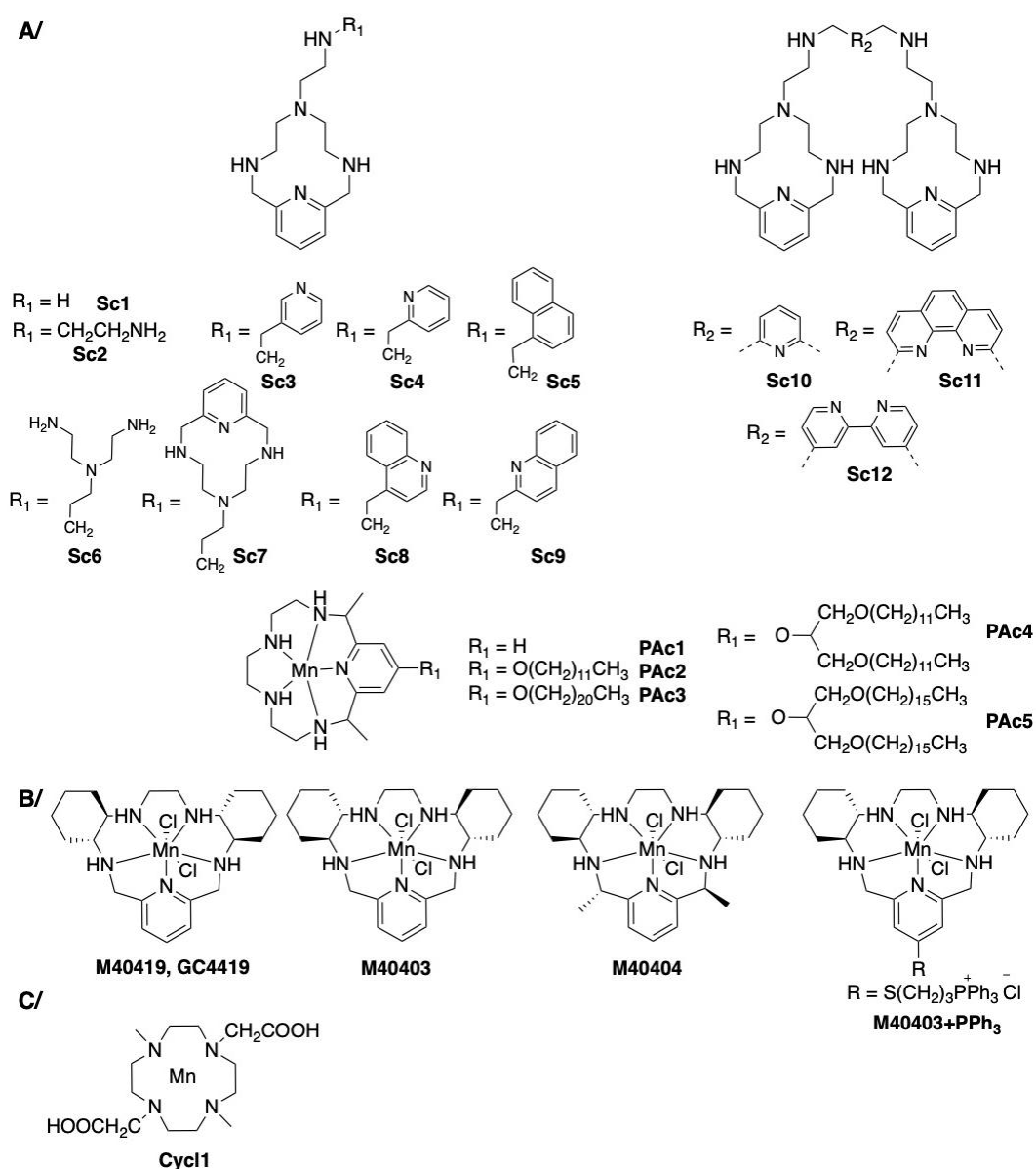


Figure 5. Structure of complexes or ligands involving an aza macrocycle. A/ Scorpion-like ligands. B/ Constrained scorpion-like ligands C/ Cyclen-derived ligands.

As superoxide is a negatively charged ROS, its ability to cross negatively charged membranes is limited. Hence, as we already suggested in various contexts [36,70], the apparent bioactivity (AB), measured here macroscopically as growth restoring capacity of a collection of cells, is the combination of an intrinsic activity (I) modulated by penetration in cells or in bacteria (P), with a simple form could be $AB = I \times P$. In the above-mentioned cases, the mimics were probably not present in sufficient amount in the right compartment where superoxide was generated due to mislocalization, low cellular uptake and/or low stability of the mimics in the biological medium.

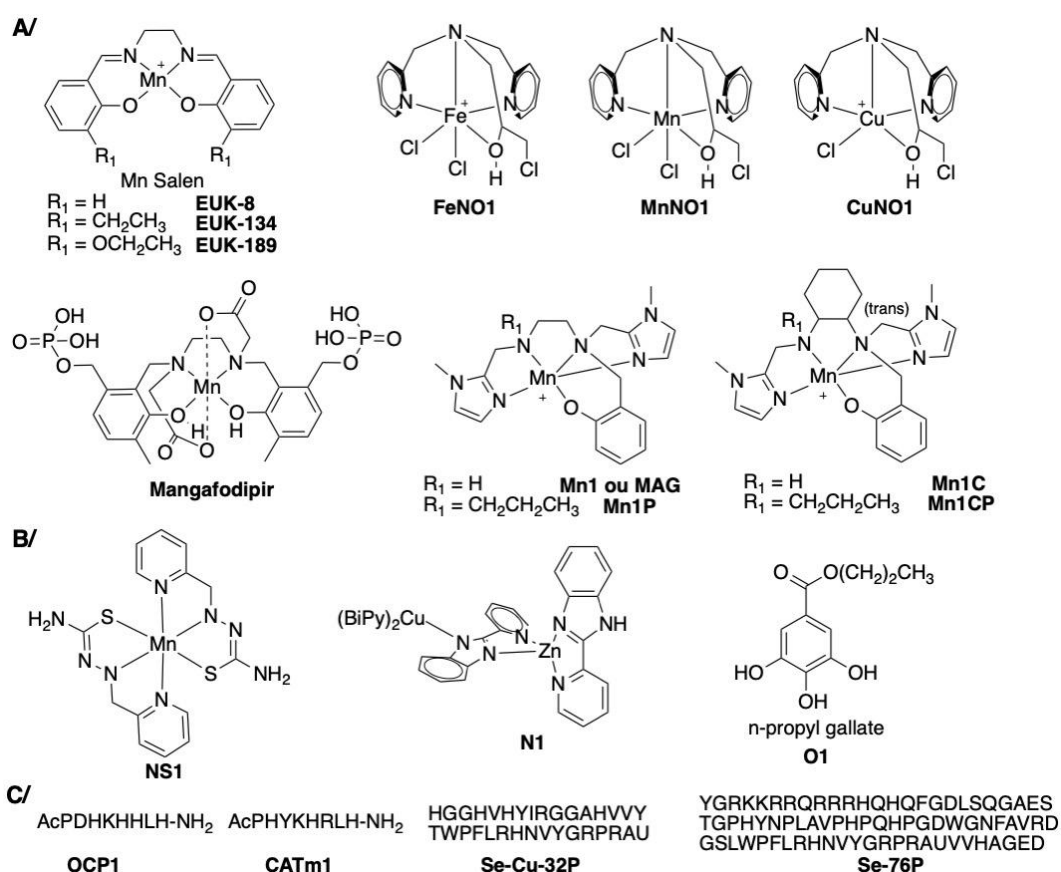


Figure 6. Structure of opened-chain ligands or corresponding complexes having a SOD-like activity. A/ Complexes showing N and O donors in the coordination sphere. B/ S and N, only N or only O donors-based ligands or complexes. C/ Peptide sequences that are able to coordinate metal(s) and that showed catalytic activities for superoxide dismutation.

This highlights the importance of the detection, identification and quantification of SODm in cells to evaluate their cellular uptake, their biodistribution and their speciation in cells and

distinguish between a lack of activity associated with a low bio-availability from an inactivation in cells. For that purpose, many analytical tools have been developed [29].

Although very useful, SOD-deficient *E. coli* and *S. cerevisiae* encounter some limitations. Particularly, after long incubations in restricted media (i.e. more than 10-15 hours), bacteria and cells may accumulate mutations and acquire the ability to overcome their autotrophy for amino acids, and thus return back to a normal growth rate [60]. This can bias the results obtained from such experiments.

The human fungal pathogen *Cryptococcus neoformans* constitutes another interesting biological model for SODm evaluation as a strong correlation between its resistance to oxidative stress and its virulence potential has been reported. S. Giles *et al.* constructed a SOD2-deficient strain via the allele-specific homologous integration in the SOD2 locus of a SOD2 deletion construct generated by polymerase chain reaction (PCR) overlap [71]. This reverse-genetics approach revealed the contribution of SOD2 to maintain one of the essential *C. neoformans* phenotype required for virulence: the ability to grow at 37°C (Figure 7, C.). Using this model, the authors investigated whether this temperature-sensitive phenotype observed in SOD-deficient mutants could be suppressed by the Mn-salen and MnP SODm addition [71].

A model of mitochondrial oxidative stress, useful to predict the biological efficacy of SODm, was established by Patel [72]. It relies on SOD-deficient neuronal cultures isolated from cerebral cortices of MnSOD knockout mice embryos and recapitulates age-related mitochondrial oxidative stress. Using a cytotoxicity assay based on LDH release measurement, Patel *et al.* screened the biological efficacy of MnPs (MnTBAP and MnTE-2-PyP, Figure 3) for prolonging cell survival and delaying cell death resulting specifically from increased mitochondrial oxidative stress (Figure 7D) [72].

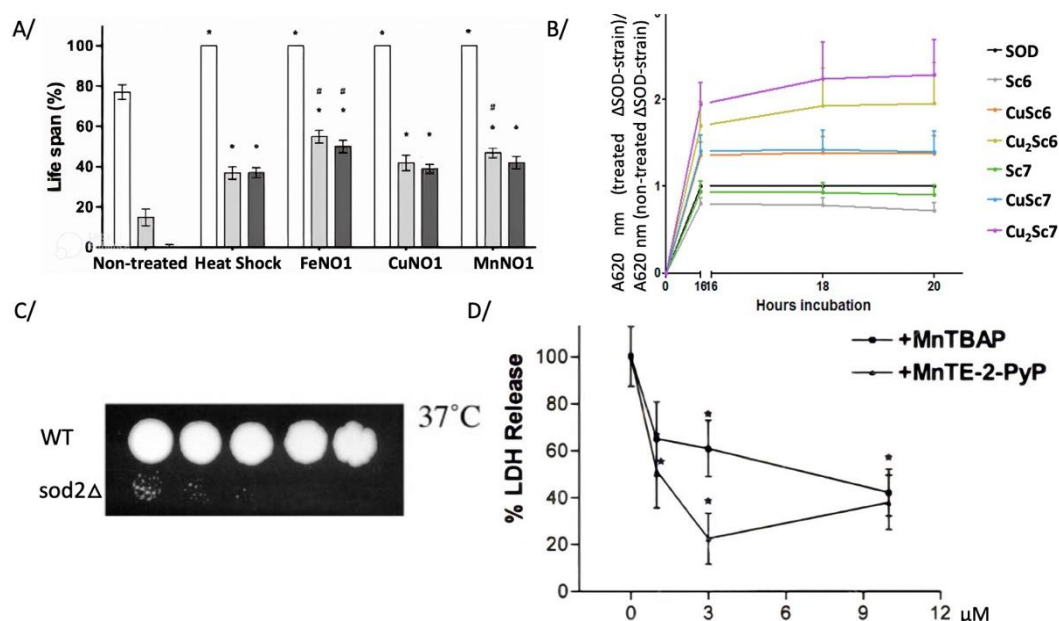


Figure 7. Protective effects of SODm in SOD-lacking microorganisms: *S. Cerevisiae* yeast strain, *C. neoformans* and murine neuronal cells. A/ Figure from [68]. Extension of life span in *S. cerevisiae* mutants lacking *sod1*, exposed to chronologic aging and treated with metal-based SODm at 25 μ M for 1h. Y-axis corresponds to the percentage of live cells. B/ Aerobic growth curve of *sod1*-deficient (Δ SOD) *S. Cerevisiae* strain in presence of SODm metals complexes (10 μ M) whose ligand are represented on the right. Adapted with permission from [67]. Copyright 2017 American Chemical Society. C/ Figure from [71]. Culture on agar plates at 37°C of wild-type and SOD2-deficient *Cryptococcus neoformans* strains. D/ Figure from [72]. Evaluation of neuronal cell death by lactate dehydrogenase (LDH) assay in SOD2-deficient mutants incubated with 2 MnPs at concentrations varying between 1 to 10 μ M.

Cellular model	Type of SOD affected	Strategy to decrease SOD expression	Read out	SODm tested	Advantages/drawbacks	References
<i>Escherichia coli</i>	MnSOD and FeSOD	allelic exchange with mutated genes in plasmids [59,73]	growth rate in aerobic conditions	MnP, M40403, EUK, Sc (Figure 3, Figure 5 and Figure 6)	<ul style="list-style-type: none"> non-commercially available cells routine assay long incubation times (mutations, stability of SODm) 	[49,54–58,63,65,66]
<i>Saccharomyces cerevisiae</i>	Cu,ZnSOD or MnSOD	deletion-replacement mutations [60]	growth rate in aerobic conditions	MnP, M40403, EUK, Sc, MnNO1 (Figure 3, Figure 5 and Figure 6)	<ul style="list-style-type: none"> commercially available yeast routine assay long incubation times (mutations, stability of SODm) 	[49,58,65,67,68]
<i>Cryptococcus neoformans</i>	MnSOD	allele-specific homologous integration of deletion construct at the SOD2 locus	growth rate at elevated temperatures	EUK, MnP (Figure 3 and Figure 6)	<ul style="list-style-type: none"> non-commercially available cells easy to use poor penetration of cationic SODm 	[71]
neuronal cells	MnSOD	neuronal cultures from cerebral cortices of MnSOD knockout mice embryos	LDH assay	MnTBAP and MnTE-2-PyP ⁵⁺ (Figure 3)	<ul style="list-style-type: none"> non-commercially available cells (cells difficult to obtain) routine assay 	[72]
human keratinocytes (HaCaT)	MnSOD	Lentiviral constructs expressing shRNA	UV-induced EGFR activation by WB	MnTnBuOE-2-PyP ⁵⁺ (Figure 3)	<ul style="list-style-type: none"> commercially available cells routine assay requires lentivirus preparation and UV irradiation 	[74]
HEK293T cells	MnSOD	CRISPR/Cas9 to generate biallelic SOD2 disruption	clonogenic assay	GC4419 (Figure 5)	<ul style="list-style-type: none"> commercially available cells requires molecular biology experiments to modify the cells routine assay long treatment (10 days) 	[75]

Table 1. SOD deficient cellular models used to study SOD mimics

Although many studies on human MnSOD have been reported in the literature, only a few of them explored the ability of SODm to abrogate the biological consequences of a lack

of MnSOD activity in human cells. Holley *et al.* demonstrated the efficiency of a MnP to substitute for SOD enzyme for inhibiting the UV-induced activation of epidermal growth factor receptor (EGFR) in MnSOD-silenced HaCaT cells. In this study, a lentivirus containing a short hairpin RNA (shRNA) targeted against MnSOD was used to silence MnSOD in the human keratinocyte cell line [74]. More recently, using the HEK293T cell line, Cramer-Morales *et al.* generated a novel human cellular model that is completely devoid of detectable MnSOD protein expression and enzyme activity using the strategy based on the CRISPR/Cas9 system to generate biallelic SOD2 disruption. They showed that treating the SOD2-null cells with a SODm allowed the rescue of their growth and survival (Figure 8) [75].

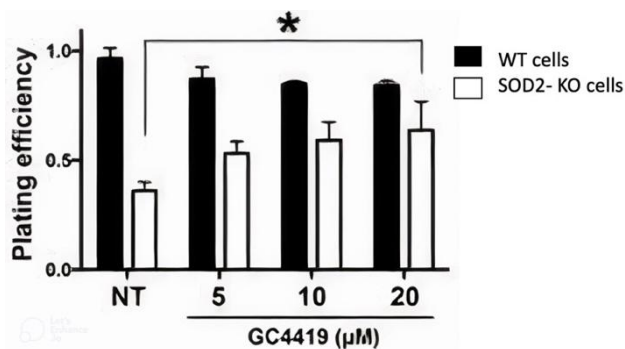


Figure 8. Figure from [75]. The pharmaceutical SODm labelled GC4419 is able to restore the clonogenic activity of SOD2 null HEK293T cells in a dose dependent manner. Black bars: wild-type (WT) cells. White bars: SOD2-knockout (KO) cells. Copyright © 2015 Elsevier Inc. All rights reserved.

2.2. Other cellular models of oxidative stress

SOD deficient microorganisms appeared as excellent models to investigate the activity of SODm. However, they are far from the oxidative stress events occurring in most physiopathologies. In this context, others cellular models based on more physiological induction of oxidative stress have been developed and are widely used. In these models, oxidative stress is generated and SODm are evaluated for their ability to restore a normal functioning of cells. These cellular models are classified into four categories depending on the oxidative stress triggering pathway:

Class 1: cellular models exposed to exogenous ROS, added directly in the culture medium or generated enzymatically outside the cells or cells naturally rich in endogenous H₂O₂ (Table 1).

Class 2: cellular models exposed to anticancer drugs or treatments whose primary mechanism of their pharmacological action is ROS production (Table 2).

Class 3: cellular models exposed to drugs whose ROS production is an adverse side effect (Table 3).

Class 4: cellular models closely mimicking physiopathological situations i.e., endogenous production of ROS species upon activation by a natural triggering signal (Table 5).

2.2.1. Class 1: cells exposed to exogenous ROS, added directly in the culture medium or generated enzymatically or cells naturally rich in endogenous H₂O₂

Many cellular models of oxidative stress are based on an exogenous enzymatic production of ROS. The exogenous extracellular ROS H₂O₂ that is less reactive than the hydroxyl radical and superoxide can diffuse and partially penetrate inside the cells, which leads to an increased cellular ROS content and cytotoxic effects [76,77]. The historically-used system is composed of xanthine and xanthine oxidase (XO). XO is an enzyme that catalyzes the oxidation of xanthine and hypoxanthine into urate while consuming dioxygen. XO proceeds to dioxygen reduction *via* an univalent and a divalent (or direct) pathway leading respectively to superoxide and hydrogen peroxide generation. Because XO is a high molecular weight protein, it does not enter cells unless active endocytosis *via* vesicular transport occurs. ROS are thus produced mainly in the extracellular medium and have to diffuse across membranes to reach intracellular targets. Consequently, superoxide molecules generated extracellularly will dismutate into H₂O₂ which can then cross the cell membrane

[78]. This xanthine/XO system thus provides an intracellular H₂O₂ stress and can *a priori* be used with any cell type in culture: cell lines of animal or human origins but also cells in primary culture or explants. Moreover, ROS production can be controlled by manipulating the substrate (xanthine, hypoxanthine) and enzyme concentrations. Moriscot *et al.* incubated insulin-secreting cells and human pancreatic islets in presence of XO and hypoxanthine and evidenced the beneficial effect of MnTMPyP on ROS production and cell viability (Figure 9) [79].

ROS localization	Generation system	Primary ROS generated	Cellular models tested	SODm tested	Advantages/drawbacks	Ref.
Extracellular	Xanthine/ xanthine oxidase	superoxide, H ₂ O ₂ Continuous slow flow of (physiological relevance)	Green monkey kidney cells (Vero cells)	Se-Cu-32P (Figure 6)	<ul style="list-style-type: none"> commercially available cells non-human derived from normal kidney cells not immortalized cells 	[80]
			Rat cardiomyocyte cell line H9c2(2-1)	NS1 (Figure 6)	<ul style="list-style-type: none"> commercially available cells model to study diabetes, ischemia-reperfusion injury, cardiomyopathy, mitochondrial metabolism etc 	[81]
			Rat insulinoma cell line (INS-1)	MnTMPyP (Figure 3)	<ul style="list-style-type: none"> commercially available cells basic diabetes cellular model widely used to study the effect of drugs on insulin secretion 	[79]
			Human embryonic kidney cells (HEK 293)	NS1 (Figure 6)	<ul style="list-style-type: none"> commercially available cells widely used in biotechnology ease of transfection and able to produce large amounts of recombinant proteins 	[82]
			Rat aorta smooth muscle cells (RASM)	Cycl1 (Figure 5)	<ul style="list-style-type: none"> commercially available cells good physiological relevance widely used to study cardiovascular function and disease 	[83]
	H ₂ O ₂ added to the culture medium	H ₂ O ₂	Primary rat cortical neurons	MnTMPyP (Figure 3)	<ul style="list-style-type: none"> non-commercially available cell line isolated from rat brain physiological good physiological relevance well suited to study OS effect in neuronal diseases 	[84,85]
			Rabbit lens epithelial cells	O1 (Figure 6)	<ul style="list-style-type: none"> non-commercially available cell line Isolated from new born rabbit good physiological relevance 	[86]
			Rat primary neurons	EUK-134, EUK-189 (Figure 6)	<ul style="list-style-type: none"> non-commercially available cell line isolated from rat brain physiological good physiological relevance well suited to study OS effect in neuronal diseases 	[87]
	Glucose/ glucose oxidase	H ₂ O ₂ Continuous slow flow of (physiological relevance)	Human dermal fibroblasts	EUK-8, EUK-134 (Figure 6)	<ul style="list-style-type: none"> commercially available cells human cells good physiological relevance but more expensive to culture 	[32]
			Calf pulmonary endothelial cells	MnTMPyP, MnTBAP (Figure 3)	<ul style="list-style-type: none"> commercially available cells Study of neutrophil-mediated destruction of endothelial cells in inflammatory processes 	[89]
Intracellular	Endogenous H ₂ O ₂	H ₂ O ₂	HeLa HyPer cells	CATm1 (Figure 6)	<ul style="list-style-type: none"> non-commercially available cell line no need for external probes/assay high sensitivity to detect H₂O₂ 	[90]
				MnTnE-2-PyP ⁵⁺ , MnTnBuOE-2-PyP ⁵⁺ , MnTBAP, M40403, EUK-134 (Figure 3, Figure 5 and Figure 6)		[91]

Table 2. Summary of class 1 cellular models of oxidative stress exposed to exogenous ROS, added directly in the culture medium or generated enzymatically outside the cells or cells naturally rich in endogenous H_2O_2 , mentioned in the text.

Furthermore, Zou *et al.* demonstrated that a Se and Cu peptide mimicking SOD was able to rescue green monkey kidney cells (Vero cells), damaged by XO/xanthine/ Fe^{2+} with Fe^{2+} meant to catalytically generate HO° from H_2O_2 and superoxide through Fenton mechanism [80]. Likewise, Kain *et al.* determined the ability of a Mn SODm Mn-NS₁ (Figure 6) to inhibit the cell death of H9c2 cardiomyocytes caused by the superoxide generator XO/xanthine [81]. The measurement of uric acid production by xanthine/XO in parallel experiments showed that the antioxidant action of the studied mimic was not due to the blockade of XO enzymatic activity but rather to a specific quenching of superoxide. This control was also conducted by P. Failli *et al.* to demonstrate the efficacy of Mn-based SODm (Cycl1) as an efficient superoxide scavenger [83].

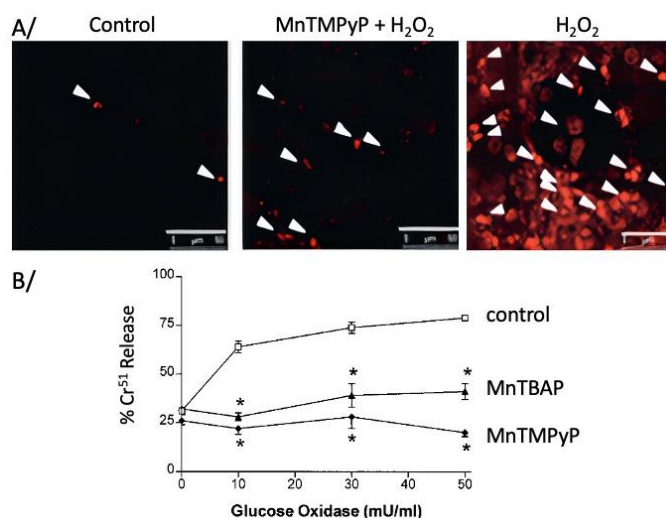


Figure 9. Protective effect of MnTMPyP SODm on two cellular models exposed to exogenous ROS: A/ H_2O_2 added directly in the culture medium or B/ generated enzymatically with the glucose oxidase system. A/ Figure from [85]. Imaging by laser scanning confocal microscopy of intracellular superoxide radical with the use of superoxide-specific DHE probe. Primary Cortical Neuron Culture were exposed or not to H_2O_2 bolus at $100 \mu M$ for 2 hours and treated or not with MnTMPyP MnP at $5 \mu M$. B/ Figure from [89]. Effect of MnTBAP and MnTMPyP SODm on the injury mediated by glucose oxidase in endothelial pulmonary cells labelled with Cr^{51} . Cell injury was assessed by measuring the release of Cr^{51} into the culture medium 5h after glucose oxidase stress. Copyright © 1997 Academic Press. All rights reserved.

Another example of the use of the xanthine/xanthine oxidase system was provided by Vyas *et al.* to generate an oxidative stress in human embryonic kidney cells (HEK 293) [82]. They demonstrated that manganese complexes of thiosemicarbazone ligands display a

protective effect and were useful to avert the ROS-induced acute nephrotoxicity observed in patients suffering from renal failure.

Another commonly used and simple model consists of the treatment of cells with H_2O_2 , that was shown to trigger the generation of superoxide radical anion according to ROS assays based on ROS-specific fluorescent probes (see section 3.1) [92]. Indeed, H_2O_2 can cross cell membranes and penetrate cells, where it may initiate various redox-mediated pathways [78]. Several papers report the protective effect of MnTMPyP against H_2O_2 -induced oxidative stress in primary rat cortical neurons (Figure 9A) [84,85]. More precisely, authors investigated how MnPs prevent apoptotic cell death and cellular oxidation, and how MnTMPyP preserves the mitochondrial and endoplasmic reticulum functions, following H_2O_2 injury. Other examples of antioxidant activity in H_2O_2 -injured cells include the protection of rabbit lens epithelial cells by n-propyl gallate from H_2O_2 insult [86] and the efficiency of salen SODm (EUK-134) to protect rat primary neurons from H_2O_2 [87].

Rather than being administered as a bolus, H_2O_2 can be generated enzymatically by using a glucose/glucose oxidase system. The advantage of this system is to produce a continuous slow flow of hydrogen peroxide. It has been used by Doctrow *et al.* to evaluate the cytoprotective effects of a series of salen manganese complexes in human dermal fibroblasts [32]. Likewise, Crapo *et al.* used this enzymatic system to demonstrate the ability of MnTMPyP and MnTBAP to protect calf pulmonary artery endothelial cells against H_2O_2 -mediated injury (Figure 9B) [89].

Lastly, another model of interest to be mentioned in this section is that of the HeLa HyPer cells [93]. These cells are naturally rich in H_2O_2 making the addition of exogenous ROS not required to assess the antioxidants effect of SODm. Briefly, HeLa Hyper cells express a ratiometric fluorescent sensor of H_2O_2 , named HyPer [93]. Measuring this normalized

fluorescence ratio allows to monitor the intracellular concentration of H₂O₂. This model was notably used by our team to evaluate and compare the antioxidant effects of the commonly-known SOD and catalase mimics, Mn1, MnTnBuOE-2-PyP⁵⁺, M40403, MnTBAP, MnTE-2-PyP⁵⁺ and EUK-134 [91]. While M40403 and MnTBAP had no effect on the normalized fluorescent ratio, Mn1, MnTnBuOE-2-PyP⁵⁺, MnTE-2-PyP⁵⁺ and EUK-134 were able to significantly decrease the levels of intracellular H₂O₂ when incubated at 100 μM.

2.2.2. Class 2: cellular models involving anticancer drugs or treatments whose primary mode of action is ROS production

ROS localization	Generation system	Primary ROS generated	Cellular models tested	SODm tested	Advantages/drawbacks	Ref.
Intracellular	Oxaliplatin, paclitaxel, 5-fluorouracil	Superoxide H ₂ O ₂	Human leukocytes, murine colon cancer cells (CT26), human lung cancer A549 cell line	MnTBAP, Mangafodipir (Figure 3, Figure 6)	<ul style="list-style-type: none"> CT26, A549: commercially available cells Human leukocytes: good physiological relevance, non-commercially available cells 	[45]
			Fibroblast cell line (NIH/3T3), colon cancer cell lines (HT29 and CT26)	Mn1 (Figure 6)	<ul style="list-style-type: none"> commercially available cells 	[94]
	Irradiation	superoxide, H ₂ O ₂ , HO [•]	Lymphoblastoid cells from Ataxia-Telangiectasia patients (A-T cells)	MnTM-2-PyP ⁵⁺ , MnTE-2-PyP ⁵⁺ , MnTnHex-2-PyP ⁵⁺ , MnTTEG-2-PyP ⁵⁺ , MnBr ₈ TSPP ³⁻ , M40403, M40404, EUK-8, EUK-134, EUK-189, (Figure 3, Figure 5 and Figure 6)	<ul style="list-style-type: none"> non-commercially available cells radiosensitive cells with increased ROS levels and impaired mitochondrial function 	[95]

Table 3. Summary of class 2 cellular models of oxidative stress, exposed to anticancer drugs or treatments whose primary mechanism of their pharmacological action is ROS production, mentioned in the text.

Oxaliplatin, paclitaxel and 5-fluorouracil are other ROS-generating chemical agents that are mainly used as anti-cancer agents, leading to cancer cell death through the production of an intracellular oxidative stress (Figure 10). Their anti-tumoral efficacy is associated with deleterious side effects, particularly peripheral neuropathy. As this neurotoxicity involves ROS production, these agents provide interesting cellular model to assess the ability of SODm to modulate the oxidative stress [94,96]. The group of F. Batteux exposed healthy human leukocytes and murine colon cancer cells CT26 to these three chemotherapeutic agents and observed significantly increased intracellular levels of superoxide and hydrogen peroxide in both cells types, using a spectrofluorometric assay [45]. Interestingly, treatment with the SODm mangafodipir, composed of a vitamin B6 derivative ligand, decreased the lysis of healthy leukocytes exposed to paclitaxel, oxaliplatin, or 5-fluorouracil by respectively,

46%, 30.5% and 15%. However, treatments of CT26 cells with mangafodipir enhanced the cytotoxicity of the three anticancer chemotherapeutic agents which was associated to an increased dismutation of superoxide into H₂O₂. This can be explained by the increased sensitivity of cancer cells toward H₂O₂ compared to healthy cells. Guillaumot *et al.* demonstrated the activity of a low molecular weight SODm labelled MAG (or Mn1) on normal fibroblast cells (NH3T3) and on colon cancer cells (HT29 and CT26) treated with oxaliplatin [94]. This SODm increases levels of hydrogen peroxide via the detoxification of superoxide with an increase of the cytotoxicity of oxaliplatin, probably through an increase of H₂O₂. But MAG also induced a decrease of oxidative-stress mediated neuropathy in an *in vivo* model. In a subsequent study, they showed that a compound directly derived from Mn1, when administrated in combination with oxaliplatin, was not affecting the antitumoral activity meanwhile improving the tolerance to oxaliplatin [97].

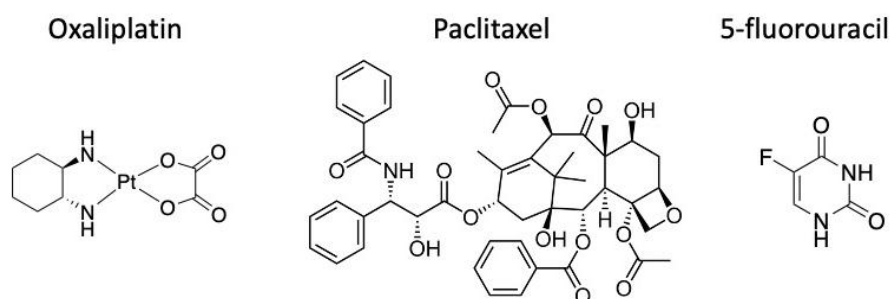


Figure 10. Structure of the ROS-generating anti-cancer agents

Many papers show that exposure of cells to irradiation leads to the generation of ROS that are then responsible for DNA damages and cell death [98–100]. Thus, SODm appear as potent radiation protectors as they are able to scavenge ROS and thus to abrogate the ROS-mediated damages. Lymphoblastoid cells derived from Ataxia-Telangiectasia (A-T) patients have been used as a radiation-induced oxidative stress model for the screening of radioprotectant and antioxidant SODm [95]. A-T patients cells indeed display a high ROS content, according to ROS-specific fluorescent labelling, associated with a strong radio

sensitivity and an impaired mitochondrial function [101]. Cells were irradiated and incubated in presence of different SODm [95]. Measurement of radiation-induced cell death, apoptosis and DNA damages allowed demonstration of the radioprotectant potential of each compound.

2.2.3. Class 3: cellular models exposed to drugs whose adverse effects generate ROS

ROS localization	Generation system	Primary ROS generated	Cellular models tested	SODm tested	Advantages/drawbacks	Ref.
Intracellular	Menadione (vitamin K3)	superoxide, H ₂ O ₂ , HO [•]	Insulin-secreting cells (INS-1)	MnTMPyP (Figure 3)	<ul style="list-style-type: none"> commercially available cells basic diabetes cellular model widely used to study the effect of drugs on insulin secretion 	[79]
			Bovine aortic endothelial cells (BAECs)	MnTBAP (Figure 3)	<ul style="list-style-type: none"> commercially available cells widely used in cancer and cardiovascular diseases good physiological relevance 	[102]
Intracellular	Paraquat (herbicide)	superoxide, H ₂ O ₂ , HO [•]	Human epithelial cervical cancer cells (HeLa cells)	N1 loaded in functionalized mesoporous silica	<ul style="list-style-type: none"> commercially available cells very sensitive to oxidative stress 	[103]
			Neuronal and glial cells from embryonic rat cerebral cortices	MnTBAP (Figure 3)	<ul style="list-style-type: none"> non commercially available cells good physiological relevance used to study toxin-induced neuronal excitotoxicity and potential benefits of SODm 	[104]
			Rat Dopaminergic Neural Cell Line (1RB3AN27) and primary Mesencephalic cells	EUK-134, EUK-189 (Figure 6)	<ul style="list-style-type: none"> 1RB3AN27: commercially available cells widely used dopaminergic neuron model Primary mesencephalic cells: isolated from mouse embryos, good physiological relevance 	[105]
Intracellular and extracellular	SIN-1 (3-morpholino-sydnonimine)	NO, superoxide peroxynitrite	Bovine aortic endothelial cells (BAECs)	MnTnHex-2-PyP ⁵⁺ MnTnBuOE-2-PyP ⁵⁺ (Figure 3)	<ul style="list-style-type: none"> commercially available cells widely used in cancer and cardiovascular diseases good physiological relevance 	[106]
			Insulin-secreting cells (INS-1)	MnTMPyP (Figure 3)	<ul style="list-style-type: none"> commercially available cells basic diabetes cellular model widely used to study the effect of drugs on insulin secretion 	[79]
mitochondria	Stavudine	superoxide, H ₂ O ₂ , HO [•]	Human liver cancer cell line (HepG2)	MnTBAP (Figure 3)	<ul style="list-style-type: none"> commercially available cells high abundance of mitochondria cells sensitive to stavudine well-suited to investigate the development of hepatic steatosis and lactate acidosis 	[107]

Table 4. Summary of class 3 cellular models of oxidative stress exposed to drugs whose ROS production is an adverse side effect, mentioned in the text.

Other pharmacological compounds used for human therapy or chemicals that may be absorbed accidentally by humans lead to ROS production, as deleterious side effects. Cellular models treated with these compounds have thus been used to test the efficacy of SODm. Such ROS-inducing agents include menadione and paraquat (1,10-dimethyl-4,40-bipyridylum dichloride, PQ). Menadione (medication for normal blood clotting) and

Paraquat, one of the most widely used herbicides in the world, leads to an acute generation of superoxide via redox cycling carried out by one-electron reductive enzymes [108–110] which can lead to cell death [102]. Moriscot *et al.* showed that addition of the MnP SODm MnTMPyP to insulin-secreting cells (INS-1) or human pancreatic islets during a menadione stress period led, in both cases, to reduced ROS production and improved cell survival [79]. Interestingly, a Cu/ZnSODm loaded in functionalized mesoporous silica was able to inhibit the PQ-induced oxidative damages and apoptosis of HeLa cells (Figure 11a) [103]. PQ treatment of rat dopaminergic cells and primary mesencephalic cultures also permits to illustrate the capacity of salen manganese complexes (EUK-134 and EUK-189) to protect against oxidative stress-induced neurotoxicity (Figure 11b) [105].

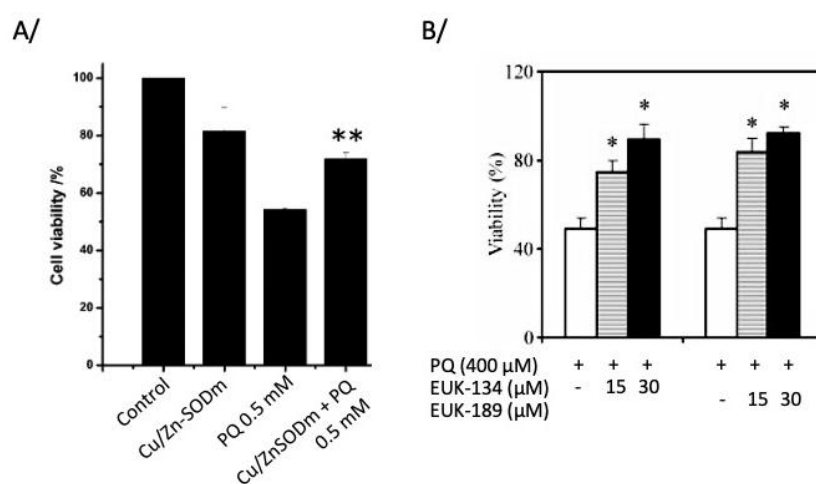


Figure 11. Effect of SODm on cells exposed to Paraquat (PQ), a ROS-generating chemical. (A) Figure from [103]. A/ vectorized Cu/Zn SODm was able to improve the cell viability of HeLa cells stressed by PQ. B/ Figure from [105]. Manganese salen complexes attenuate the cell death resulting from PQ action in dopaminergic neuron cells.

Cell treatment with SIN-1 (1,3-morpholinosydnonimine, a vasodilator) constitutes another relevant model of oxidative stress. Indeed, the decomposition of SIN-1 simultaneously releases nitric oxide and superoxide which then react together to form peroxynitrite, a powerful oxidizing and nitrating agent [111]. Known as fast reductants of peroxynitrite, MnPs provided promising results for their capacity to reduce SIN-1-induced ROS generation and thus to protect bovine aortic endothelial cells against peroxynitrite-mediated

cytotoxicity [106]. In their above-cited paper, Moriscot *et al.* also showed that a MnP preserved INS-1 cells and human pancreatic islets viability upon exposure to SIN-1 [79].

Mitochondrial oxidative stress can result from the toxicity of nucleoside reverse transcriptase inhibitors (NRTIs), drugs used in antiretroviral therapy. For example, the mitochondrial superoxide level increases in HepG2 cells (a human liver cancer cell line) treated with NRTI stavudine (2'-3'-didehydro-2',3'-deoxythymidine), as shown by monitoring the decrease of aconitase activity upon treatment [107]. These authors also evaluated the ability of MnTBAP to reverse the stavudine-induced mitochondrial dysfunction linked to oxidative stress, the altered mitochondrial DNA amplification and the disrupted cellular energetics.

*2.2.4. Class 4: cellular models closely mimicking physiopathological situations:
ROS production upon activation of native cellular pathways*

The last class of cellular models used to assess SODm efficacy relies on ROS generation by the cells themselves upon stimulation of endogenous pathways. Cellular models of immune response, cancer, diabetes and inflammatory diseases for instance are of particular interest in this context. In these models the pathological pathways that involve oxidative stress can be activated using specific triggers. Owing to their similarity with the real physiopathological situations, the oxidative stress produced occurs with a similar amplitude and in the same cell compartments as in the studied diseases.

ROS localization	Generation system	Primary ROS generated	Cellular models tested	SODm tested	Advantages/drawbacks	Ref.
Intracellular and extracellular	IFN- γ , LPS	ROS and NOS	Mouse macrophage cell line (RAW 264.7)	M40403, PAC1-5 (Figure 5)	<ul style="list-style-type: none"> commercially available cells widely used can produce high levels of ROS following immune stimulation 	[112]
	IFN- γ , LPS + PMA			Mn1 (Figure 6)		[113]
	IFN- γ , LPS + PMA			OCP1 (Figure 6)		[113]
	LPS			MnTM-4-PyP ⁵⁺ -MPP, MnTM-4-PyP ⁵⁺ (Figure 3)		[114]
	N-formyl- Met-Leu-Phe peptide (fMLP)			Cycl1 (Figure 5)		[83]
	Hyperthermia (43°C)			Not tested with SODm		[115]
	fMLP-stimulated macrophages RAW 264.7	ROS and NOS	Rat aorta smooth muscle cells (RASM)	Cycl1 (Figure 5)	<ul style="list-style-type: none"> commercially available cells good physiological relevance widely used to study cardiovascular function and diseases 	[83]
	LPS or PMA		Rat alveolar macrophages (CRL-2192)	M40403 (Figure 5)	<ul style="list-style-type: none"> commercially available cells can produce high levels of ROS following immune stimulation used to study the role of alveolar macrophages in protecting lung tissue during respiratory infection 	[116]
	DMSO + PMA		Superoxide and others ROS	Human leukemia cell line (HL-60) differentiated into macrophages-like cells	Phth1-7, MnTMPyP (Figure 3) MnTMPyP (Figure 3)	<ul style="list-style-type: none"> commercially available cells can be differentiated to granulocyte-like cells similar to phagocytic cells they cause an extracellular release of superoxide upon activation by PMA
	PMA + LPS	Superoxide and other ROS	Human monocyte cell line (THP-1) differentiated into macrophages	Sc1-12 (Figure 5)	<ul style="list-style-type: none"> commercially available cells very popular cell line need to be differentiated them into macrophages More reliable than Raw 264.7 cells for some assays: they express the apoptosis-associated speck-like protein, necessary for the activation of NLRP3 inflammasome 	[66]
	Hypoxia	Superoxide and other ROS	Alveolar macrophages from rat lung tissues	MnTE-2-PyP ⁵⁺ (Figure 3)	<ul style="list-style-type: none"> can produce high levels of ROS following immune stimulation used to study the role of alveolar macrophages in protecting lung tissue during respiratory infection and hypoxia good physiological relevance. 	[119]
	Hyperglycemia (high amount of glucose)	ROS and NOS	Rat cardiac myoblastic cell line (H9c2)	NS1 (Figure 6)	<ul style="list-style-type: none"> commercially available cells Widely used model to study diabetes, ischemia-reperfusion injury, cardiomyopathy, mitochondrial metabolism etc. 	[81]
	NMDA (N-methyl-D-aspartate)	ROS	Neuronal and glial cells from embryonic rat cerebral cortices	MnTBAP (Figure 3)	<ul style="list-style-type: none"> primary cells physiologically relevant cortical cell model to study toxin-induced neuronal excitotoxicity 	[104]
	Mechanical and chemical (IL-1b) stress	ROS	Human isolated pancreatic islets	AEOL10150 (Figure 3)	<ul style="list-style-type: none"> non-commercially available cells physiologically relevant model to study the benefits of SODm for preserving the pancreatic islet from mechanical and chemical stress during transplantation 	[120]
			Rat pancreatic islets	AEOL10150 (Figure 3)		[121]
	LPS	Superoxide and other ROS	Human colon cancer epithelial cell line stably transfected with MD2 (HT29-MD2)	Mn1 (Figure 6)	<ul style="list-style-type: none"> non-commercially available cells stably transfected to overexpress MD2 protein increased sensitivity to LPS with a strong inflammatory response 	[36]
Mn1 functionalized with cell-penetrating peptide (Figure 6)				[122]		
Mn1, Mn1P, Mn1C, Mn1CP (Figure 6)				[123]		
MnPs, M40403' EUK-134 (Figure 6)				[91]		

				3, Figure 5 and Figure 6)		
				OCP1 (Figure 6)		[124]

Table 5. Summary of class 4 cellular models of oxidative stress closely mimicking physiopathological situations, mentioned in the text.

2.2.4.1. Cellular model of oxidative stress based on immune response activation

ROS and RNS play a major role in the innate defense against extracellular pathogens and more largely in the immune system by regulating cytokine response and immune cell survival, and by participating to immunologically important signaling pathways [125]. They are mainly generated by macrophages in the context of a specific type 1 T-helper cell response. As macrophages are major actors in the production of ROS and RNS species under immune stimulation, they constitute an interesting model for oxidative stress [126]. The team of I. Ivanovic-Burmazovic demonstrated the effect of manganese SODm (the amphiphilic analogues of Mn(II)pyaneCl₂, PAC1-5) on the superoxide level present in the cytosol of a murine macrophage cell line, RAW 264.7 cells, stimulated with interferon-γ (IFN-γ) and lipopolysaccharide (LPS) (Figure 12B) [112]. They also evidenced that the parent Mn(II)pyaneCl₂ acts mainly as nitric oxide dismutases [127]. Similarly, our team investigated the effect of a low-molecular weight SODm labeled Mn1 in Raw 264.7 cells, immuno-activated with IFN-γ, LPS and phorbol-12-myristate-13-acetate (PMA), a NADPH oxidase activator (Figure 12C) [113]. Mn1 was shown to efficiently alter the flow of O₂^{•-}, ONOO⁻ and H₂O₂ in extracellular medium. More recently, the same team used these stimulated macrophages to demonstrate the antioxidant properties of a peptidyl copper complex mimicking SOD [124]. This cellular model was also one of the models used to evaluate the SOD activity of a series of SODm [91]. MnP activity in immuno-activated macrophages has also been evaluated by the team of Kawakami. They notably described the antioxidant properties of a MnP-oligopeptide conjugate that restores the viability of LPS-stimulated

macrophage RAW 264.7 cells (Figure 12A) [114]. The group of Valtancoli used also RAW 264.7 macrophages stimulated with N-formyl-Met-Leu-Phe peptide (fMLP) and assessed the ability of Mn(II) complexes with polyamine-polycarboxylate ligands to prevent superoxide-dependent cytochrome *c* oxidation and thus indirectly to scavenge superoxide [83]. They also provided an innovative example of activated macrophages co-incubated with rat aorta smooth muscle (RASM) cells. ROS generation induced by stimulated macrophages resulted in significantly increased lipid peroxidation in co-incubated RASM cells, which was partially decreased by the addition of the mimic. For their part, the group of D. Salvemini advantageously used rat alveolar macrophages CRL-2192 as a lung derived cell culture model, since these cells exhibit a higher capacity to generate ROS in response to gram negative bacterial endotoxin (*E. coli* LPS or PMA) compared with macrophages from other anatomic compartments [116]. This model of acute lung injury was suitable for studying the implication of ROS in exacerbating inflammatory responses through modulation of pro-inflammatory cytokines production as well as the ability of SODm M40403 to decrease superoxide concentration and cytokines overexpression following cell stimulation.

Macrophages are also known to produce ROS in response to hypoxia [119]. Jackson *et al.* incubated alveolar macrophages under hypoxic (0.5% O₂) and normoxic (20% O₂) conditions, measured the levels of superoxide by monitoring the reduction of cytochrome *c* by superoxide and established that low oxygen stress activates a significant increase in superoxide production by macrophages [119]. Treatment of macrophages challenged by hypoxia with the SODm MnTE-2-PyP⁵⁺ allowed to maintain superoxide concentration at the level observed under normoxia. The same group identified hyperthermia as an additional stimulus to activate the respiratory burst of macrophages [115]. Incubation of RAW 264.7

macrophages at 41°C under normoxia stimulates a significant production of superoxide, as measured by cytochrome *c* assay (see section 3.1.2).

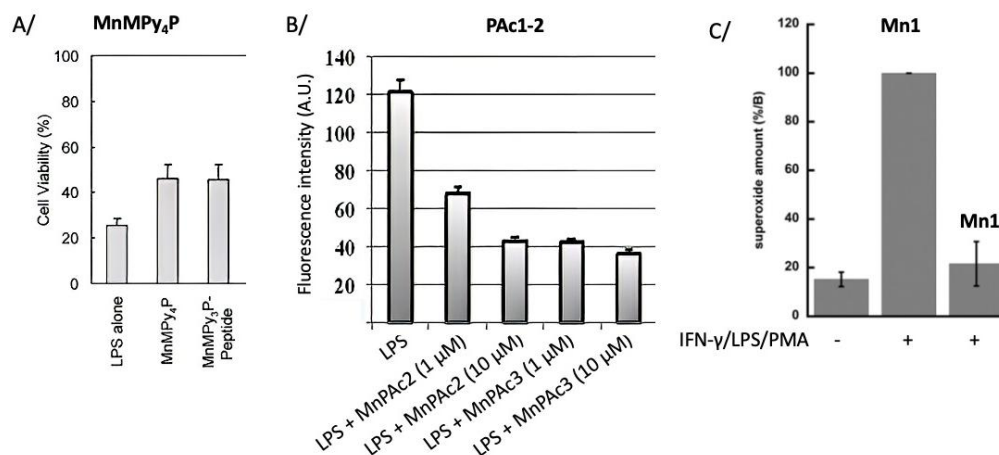


Figure 12. Effect of SODm on stimulated murine RAW 264.7 macrophages. A/ Increase in the viability of LPS-stimulated RAW 264.7 cells after treatment with MnTMPyP or its analog conjugated to a signal peptide for mitochondrial targeting. Adapted with permission from [114]. Copyright 2006 American Chemical Society. B/ Measurement of intracellular superoxide levels in immune-stimulated cells via the use of the HE probe. Treatment with 2 amphiphilic pentaazamacrocyclic manganese complexes (MnPACx) reduced superoxide levels. Adapted with permission from [112]. Copyright 2014 American Chemical Society. C/ Figure from [113]. Evaluation of Mn1 effect on extracellular superoxide levels in IFN-γ/LPS/PMA stimulated RAW 264.7. Superoxide was quantified in extracellular media using cytochrome *c* reduction in the extracellular medium.

Human leukemia cells are also widely used as a superoxide-producing cell model. Human promyelocytic leukemia cells (HL-60) differentiate into macrophage-like cells when treated with DMSO and the incubation of these differentiated cells with PMA leads to an increase in extracellular superoxide production through NADPH oxidase pathway. The detection and quantification of both intracellular and extracellular superoxide by dihydroethidium fluorescence analysis then allowed to evaluate the activity of MnP [118] and Mn-Phthalocyanines as SODm [117]. Another model reported by González-García *et. al* is the human monocyte cell line THP-1 differentiated into macrophages upon PMA treatment and then immune-stimulated with LPS [66]. This cellular model was notably used to evaluate the intracellular activity of manganese complexes composed of tail-tied aza-scorpionid ligands [66].

2.2.4.2. Cellular model of OS related to diabetes context

Another model of oxidative stress based on endogenous production of reactive oxygen and nitrogen species consists of inducing hyperglycemia by adding high amount of glucose in the culture medium. Indeed, hyperglycemia is known to induce oxidative stress, contributing notably to the apoptosis of cardiac cells in diabetic cardiomyopathy [128]. The SODm designed by the group of S. Sitasawad afforded high protection against hyperglycemia-induced oxidative stress in the rat cardiac myoblastic cell line H9c2 [81].

Furthermore, pancreatic islets detached from the surrounding extracellular matrix for subsequent transplantation (for severe type I diabetes cases) or for research were reported to undergo mechanical and chemical insults associated to oxidative stress and leading to significant ROS-induced cell damages [129]. The mechanical and chemical stresses notably induce a loss of the islet mass as well as islet cells necrosis and apoptosis [120]. Bottino *et al.* cultured human isolated pancreatic islets in order to test the ability of SODm compounds to block oxidative stress and thus to preserve the normal β -cell phenotype after a mechanical stress [120]. The group of Papaccio cultured rat pancreatic islets and simulated a mechanical stress by treating cells with long periods of collagenase digestion during the separation procedure while chemical stress was induced through the addition of cytokine IL-1b [121]. Both papers revealed that the addition of the MnP SODm named AEOL-10150 was able to counteract the negative effect of the mechanical stress, as illustrated by a significantly higher islet cell mass and an improved cell survival, while it had a negligible impact on cytokine-induced cytotoxicity.

2.2.4.3. Cellular model of OS mediated by inflammation

A model of oxidative stress induced by inflammation was developed based on the intestinal epithelial cell line HT-29. HT-29 cells, which express TLR4, were stably transfected to overexpress a LPS co-receptor molecule, the myeloid differentiation receptor MD-2,

abrogating LPS tolerance [130]. The resulting HT29-MD2 cell line has thus an increased sensitivity to LPS, which induces a strong inflammatory reaction in cells illustrated by the release of pro-inflammatory cytokines such as interleukin-8 (IL-8). The inflammatory response is known to be accompanied with an overproduction of superoxide by NADPH oxidase (NOX) [131]. In this model, it has been demonstrated that a LPS challenge induces an overexpression of MnSOD, which support the onset of an oxidative stress mediated by LPS [36].

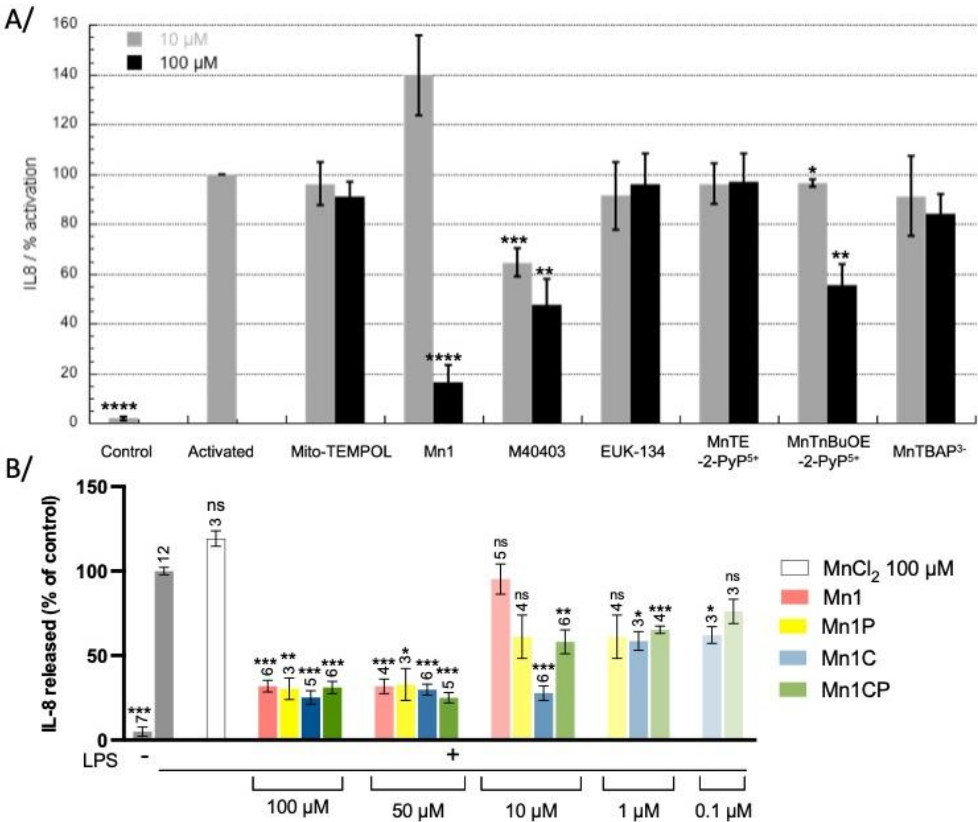


Figure 13. Evaluation of the effect of A/ Mn1 and compounds commonly known as SOD or CAT mimics (figure from[91]) and B/ SODm derived from Mn1 with improved inertness (figure from[123]), on the LPS-induced secretion of IL-8 in HT29-MD2 cells.

Herewith, LPS-activated HT29-MD2 cells constitute a cellular model of inflammation that can contribute to the investigation of the intracellular SOD-like activity of SODm. The low-molecular weight manganese complex Mn1, its newly-designed less labile analogs, and Mn1 derivatives functionalized with a cell penetrating peptide were all able to partially blunt the MnSOD upregulation and to reduce the release of interleukin-8 in the cell model HT29-MD2

activated by LPS (Figure 13). Likewise, the anti-inflammatory activity of various well-studied commercial SODm were examined on HT29-MD2 cells and compared to that of Mn1 (Figure 13) [91]. Lastly, a peptidyl copper complex mimicking SOD displayed similar beneficial antioxidant and anti-inflammatory effects in LPS-activated HT29-MD2 cells [124].

2.2.4.4. Cellular model of OS related to excitotoxicity

Lastly, Patel *et al.* described an oxidative stress model associated to excitotoxicity of neuronal cultures due to excessive accumulation of calcium ions in post synaptic neurons [132]. This pathological process can lead to cell death. Excitotoxicity can be induced by cell treatment with N-methyl-D-aspartate (NDMA), a neurotransmitter and neuroendocrine regulator that becomes excitotoxic at high dose. Excitotoxicity results in intracellular superoxide generation which has been evidenced by the inactivation of aconitase. They have investigated how MnTBAP can protect mature neuronal cultures from excitotoxic injury by scavenging intracellular superoxide radicals.

To conclude on this part, it is important to note that depending on the model used, ROS can be produced in different cellular compartments or extracellularly. When cell penetration is required, the observed effect of the SODm is thus a combination of their intrinsic catalytic activity and their ability to translocate into cells and reach their target.

3. Assays to evaluate SODm activity in cells

The previous section was meant to offer an in-depth review of biological systems available for researchers as relevant tools to evaluate the biological activity of SODm. These oxidative stress models have been widely used to investigate the direct effects of SODm on ROS scavenging, their protective effects against cell injury, and their indirect effects on proteins, DNA, lipids and other biomolecules. The subsections below focus on the assays that are used to characterize the bioactivity of SODm using the above-presented cellular models.

3.1. Evaluation of the direct effects of SODm on ROS scavenging in cells

The effect of SODm on oxidative stress can be directly assessed by quantifying the cellular amount of ROS. Indeed, SODm are expected to exert a beneficial antioxidant activity in cells by quenching superoxide radical. To confirm this assumption but also to provide a better understanding of SODm mechanisms of action, researchers have attempted to sensitively and selectively detect superoxide. However, this transient species has a short lifetime in cells and cannot be easily detected. Numerous tools including fluorescent probes or electrochemical techniques have been employed to inform on the overall redox status of cells but their use as superoxide marker is still under debate.

The two following sections offer an overview of the probes used to measure the levels of superoxide in the presence or not of a SODm and thus enabling to characterize the SODm efficiency in limiting oxidative stress. The structures of these probes are summarized in the following Table 6.

3.1.1. Cell permeant fluorescent probes

3.1.1.1. Hydroethidine (HE) / dihydroethidium (DHE)

Hydroethidine (HE) (also called dihydroethidium (DHE)) is the most popular fluorogenic probes used for detecting intracellular superoxide ions. The capacity of HE to penetrate into cells was first reported in 1984 by Gallop *et al.* [133]. The study was completed in 1990 by Rothe and Valet [134] who showed that HE can then react intracellularly with superoxide to form the fluorescent two-electron oxidized product, ethidium (E^+). However, contrary to the consensus, HE probe is not specific to superoxide as it can react with other oxidants. For instance, HE can be oxidized through non-superoxide dependent intracellular processes, involving oxidases or cytochromes [135]. For a long time, HE has been considered mistakenly as a superoxide-specific marker. Moreover, the fluorescence of E^+ (excitation, 500-530 nm; emission, 590-620 nm) is enhanced upon intercalation into DNA which may bias the results [136]. Nevertheless, HE has been extensively used as a fluorescent sensor of the cellular redox state. Afterwards, in 2003, the group of Kalyanaram showed by using mass spectrometry and NMR that the reaction between superoxide and HE generates another red fluorescent compound at much lower concentration than E^+ , the hydroxylated product 2-hydroxyethidium (2-OH- E^+) (excitation, 480 nm; emission, 567 nm) [137]. Interestingly, 2-OH- E^+ is more specific of the reaction of HE with superoxide [138]. The improved selectivity of 2-OH- E^+ for superoxide was notably investigated by Bindokas *et al.* [139]. They observed that 2-OH- E^+ was not obtained by oxidation by HO^\bullet , NO, $OONO^-$, H_2O_2 , hypochlorite or singlet O_2 but only by superoxide. To our knowledge, this selectivity was not explained yet [139]. Because both oxidation products E^+ and 2-OH- E^+ are fluorescent in the same wavelength range, a simple reading of fluorescence is not sufficient to specifically determine the superoxide content. Indeed, the distinct detection of E^+ and 2-OH- E^+ using filter-based optical systems may lead to misreporting of the species of ROS being generated due to excitation and emission overlapping. An HPLC protocol has thus been developed allowing

the selective detection and quantification of 2-OH-E⁺ in Bovine Aortic Endothelial Cells (BAEC) exposed to menadione or antimycin A, based on the difference in elution between E⁺ and 2-OH-E⁺ [102]. The group of S. Dikalov adapted this HPLC-based assay to demonstrate that the formation of 2-OH-E⁺ from HE is proportional to the rate of superoxide formation in endothelial cells [140]. In a review, Zielonka and Kalyanaraman conclude on the requirement of HPLC to accurately quantify HE derivatives, and the unsuitability of conventional fluorescence-based techniques that do not distinguish E⁺ and 2-OH-E⁺ for quantifying superoxide [141].

Overall, both methods, i.e., fluorescence measurement coupled or not with HPLC, have been widely used for the investigation of SODm activity in cells (general antioxidant activity or specific anti-superoxide activity). Examples of HE/DHE used for the evaluation of SODm ability to quench superoxide include a work from Ndengele *et al.* which focused on the role of ROS in NF- κ B activation and cytokine production in alveolar macrophages [116]. By measuring the intracellular E⁺ fluorescence emitted by macrophages (488/610 exc/em), they found that PMA stimulation briskly enhanced the generation of ROS and this latter was partially suppressed in a dose-dependent manner by the SODm M40403. Similarly, the group of Ivanovic-Burmazovic explored the capacity of amphiphilic pentaazamacrocyclic complexes to remove ROS and subsequently prevent the oxidation of HE in immune-stimulated RAW264.7 cells [112]. Furthermore, Mathieu *et al.* used HE for the detection of cytosolic ROS in HT29-MD2 cells [36]. They observed that the synthetic low molecular weight SODm Mn1 was able to reduce ROS levels below the basal levels. In their work, Matemadombo *et al.* performed an HE assay on DMSO-treated HL-60 cells exposed to Mn-Phthalocyanines which are assumed to act as proficient SODm [117]. Considering (i) the advantageous intracellular photostability of 2-OH-(E⁺) and (ii) the fact that 2-OH-(E⁺) is not produced by

other ROS or RNS than superoxide [137], they preferentially monitored 2-OH-E⁺. Results evidenced a strong intracellular oxidation of HE interpreted as a strong production of superoxide in DMSO-treated HL-60 cells without PMA stimulation and an increased extracellular production after PMA stimulation. The HE fluorescence intensity was reduced by addition of Mn-phthalocyanines, which illustrates the inhibition of intracellular and extracellular superoxide concentration by these complexes.

3.1.1.2. MitoSOX

Mitochondria are recognized to play a crucial role in the intracellular generation of ROS in physiopathological conditions [58,142], by leakage of the respiratory complexes that are a major source of superoxide [3]. Indeed, mitochondria is a fragile organelle that needs to be specifically protected against oxidative stress. This is achieved by mitochondrial MnSOD and its knock-out is lethal for mice, whereas that of cytosolic CuSOD is not [143]. For this reason, the development of methods to assess the mitochondrial superoxide generation has been of great interest and led to the development of the commercially available MitoSOX red, a cell-permeant dye widely used as a mitochondrial superoxide indicator [144]. MitoSOX red comprises a HE moiety, which confers the probe a similar reactivity as HE's one. The HE moiety is covalently linked to a hexyl triphenylphosphonium cation (TPP⁺) to form the MitoSOX red probe. The particular electronic structure of TPP cations made of a positive charge on the phosphonium delocalized over the three lipophilic phenyl groups facilitates its translocation across phospholipid bilayers and its accumulation into the mitochondrial matrix in response to the negative membrane potential within the mitochondria [145]. TPP⁺ is thus able to carry the HE-linked group to mitochondria where it exhibits fluorescence upon oxidation. On its own, unconjugated HE is homogeneously distributed in the cells without preferential localization in the mitochondria. As for E⁺, the fluorescence quantum yield of E⁺-

TPP⁺ is boosted upon binding to mitochondrial DNA. Robinson *et al.* discovered that the superoxide-derived product of MitoSOX red (2-OH-E⁺-TPP⁺) has a distinct excitation wavelength at 396 nm that was not present for other nonspecific oxidation products (E⁺-TPP⁺) [144]. Monitoring the oxidation of MitoSOX red by exciting at 396 nm thus appears to improve the selective detection and imaging of intracellular superoxide production which is overestimated when monitored at 510 nm (detection of E⁺-TPP⁺). Since then, numerous studies have validated the use of MitoSOX red with fluorescent/confocal microscopy or flow cytometry for the selective detection of mitochondrial superoxide production in various cell types including keratinocytes, fibroblasts, neurons, epithelial, endothelial and lymphoid cells [146]. In particular, the group of Pacher established a quantitative method for mitochondrial superoxide detection simultaneously in rat cardiac myocytes (H9c2 cells) and in human coronary artery endothelial cells (HCAECs), that can be easily adapted for virtually any cell types [147]. The MitoSOX red probe has been widely applied to the investigation of SODm ability to scavenge mitochondrial superoxide. Lieb *et al.* used MitoSOX red to show the efficiency of amphiphilic pentaazamacrocyclic in decreasing the basal mitochondrial level of superoxide [112]. Furthermore Kain *et al.* examined the effect of thiosemicarbazone ligands bearing bipyridyl or aminoethanethiol group as ancillary ligands in high-glucose injured cardiac H9c2 cells [81]. They determined the intracellular levels of mitochondrial superoxide and peroxynitrite using MitoSOX red and dihydrorhodamine-123, respectively. The antioxidant properties of these compounds correlated positively with the elimination of ROS in mitochondria since they drastically reduce the superoxide and peroxynitrite flows. MitoSOX red probe is eventually a suitable mitochondria-targeted superoxide probe, relevantly used for the evaluation of SODm effect.

3.1.1.3. 2',7'-Dichlorodihydrofluorescein diacetate (DCFH-DA)

Numerous studies investigating SODm activity on ROS levels involved the 2',7'-dichlorodihydrofluorescein diacetate (DCFH-DA) assay. The DCFH-DA probe enters cells, accumulates mostly in cytosol and is herein easily deacetylated by intracellular esterases into the non-fluorescent form dichlorofluorescein (DCFH). The subsequent oxidation of DCFH by ROS yields DCF, which is highly fluorescent with an emission at ca. 525 nm when excited at ca. 488 nm (see Table 6). As DCFH can be converted to DCF by various ROS including peroxynitrite and numerous radicals, DCF fluorescence is not a direct assay of superoxide but an assay of generalized oxidative stress [148]. To study the global oxidative activity of INS-1 cells subjected to a xanthine/XO challenge, Moriscot *et al.* loaded cells with both DCFH-DA and DHE probes at the end of the stress period [79]. Flow cytometry analysis showed an increase of both DCF and HE fluorescence in stressed cells compared to non-stressed cells, revealing the higher levels of cytosolic ROS. When the SODm MnTMPyP was added, fluorescence increased less sharply for DCFH-DA and no increase was observed for HE. This suggests that the DCFH-DA probe can be oxidized by a larger number of oxidants than HE and supports the SODm intracellular activity of MnTMPyP. Likewise, Pollard *et al.* employed both DCFH-DA and DHE to examine the SOD activity of other MnPs in lymphoblastoid cells derived from Ataxia-Telangiectasia (A-T) patients (A-T cells) [95]. As described above (section 2.2.2), A-T cells are strongly sensitive to irradiation which results in higher levels of ROS. Treatment with MnTnHex-2-PyP and a mixture of MnTM-2-PyP⁺ derivatives (isomers) reduced the radiation-induced ROS level. The group of Xia measured the formation of ROS in rat cortical neurons exposed to H₂O₂ using laser scanning microscopy after staining with HE and DCFH-DA (Figure 14) [84,85]. ROS levels were markedly higher in H₂O₂-injured cells compared to control cells. However, pre-treatment of

the neurons with MnTM-4-PyP MnP significantly decreased the ROS level, which corroborates the MnP antioxidant activity.

Likewise, Peshavarya *et al.* investigated the effect of MnTMPyP on differentiated HL-60 cells and on human microvascular endothelial cells (HMEC-1 cells) incubated with diethyldithiocarbamate (DETCA), known to inactivate endogenous SOD [118]. To do so, they measured the total ROS production using DCFH-DA probe.

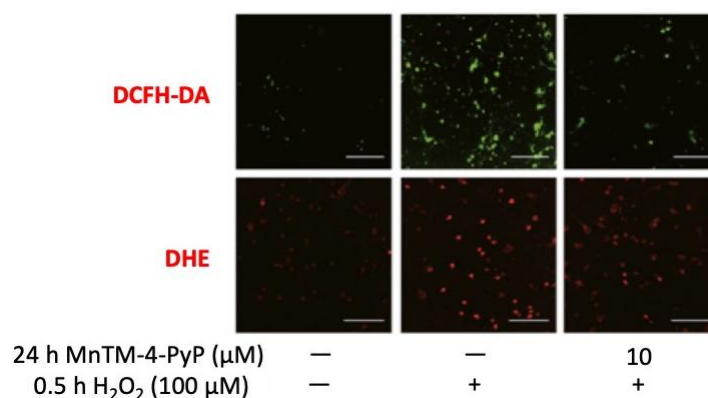


Figure 14: Fluorescence microscopy images illustrating the use of the ROS fluorescent probe mentioned in the text to evaluate the effect of SODm on cellular ROS content. Figure from [84]. H₂O₂-challenged rat cortical neurons treated with MnTMPyP SODm display lower ROS levels according to DCFHDA and DHE staining.

To conclude on this part, the fluorescent probes presented here allow to monitor qualitatively or semi-quantitatively the changes in cellular superoxide generation and their site of production. However, they still suffer from main limitations, in particular, they lack ROS specificity, except MitoSOX which is much more specific to superoxide and localized in mitochondria.

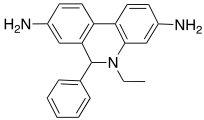
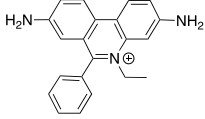
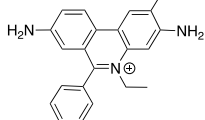
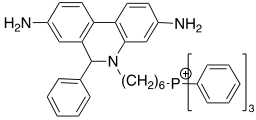
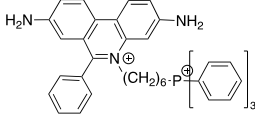
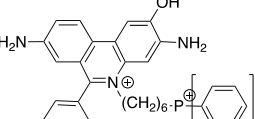
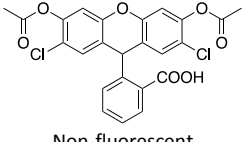
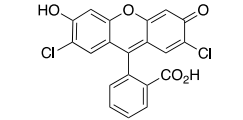
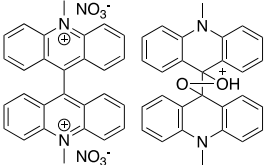
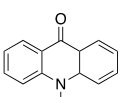
3.1.1.4. Lucigenin

Lucigenin is a chemiluminescent probe described in 1983 by Minkenberg and Ferber and commonly used for the detection of superoxide in cells and tissues [149]. This probe was shown to be first reduced to a radical cation and then to react with superoxide to generate unstable dioxetane (see Table 6) [150]. This latter breaks down into two N-methylacridone and generate photons. However, this probe is subject to redox cycling in the presence of

endogenous cellular reductases resulting in the artifactual generation of superoxide by the probe itself [151]. The measured amount of superoxide is thus overestimated, limiting the use of this probe for quantification. Nevertheless, this probe can be used in first approach as a very simple qualitative tool. Peshavarya *et al.* observed that MnTMPyP was able to abolish the increase in lucigenin chemiluminescent signal observed in PMA-stimulated HL-60 cells and in HMEC-1 cells exposed to NADPH [118].

3.1.2. Colorimetric non-cell-permeant probes

Other kinds of superoxide indicators are greatly limited by their cell-impermeability and subsequently their inability to probe intracellular superoxide. However, they provide a qualitative method to assess the effect of SODm on extracellularly released superoxide. These probes for superoxide detection include the UV-visible markers cytochrome *c* (12 kDa protein) [152] and the tetrazolium salt: 2,3-Bis-(2-méthoxy-4-Nitro-5-sulfophenyl)-2H-tetrazolium-5-carboxanilide (XTT) [153]. As a reminder, XTT dye is also used in cell cytotoxicity assay but require an electron coupling reagent to efficiently transfer the electrons from the cells to XTT. The use of XTT for the quantification of extracellular superoxide is limited by the unspecific reduction of XTT by cellular components via trans-plasma membrane electron transport that occurs even (but slowly) in absence of electron coupling reagent [154]. This probe can thus provide two different end points according to the experimental conditions and the time scale. The cytochrome *c* method based on the spectrophotometric monitoring of ferric cytochrome reduction to ferrocytochrome *c* at 550 nm was successfully applied to the determination of superoxide produced by RAW 264.7 macrophages in the extracellular medium (see section 2.2.4.1).

	Probe	Reduced form	Oxidized (detected) form	Selectivity	Advantages/drawbacks	References
Cell-permeant fluorescent probes	hydroethidine (HE) also called dihydroethidium	 <p>Blue fluorescence</p>	 <p>Ethidium (E⁺): 480-500/575-595 nm (exc/em)</p>	ROS	<ul style="list-style-type: none"> -E⁺ binds to DNA, which increases fluorescence 	[36,112,116,137]
			 <p>2-hydroxyethidium (2-OH-E⁺): 480-500/575-595 nm (exc/em)</p>	superoxide	<ul style="list-style-type: none"> separation of 2-OH-E⁺ from E⁺ by HPLC is required to selectively observe superoxide 	
	MitoSOX		 <p>E⁺-TPP⁺: 480-500/575-595 nm (exc/em)</p>	ROS	<ul style="list-style-type: none"> TPP⁺ favors mitochondria accumulation E⁺-TPP⁺ binds to mitochondrial DNA, which increases fluorescence 	[81,82,112]
			 <p>2-OH-E⁺-TPP⁺: fluorescence 480-500/575-595 nm (exc/em)</p>	superoxide	<ul style="list-style-type: none"> 2-OH-E⁺-TPP⁺ has a selective λ_{exc} at 396 nm for superoxide detection detection by fluorescence microscopy, flow cytometry 	
	Dichlorodihydrofluorescein diacetate (DCFH-DA)	 <p>Non-fluorescent</p>	 <p>DCF: 480-500/515-525 nm (exc/em)</p>	ROS	<ul style="list-style-type: none"> high background (photo-oxidation) not specific for superoxide detection by fluorescence microscopy, flow cytometry, microplate reader 	[79,84,85,95,118]
	Lucigenin	 <p>Lucigenin dioxetane</p>	 <p>N-methylacridone</p>	superoxide	<ul style="list-style-type: none"> redox cycling of the probe generating superoxide production leading to superoxide overestimation 	[118]

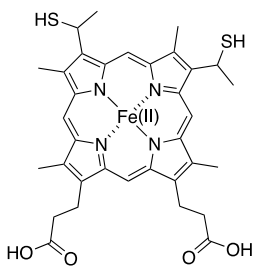
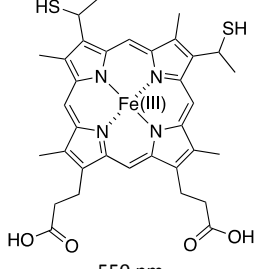
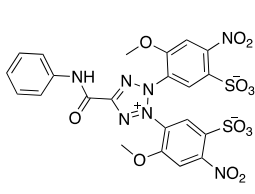
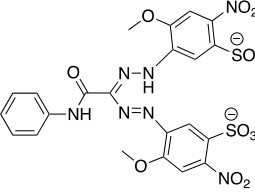
Colorimetric, non-cell permeant probes	Cytochrome <i>c</i>			superoxide	<ul style="list-style-type: none"> • detection of extracellular superoxide only • redox cycling of the probe with Cu leading to false positive results 	[83,113,119,124]
	XTT			perhydroxyl superoxide	<ul style="list-style-type: none"> • only detects extracellular ROS • less selective than cytochrome <i>c</i> • usable with Cu 	[124]

Table 6. List and structures of the fluorescent or colorimetric ROS probes mentioned in the text and applied for the evaluation of SODm anti-ROS activity.

Using this cytochrome assay, Jackson *et al.* showed that MnTE-2-PyP⁵⁺ was efficient to reduce to basal levels the amount of extracellular superoxide released by this macrophage cell model after hypoxic treatment [119]. Similarly, the groups of C. Policar [113] and B. Valtancoli [83] reported the ability of SODm, respectively Mn1 and manganese complexes with polyamine-polycarboxylate ligands, to prevent the increase of superoxide secreted by stimulated macrophages (see section 2.2.4.1). Additionally, the group of C. Policar used the cytochrome *c* assay for the evaluation of a peptidyl copper complex, which revealed a dose-dependent effect on superoxide concentration produced by macrophages [124]. To complete their study, they also performed the XTT assay, even if XTT is less selective for superoxide than cytochrome *c*. They observed a similar promising effect of the peptidyl copper complex that was able to diminish the levels of reduced XTT in supernatant of stimulated macrophages [124].

As emphasized in this section, fluorescence-based systems or redox-sensitive dyes are adapted to monitor the concentration of ROS in real time and have been applied to the assessment of SODm activity. New generations of fluorescent probes, such as dual-activated sensors are currently designed. They aim at exhibiting high sensitivity and selectivity toward

superoxide in the presence of other ROS or strong oxidants found in cells [155,156]. However, they do not overcome the drawback associated to the fact that they are exogenously added: they may alter cell structure and functions and subsequently bias the obtained results. The following sections focus on alternatives techniques for ROS detection that do not require addition of exogenous probes.

3.1.3. Aconitase activity assay

One of the main effects of superoxide in biological environments is its effect on aconitase, an enzyme that catalyzes the isomerization of citrate to isocitrate *via* cis-aconitate in the tricarboxylic acid cycle, also known as the Krebs cycle, which occurs in the matrix of mitochondria. Aconitase is an iron-sulfur 4Fe-4S enzyme, inactivated in a superoxide concentration dependent fashion by the oxidative loss of one iron from the cluster [157]. Hence, aconitase has been described since a long time as a physiological intracellular target of oxidizing conditions that can serve as an indirect superoxide detector via the spectrophotometric monitoring of its inactivation at 240 nm [158–160]. The inactivation of aconitase in presence of a superoxide generator such as xanthine/XO or paraquat validated the use of aconitase as a marker for superoxide generation [132]. Nevertheless, the aconitase is subjected to inactivation by other intracellular oxidants like peroxynitrite [161]. The iron-sulfur cluster actually exposes a local positive charge on one iron, which offers an electrostatic attraction for the anionic oxidants. This iron-sulfur cluster-containing enzyme is thus not selectively inhibited by superoxide but rather constitutes a global marker of oxidative stress. Patel *et al.* demonstrated that the SODm MnTBAP was able to attenuate the aconitase inactivation selectively induced by paraquat in cortical neurons cultures [104]. The group of Day also used the inactivation of aconitase by superoxide to evidence the efficacy of MnTBAP treatment to counteract the stavudine-induced mitochondrial oxidative stress in

HepG2 cells [107]. Furthermore, the pentaazamacrocyclic manganese MitoSOD (M40403 + PPh_3 , Figure 5) was assessed for its potential to protect the mitochondrial activity of isolated heart mitochondria that is remarkably decreased following exposition to paraquat [162]. MitoSOD was designed by conjugating a TPP lipophilic cation to the pyridine ring of M40403 to improve its accumulation in mitochondria and increase dismutation of superoxide within mitochondria. MitoSOD successfully protected aconitase from paraquat-induced superoxide damages.

3.1.4. Electrochemical detection of ROS

The lack of reliable fluorescent probes for the accurate detection of superoxide and the requirement of novel techniques to investigate ROS signaling led to the development of innovative electrochemical approaches. Electrochemical experiments conducted with ultramicroelectrodes were shown to offer a unique possibility of in situ, real-time, and direct measurements of extracellular ROS and RNS produced by a single cell [163]. Briefly, it consists of positioning a platinized carbon-disk microelectrode in close proximity to the plasma membrane of a single cell, such as a macrophage, with a micromanipulator. The electric current is then monitored at a series of constant potentials, chosen based on voltametric studies out of any cellular context (+300 mV, +450 mV, +650 mV, and +850 mV versus sodium-saturated calomel reference electrode). The weight of ROS contribution to each current were determined from these voltammograms. Then, the detected currents at each potential can be written as linear combinations of the responses of H_2O_2 (product from superoxide dismutation by SOD), ONOO^- , NO^\bullet , and NO_2^- (see Figure 15 (A)). Eventually, the integration of the current curves over time associated with the resolution of the system of linear equations and the application of Faraday's law allow the individual quantification of the four electroactive species mentioned above released by the macrophages. Amatore *et*

al. conducted such amperometric analysis on single immuno-stimulated macrophages and succeeded in quantifying the amount of ROS and RNS, that were shown to be generated in higher quantities over the course of the inflammatory response [164]. The recording of ROS and RNS release allows an accurate prediction of their metabolic fate during oxidative stress and, in the particular case of SODm, it is useful to provide further insights on the mimics actions in biological conditions.

To investigate the potential of SODm, the groups of Ivanovic-Burmazovic and Policar performed the protocol reported by Amatore *et al.* and retrieved the amounts of H_2O_2 , ONOO^- , NO^\bullet and NO_2^- released extracellularly by the macrophages [113,127]. Using this technique, the group of Ivanovic-Burmazovic achieved a direct quantification of ROS/RNS production in single immuno-stimulated macrophages that had, or had not, been treated with a manganese(II) pentaazamacrocyclic SODm [127]. Amperometric measurements revealed a significant increase in H_2O_2 extracellular fluxes following SODm treatment, which reflects the SOD-like activity of the mimic (Figure 15B). They also observed a complete loss of the extracellular fluxes of ONOO^- and NO^\bullet and a 4-fold increase in NO_2^- amount in presence of the mimic. These results suggest the ability of the complex to react with NO^\bullet and ONOO^- , in addition to its SOD activity (Figure 15 (B)). Bernard *et al.* similarly evaluated the effect of Mn1 on the ROS and RNS fluxes recorded by amperometry in stimulated macrophages [113]. Incubation of the complex resulted in a reduction of the ONOO^- amount released during the oxidative burst accompanied with a slight increase in H_2O_2 amount compared to control cells (Figure 15 (C)). However, the complex had no effect on NO_2^- and NO^\bullet concentration. Moreover, from the admitted scheme for evolution of ROS in macrophages (Figure 15 (A)), the initial fluxes of superoxide and nitric oxide can be back-calculated and no effect on the initial flux in superoxide was observed, indicating that the

complex was not inhibiting superoxide nor nitric oxide production. The authors concluded on the ability of the complex to accelerate the superoxide dismutation into hydrogen peroxide, without any effect regarding inhibition of the production of superoxide.

As depicted in Figure 15, the dismutation pathway is in competition with the reaction between NO^\bullet and superoxide leading to ONOO^- , which thus explains the decrease in the peroxynitrite amount detected at the electrode. According to the stoichiometry of superoxide dismutation and superoxide–nitric oxide reaction, the overall peroxynitrite decrease should be twice that of H_2O_2 increase. However, they observed a weaker increase of H_2O_2 than what expected. This suggest that the complex displays a weak catalase activity (which fasten H_2O_2 dismutation), that could account for this observation.

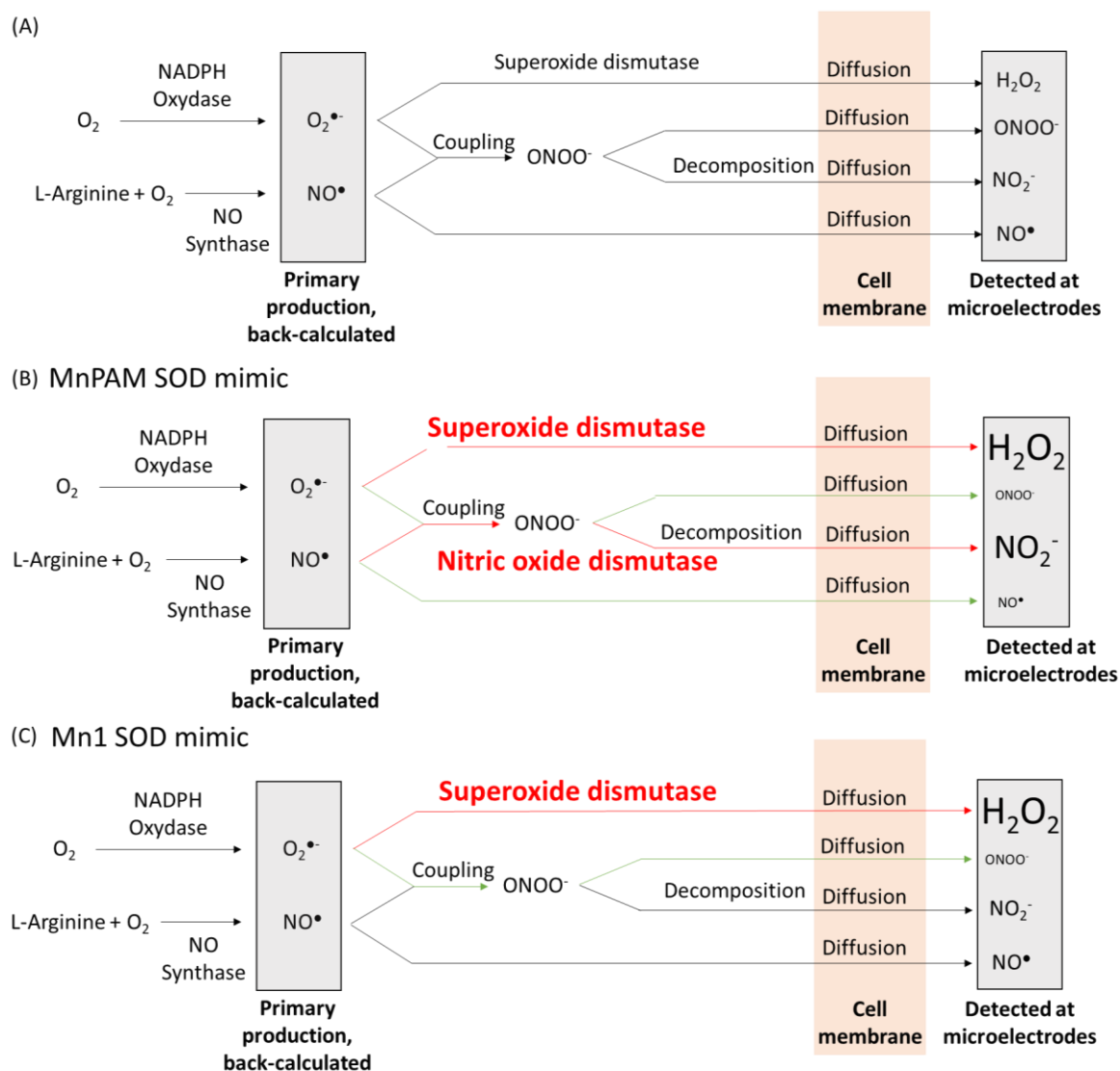


Figure 15. (A) Reaction scheme describing the metabolic fate of ROS and RNS during the oxidative burst of RAW 264.7 macrophages, inspired from the papers of Bernard et al. [113] and Filipovic et al. [127]. (B) Impact of a MnPAM SODm on the generation of ROS by macrophages measured by amperometric analyses, according to a study of Filipovic et al. [127]. (C) Impact of Mn1 labelled SODm on the generation of ROS by macrophages measured by amperometry, according to a study of Bernard et al. [113]. Green arrows correspond to the pathways that are inhibited in presence of the SODm. Red arrows correspond to the pathways that are enhanced in presence of the SODm.

3.2. Evaluation of the protective effects of SODm in cells

This section presents assays performed to evaluate the protective effects of SODm in oxidative stress-injured cells. This includes methods that measure the general health status of the cells (cell morphology, cell growth, cell viability, cell death) to more specific methods that evaluate one precise cellular activity (cell cycle...) or the activity of specific organelles to specify a mechanism of action (see Table 7). It has to be noted that many of the cell viability and cell death assays described below were also used to evaluate the cytotoxicity induced by

the SODm in healthy cellular models. This way, the half maximal inhibitory concentration IC_{50} of SODm can be calculated and an appropriate incubation concentration for SODm treatment can be determined.

3.2.1. Observation of the cell morphology by optical microscopy

Using a phase contrast microscope, an apparatus that is present in most cell culture rooms, the observation of the morphology of cells in culture is a convenient and rapid tool to assess their health status after any treatment. This only requires a good knowledge of the normal characteristics of the cell type tested, particularly in term of cell shape, size, adhesiveness, refringence, etc. In some cases, oxidative stress-injured cells exhibit a different morphology as compared to control cells, such as blebbing [86], and the examination of the cell morphology in presence of SODm may give an indication of the cell recovery. Although this is not a quantitative method, the advantage is that the same cell culture can be looked at and returned back in the incubator many times: it is not a destructive method as compared to all the methods that will be described hereafter. For instance, phase contrast inspections confirmed that the SODm MnTBAP prevents cell death induced by Paraquat stress [132]. In a work from Huang *et al.*, bright field images revealed that neurons incubated in presence of MnTM4PyP showed a morphologically superior integration of synapses, suggesting that the SODm treatment attenuated the apoptosis and necrosis induced by H_2O_2 [85].

Biological samples	Studied cell characteristics	Type of cells	Methods	Advantages/drawbacks for the specific evaluation of SODm	References
Whole cells	cell morphology	animal and human cells	phase contrast microscope observation	<ul style="list-style-type: none"> • rapid, applicable to any SODm 	[85,86,132]
	cell growth	bacteria and yeasts	cell culture optical density (600 nm)	<ul style="list-style-type: none"> • rapid, easy • OD at 600 nm so may interfere with some 	[54–56,63,65,67]

				SODm	
			colony survival assay	<ul style="list-style-type: none"> longer to implement than OD but avoids OD interference with some SODm 	[95]
		animal and human cells	cell counting	<ul style="list-style-type: none"> time consuming, applicable to any SODm 	[86]
			crystal violet staining (595 nm)	<ul style="list-style-type: none"> rapid to implement, OD measurement at 595 nm so may interfere with some permeant SODm 	[75]
Cell viability (metabolic activity)	animal and human cells		reduction of tetrazolium salts into formazans (Table 8)	(see table 8)	[32,79–81,85,95,103,165,166]
			mitochondrial respiration: Alamar Blue assay (Resazurin)	(see table 8)	[84,95,114]
cell death (Necrosis)	animal and human cells		LDH release assay (UV-vis or fluorometric detection)	<ul style="list-style-type: none"> sensitive performed on cell culture supernatants commercially available kits that use different end products, which limits OD interferences with SODm 	[72,104,107,132]
			⁵¹ Cr release assay (γ counter)	<ul style="list-style-type: none"> very sensitive restrictive regulations for the use radioactive compounds 	[89]
			Cell-impermeant nucleic acid stains: Ethidium homodimer-1 (EthD-1) and propidium iodide (similar Exc/Em) (Fluorescence microscope or flow cytometry)	<ul style="list-style-type: none"> stains nucleus of dead cells can be coupled with other markers (e.g., annexin V, calcein AM) 	[79,95,104]
cell death (apoptosis)	animal and human cells		Hoechst 33342 Cell-permeant nuclei acid stain	<ul style="list-style-type: none"> stains nucleus of cells nuclei morphology can be examined by fluorescence microscopy DNA <i>per cell</i> can be quantified by FACS. 	[104]
			DNA fragmentation (agarose electrophoresis and UV illumination)	<ul style="list-style-type: none"> test of the biochemical key feature of apoptosis long to implement. 	[104]
			Annexin V (fluorescence microscope or cell sorter)	<ul style="list-style-type: none"> stains plasma membranes of apoptotic cells. 	[95]
			activated caspase-3 (colorimetric or fluorometric assays. Detection by flow cytometry, fluorescence microscopy, microplate reader, western blot)	<ul style="list-style-type: none"> many commercial kits available based on the measure of several end products Caspase-3 is activated in the execution-phase of cell apoptosis. 	[105,121,167]
cell cycle analysis	animal and human cells		propidium iodide in fixed cells (flow cytometry)	<ul style="list-style-type: none"> allows determination of DNA content in each cell. 	[103]
Specific organelles	mitochondrial morphology	animal and human cells	Mito-Tracker™ dyes (fluorescence microscopy, flow cytometry, microplate reader)	<ul style="list-style-type: none"> dye accumulates in active mitochondria several dyes with various Exc/Em wavelength are available, which limits possible interferences with SODm handle with care. 	[84]
	endoplasmic reticulum (ER) morphology	animal and human cells	ER-Tracker™ dyes	<ul style="list-style-type: none"> Live-cell permeant dye selective for ER several dyes with various Exc/Em wavelength are available, which limits interferences with SODm. 	[84]
	ER integrity, functionality	animal and human cells	Fluo 3-AM (fluorescent dye, detection by fluorescence microscopy, flow cytometry, microplate reader)	<ul style="list-style-type: none"> live-cell-permeant dye fluorescence increases when bound to Ca²⁺ live-cell imaging possible 	[85]
	mitochondria integrity, functionality	animal and human cells	JC-1 (membrane potential dependent accumulation in mitochondria, fluorescence microscopy, flow cytometry)	<ul style="list-style-type: none"> red fluorescent aggregates in healthy mitochondria, turns green (monomers) when low membrane potential live-cell imaging possible 	[84,106]
		animal and human cells	DiOC6 (mitochondrial membrane potential, fluorescence microscopy)	<ul style="list-style-type: none"> selective for mitochondria of living cells at low concentrations at higher concentrations stains all intracellular membranes rapidly toxic for cells 	[81]

		animal and human cells	Lactate (L)/pyruvate (P) ratio (mitochondrial dysfunction, colorimetric assays, microplate reader)	<ul style="list-style-type: none"> • increased L/P ratio upon mitochondrial dysfunction • not specific • commercially available kits 	[107]
		animal and human cells	Oxygen consumption rate (OCR) (mitochondrial respiration, Seahorse analyzer technology)	<ul style="list-style-type: none"> • dedicated commercially available kits • assays based on fluorescence measurement • live cell, real-time analysis. 	[106]

Table 7. Summary of the methods used to assess the protective effect induced by SODm on various cellular features.

The group of Pena used inverted-phase contrast microscopy to investigate the protection afforded by n-propyl gallate (nPG or O1 Figure 6) SODm against H₂O₂-induced membrane blebs in epithelial cells. Counting of blebbed and unblebbed cells every 30 minutes demonstrated a lower exhibition of membrane blebbing in treated cells compared to control cells [86]. These findings were confirmed by time-lapse video microscopy. Moreover, by simply counting the cells in culture every day, it was shown that O1 could prevent H₂O₂-induced growth inhibition. The monitoring of cell growth as a way to evaluate SODm benefits is common and is detailed in the following part.

3.2.2. Assays based on cell growth determination

Historically, the effects of SODm on cell or microbial growth have been largely used as a marker of their efficiency to afford complete or partial protection against oxidative stress, particularly in SOD-deficient biological models (see section 2.1). The bacterial growth curve is commonly determined by turbidimetry, an optical density measurement tool based on the fact that light scattering is directly proportional to the number of microorganisms. The optical density is usually measured at *ca.* 600 nm. The growth rate constitutes a relevant indicator during the exponential phase of growth, representing the phase where microorganisms number increases at a constant maximum rate in opposition to the preceding lag phase, during which microorganisms do not grow as they are not adapted to their new environment yet, and to the following stationary phase, where lack of nutrient or limited space prevent a further growth [49]. Numerous studies conducted by the groups of

Fridovich, Batinic-Haberle and Salvemini reported the use of turbidimetry to evaluate the beneficial effects of various MnPs SODm on the growth rate of SOD-deficient *E. coli* by comparing the growth curves in presence and in absence of MnPs [54–56,63]. In order to minimize the interferences from the absorbance of the tested MnPs, the authors followed the rates of growth turbidimetrically at 700 nm. As others examples, Guijarro *et al.* and Clares *et al.* monitored the growth of SOD-deficient yeasts and bacteria turbidimetrically at 620 nm, and assessed the antioxidant capacity of Mn(II) complexes with polyamines ligands consisting of an aza-pyridinophane macrocyclic core (Sc1-12, Figure 5) by calculating the ratio of the growth rates of the cells incubated with and without the complexes [65,67].

As compared to bacteria and yeasts, growth curves of animal or human cells can also be analyzed by cell counting (manually using a hemocytometer or by using an automated cell counter) but this is rapidly cumbersome. To simplify it, colorimetric assays that report on cell number have been developed. Among them, a novel clonogenic assay based on the detachment of adherent cells undergoing cell death have been proposed and offered a new way to assess the biological activity of SODm. The protocol proceeds in several steps: (i) washing to detach dead cells, (ii) staining of living cells with Crystal violet, a triarylmethane dye that can bind to DNA and proteins and (iii) quantification of bound crystal violet by UV-vis spectrometry at 595 nm. The group of Domann has run this clonogenic assay coupled to a proliferation assay by counting cells daily for 7 days to determine whether the SODm GC4419 could rescue the cell growth and the cell survival in SOD2 knockout cells [75]. They observed both a reduced proliferative potential and reduction in clonogenic activity in SOD-depleted cells compared to wild type cells, that were restored by incubation with this SODm.

3.2.3. Assays based on the evaluation of the overall metabolic activity

The protective effects of SODm on cell viability are usually demonstrated through assays evaluating cell metabolism, and in particular the mitochondrial metabolic activity since mitochondria is the main cellular organelle involved in ROS production. These assays are performed in 96-well microtitration plates (or 384-well plates), the reagents and kits are commercially available, and they can be automatized. The endogenous metabolic activity is known to maintain a reduced environment while this latter becomes oxidized upon cell death. The assays described below rely on this natural reducing power of viable cells and the ability of metabolically active cells to convert redox indicators into colored or fluorescent compounds. Such probes are then efficient to monitor the cellular metabolic activity.

The MTT (3-(4,5-dimethylthiazol-2-yl)-2,5-diphenyl-2H-tetrazolium bromide), XTT (2,3-Bis-(2-Methoxy-4-Nitro-5-Sulfophenyl)-2H-Tetrazolium-5-Carboxanilide), MTS (3-(4,5-dimethylthiazol-2-yl)-5-(3-carboxymethoxyphenyl)-2-(4-sulfophenyl)-2H-tetrazolium) and WST-1 (4-[3-(4-Iodophenyl)-2-(4-nitro-phenyl)-2H-5-tetrazolio]-1,3-benzene sulfonate) assays constitute some of the most commonly used cell viability assays. They are all based on a tetrazolium core and its reduction by NADPH-dependent oxidoreductase enzymes and mitochondrial dehydrogenases contained in viable and respiring cells leads to colored formazan derivatives that can be quantified by classical UV-visible spectroscopy. Due to their negative charge, XTT, MTS and WST-1 compounds cannot penetrate inside cells and must be combined with cell-permeant intermediate electron coupling reagents, which can be reduced in cells and then exit the cell to convert tetrazolium to the soluble formazan product. Table 8 shows the structure of the tetrazolium salts and gives pros and cons of each compound. For each assay, the number of viable metabolically active cells is directly proportional to the amount of formazan produced and thus to the absorbance intensity.

Assay	Probe	Reduced quantified product	Advantages/drawbacks	References
-------	-------	----------------------------	----------------------	------------

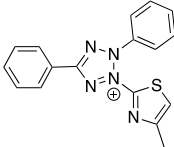
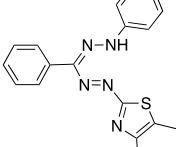
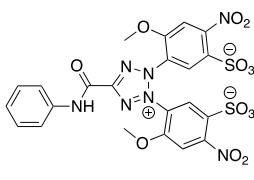
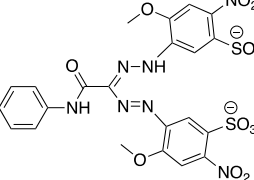
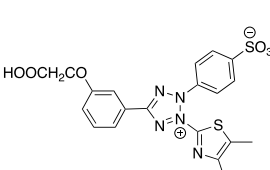
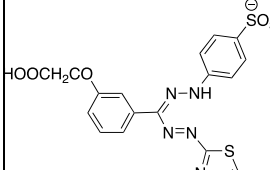
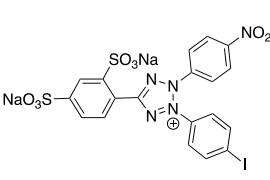
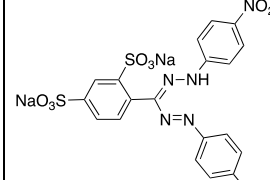
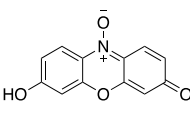
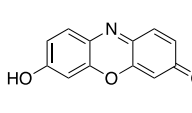
MTT			<ul style="list-style-type: none"> • formation of insoluble formazan crystals, requirement of cell lysis and solubilization of the formazan with a solvent (DMSO) • reading at 570 nm 	[80,81,165]
XTT			<ul style="list-style-type: none"> • formation of soluble formazan. No requirement of cell lysis, kinetic monitoring of the same samples possible • requirement of an electron coupling reagent for efficient reduction (phenazine methosulfate, PMS) • reading at 450 nm 	[32,95]
MTS			<ul style="list-style-type: none"> • one-step MTT assay: addition of the reagent straight to the cells without intermediate steps susceptible to enhance colorimetric interference • reduced MTS form is more soluble and less toxic than XTT formazan. Thus, cells can be returned back to incubator for further evaluation • requirement of an electron coupling reagent for efficient reduction • reading at 490-500 nm 	[85,166]
WST-1			<ul style="list-style-type: none"> • one-step MTT assay • soluble formazan product, no cells lysis required • requirement of an electron coupling reagent for efficient reduction • reading at 460 nm 	[79,103]
Resazurin (Alamar Blue™)			<ul style="list-style-type: none"> • one-step assay • resazurin (blue) is reduced into resorufin, pink and highly fluorescent (λ_{exc} 530-570 nm, λ_{em} 580-590 nm) by metabolically active cells • more sensitive than tetrazolium assays • cytotoxic but less than tetrazolium allowing longer incubations with cells • possibility of fluorescent interference from compounds being tested 	[84,95,114]

Table 8: Comparative analysis of cell viability assays used for SODm evaluation, using tetrazolium salts (MTT, XTT, MTS and WST-1) or Resazurin. All are redox indicators and reducing compounds may interfere with assays. So, various concentrations of SODm should be tested in control wells without cells. Tetrazolium are cytotoxic compounds and must be incubated with cells for relatively short periods of time (1-4 h).

The MTT viability assay proved to be valuable for evaluating the protection against ROS damage on Vero cells [80] and human fetal hepatocyte cell line (L-02) [165] afforded by peptides displaying SOD activity. Similarly, using the MTT assay, Kain *et al.* determined whether an heterocyclic thiosemicarbazone manganese complex could inhibit the ROS-induced cell death by comparing the viability of cells incubated with or without the SODm [81]. The XTT assay was notably used to show the cytoprotective effects of salen-manganese complexes [95,32], MnPs or cyclic-polyamines manganese complexes [95] against oxidative stress-induced cell injury. Based on MTS assay, Huang *et al.* revealed that the treatment of

ROS-injured cells with MnTM4PyP allowed to abrogate cell growth defects in a dose-dependent manner compared to untreated control group [85]. The MTS assay was also used by Jaramillo *et al.* to demonstrate the anti-tumor effect of MnTE-2-PyP⁵⁺ on cancer cells [166]. The authors observed that this MnP was able to enhance the dexamethasone-induced apoptosis of malignant human lymphoid cells (MOLT-4 and Jurkat cells, two human leukemia cell lines). Treatment with dexamethasone resulted in 50% decrease of cell viability, while the combined treatment with this MnP decreased the percentage of viable cells to approximately 25%, suggesting a synergy. Because it is more expensive, WST-1 assay is less commonly used while faster and simpler than classical MTT. It is based on the reduction of WST-1 by the mitochondrial succinate-tetrazolium-reductase system, strongly dependent on the glycolytic production of NADPH in viable cells. One example of application of this assay to the evaluation of SODm activity includes a work of Mou *et al.* demonstrating that a synthetic CuZnSODm N1 in Figure 6 could minimize the damages caused by paraquat stress onto HeLa cells and increased the cell viability accordingly [103]. Moreover, Benhamou group performed WST-1 assays and showed the protective effect of MnTMPyP on INS-1 cells following xanthine/XO challenge or SIN-1 stress, associated to peroxynitrite formation in cells [79]. MnTMPyP was also shown to preserve human pancreatic islet viability upon exposure to SIN-1 by WST-1 assay [79].

Lastly, resazurin based assay, such as Alamar BlueTM, is considered as a more sensitive and less toxic alternative to MTT assay. In this assay, resazurin is reduced into a pink and highly fluorescent compound specifically in respiring mitochondria. This assay is then advantageously suitable with either fluorescence or absorbance reading, and the measured intensity directly reflects the mitochondrial activity in eukaryotic cells [101]. Alamar blue assay revealed that a MnP modified with a mitochondrial signal peptide was able to rescue

immune-stimulated macrophages survival [114]. Likewise, this assay showed that the same MnP protects primary cortical neurons from oxidative stress-induced death as well [84]. Pollard *et al.* similarly observed that the rate of resazurin reduction exhibited by ataxia telangiectasia (AT) cells was significantly diminished and a return to a normal metabolism of resazurin was noticed after AT cell treatment with SODm MnMx-2-PyP-Calbio (a mixture of differently N-methylated MnT-2-PyP⁵⁺ MnPs from Calbiochem) [95]. This showed the ability of the MnPs SODm to improve the mitochondrial respiration rate of AT cells.

Other viability assays quantifying the metabolic activity of cells may be considered for the examination of SODm beneficial effects. They include for instance the commercial “CellTiterGlo” luminescent assay based on the ATP-induced oxygenation of luciferin or the Fluorescein DiAcetate and DiMethylMethylene Blue assays based on the metabolization of the probes by viable cells [168,169].

3.2.4. Assays based on cell death evaluation

Cell injury may lead to cell death, mainly via necrosis or apoptosis. In necrosis, the plasma membrane loses its integrity and the cell content leaks out into the culture medium. The quantification of cell death by necrosis thus relies on the quantification in the extracellular medium of compounds that should normally be found in cells. In contrast, in apoptosis (also called programmed cell death), there is no release of intracellular material into the extracellular space but many specific intracellular events occur and several can now be accurately and easily assessed.

3.2.4.1. Necrosis: assays based on loss of cell membrane integrity

According to many studies, SODm partially abrogate the formation of lesions in plasma membranes following oxidative stress circumstances which are indicative of cell death or

cytotoxicity. The lactate dehydrogenase (LDH) assay provides a quick and simple method to measure this phenomenon. LDH is a cytosolic enzyme that is released into the cell culture supernatant when the cell plasma membrane is disrupted. The lactate dehydrogenase activity of the extracellularly released enzyme is measured using an enzymatic coupling reaction and a colorimetric detection. In several cases, this assay was preferentially employed for the study of SODm efficiency compared to the above-mentioned assays since it is compatible with a quantitative time-course monitoring of cell damages as it only requires the sampling of small volumes of supernatants. The assay is also very sensitive since the end-point measured is an enzyme activity and LDH is present in the cytosol of almost -if not all- cell types. A strong increase of LDH release by neurons was observed after incubation with ROS-generating agents and this could be significantly prevented by treatment with MnTBAP [132]. Such neuronal injury assessed via the LDH assay was also performed in SOD-deficient neurons. Interestingly, the neuronal survival was prolonged in presence of MnTBAP and MnTE-2-PyP⁵⁺ [72]. According to LDH assay, MnTBAP was shown to exhibit markedly increased protective effects against toxicity induced by NRTI-stavudine in HepG2 cells (Figure 16) [107]. A strong LDH release occurred following cell exposure to NRTI-stavudine, that could be partly reduced by concurrent exposure to MnTBAP. The cytoprotective activity of MnTBAP was also assessed with LDH assay in neuronal cells stressed by staurosporine (Figure 16) [104].

In the same paper, Patel *et al.* described the use of the membrane impermeant ethidium homodimer-1 probe (EthD-1) as a necrotic cell marker to quantify the effect of MnTBAP on cell death. EthD-1 specifically fluoresces upon DNA binding and DNA is reachable only in permeable necrotic cells. EthD-1 staining was also used by Moriscot *et al.* to assess viability of INS-1 cells. They simultaneously stained live and dead cells using the membrane-

permeant dye Calcein-AM and EthD-1 respectively [79]. Counting of labelled cells by Fluorescence-Activated Cell Sorted (FACS) analysis then revealed that MnTMPyP addition leads to an increased percentage of viable cells. Similarly to EthD-1, propidium iodide is useful to differentiate necrotic cells from apoptotic and healthy cells, due to its enhanced fluorescence upon DNA binding combined to its inability to cross intact cell membranes [95].

Lastly, Chromium-release assay is a formerly developed technique [170] that has been scarcely used to assess the cytoprotection efficacy of SODm, such as MnTMPyP and MnTBAP. This rare use is probably because it involves ^{51}Cr , a radiolabeled compound, thus requiring specific equipment and must obey restricting regulations. This assay is used to measure the cytotoxicity mediated by natural killer cells and T lymphocytes so called effector cells. Target cells are labelled with ^{51}Cr and then cultured in presence of unlabeled effector cells. The chromium release assay consists of measuring the amount of radioactive chromium released by the target cells as an indicator of cell membrane damages which is correlated with cell necrosis. In the work of Day *et al.*, the injury of cells subjected to glucose/glucose oxidase challenge was evaluated by loading the cells with radioactive chromium and then determining the radioactivity released in the supernatant using a gamma counter [89].

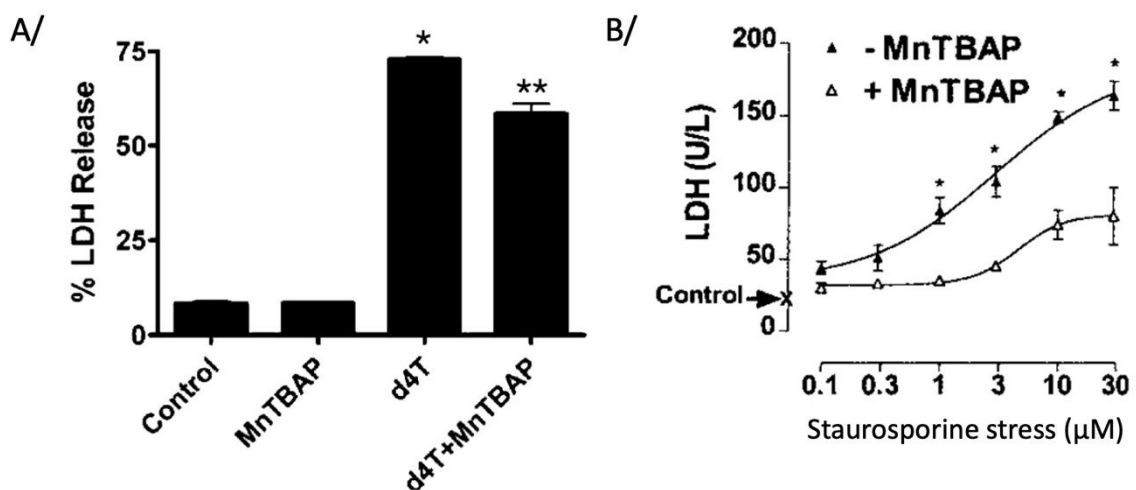


Figure 16. Examples of LDH assay application to the evaluation of SODm efficacy to protect cells membrane from ROS-induced damages. A/ Figure from [107]. Assessment of cytotoxicity of hepatoblasts exposed to stavudine (d4T) and treated with MnTBAP 100 μ M. Y-axis represents the percentage of cellular LDH released by the cells in the extracellular medium. B/ Figure from [104]. Measurement of LDH activity in the supernatant of cortical cultures stressed by various concentrations of staurosporine and treated with MnTBAP.

The decrease of radioactive chromium released by dying cells in the supernatant indicated that MnTBAP and MnTMPyP protected the integrity of the membranes of the endothelial cells against oxidative damages.

3.2.4.2. Assays relying on apoptosis evaluation

Oxidative stress is part of the factors that are known to initiate apoptosis. During apoptosis, characteristic cell changes are observed including cell shrinkage, nuclear fragmentation, chromatin condensation etc. but, at least in the early phases, the cellular membrane remains intact in contrast to necrosis. Some of these characteristics can be simply observed by fluorescence microscopy or flow cytometry via the use of Hoechst 33342 or Annexin V labelling. These methods have been used for the examination of SODm anti-apoptotic activity in oxidative stress cellular models.

A relevant example is described in the literature by Patel, whose objective was to determine the ability of MnTBAP SODm to inhibit neuronal apoptosis induced by chemical agents [104]. For this purpose, they stained cellular DNA with the permeant fluorescent dye, Hoechst 33342, and identified microscopically apoptotic nuclei thanks to their characteristic condensed chromatin (Figure 17). Fluorescently stained apoptotic cells were counted using a digital image analyzer. Alternatively, they detected apoptosis by DNA fragmentation through DNA size-based electrophoresis on agarose gel and staining with ethidium bromide. They observed a marked reduction in apoptotic death in presence of MnTBAP, that inhibits both the morphological (Hoechst) and biochemical features (DNA fragmentation) of apoptosis. The SODm was thus beneficial to protect cultured cortical neuronal cells against apoptosis suggesting the role of oxidative stress in this phenomenon.

Pollard *et al.* reported the capacity of MnTnHex-2-PyP and one manganese cyclic polyamine EUK-134 to reduce the percentage of apoptotic cells after radiations exposure [95]. To quantify the post-radiation apoptosis, they used another method based on cell membrane staining with fluorescein-labelled annexin V followed by cell analysis using flow cytometry. Annexin V binds to phosphatidylserine (PS) which appears on the outer leaflet of the plasma membrane of cells undergoing apoptosis. In healthy cells, PS is restricted to the inner leaflet of the plasma membrane, due to a flippase activity that maintains the plasma membrane asymmetry. To confirm the nature of the cell death, cells were also treated with propidium iodide that only stains necrotic cells. Carballal *et al.* performed similar flow cytometric evaluation of apoptosis and necrosis in SIN-1-exposed cells and reported an increase in PS externalization indicative of cell apoptosis. They evidenced that cell pretreatment with the SODm MnTnBuOE-2-PyP⁵⁺ has partly prevented the apoptotic cell death induced by SIN-1 [106].

Another technique to evaluate the effect of SODm on oxidative stress-mediated apoptosis relies on the monitoring of a consensus pro-apoptotic signal: the activation of caspase-3 protease enzyme [105,121,167]. Caspase-3 activation is known to be an early and central event of the apoptosis process [171]. Caspase activation can be determined using commercial kits based either on the colorimetric detection of the chromophore p-nitroanilide (pDNA) cleaved from caspase-3 when activated, or by immunofluorescence, or by Western Blot with antibodies specific for cleaved caspase-3. This alternative method was successfully applied to the assessment of the neuroprotection afforded by two salen SODm EUK-134 and EUK-189 and by MnTBAP against paraquat-induced neuron apoptotic death [105,167]. Caspase-3 activation was shown to increase following paraquat addition and this cellular response to paraquat was significantly inhibited in presence of the SODm, suggesting

their ability to prevent apoptosis. Likewise, the group of Papaccio demonstrated that the commercial MnP called AEOL10150 could protect mechanically and chemically stressed pancreatic beta islets from apoptosis [121]. Indeed, the caspase-3 activity was restored to normal when the paraquat-stressed cells were incubated with the SODm. These results were consistent with the DNA fragmentation data showing an anti-apoptotic effect of the SODm at the tested concentration (150 μ M).

3.2.5. Assays focused on the analysis of specific organelles known to be altered by oxidative stress

The dysfunction of an intracellular organelle can result in important cellular functions impairments and then in cell death. In particular, oxidative stress is known to disrupt the normal mitochondrial functions, which triggers the mitochondrial pathway of apoptosis [172] and alters the endoplasmic reticulum (ER) function, resulting in the accumulation of misfolded proteins, phenomenon known as ER stress [173]. The following section focuses on the investigations of the capacity of SODm to protect the mitochondrial and ER functions against ROS toxicity.

3.2.5.1. Morphological analysis of cellular organelles

To characterize the mitochondrial and ER protection of SODm, numerous analytical tools have been employed including the examination of mitochondria and ER morphology. Indeed, cells can be incubated with commercial Mito-tracker and ER-tracker fluorescent dyes that specifically accumulate into mitochondria and the ER respectively. The group of Xia visualized these labeled organelles by confocal laser scanning microscopy and noticed the disruption of the tubular network of mitochondria in normal neurons injured by H₂O₂ treatment (Figure 17) [84]. The prior incubation of neurons with MnTMPyP significantly minimized these damages. In the same work, they observed an alteration of the labelled ER

structure upon H₂O₂ treatment, which was restored to an uncompromised morphology with MnTMPyP pretreatment.

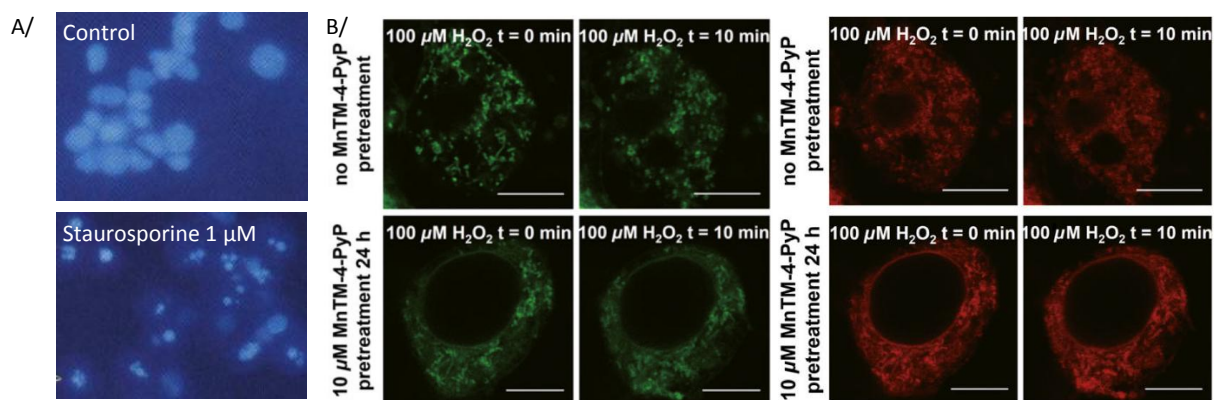


Figure 17. Fluorescence staining of subcellular organelles allowing a morphological analysis of their structure. A/ Figure from [104]. DNA staining of cortical neuronal cells with the fluorescent dye Hoechst 33342. Cells treated with staurosporine display condensed nuclei and apoptotic bodies, characteristics of apoptosis. B/ Figures from [84]. Primary rat cortical neurons staining with Mitotracker dye (left) and endoplasmic reticulum dye (right). Cells treatment with MnTMPyP restores the normal morphology of these organelles that were disrupted following H₂O₂ challenge (100 μM). Scale bars represent 7.5 μm

3.2.5.2. Examination of mitochondrial dysfunctions

The mitochondrial membrane potential ($\Delta\Psi_m$), resulting from the proton gradient generated by the proton pumps, constitutes a critical factor in maintaining the integrity of mitochondria and in subsequently regulating the apoptotic process. Indeed, $\Delta\Psi_m$ is harnessed for the mitochondrial respiratory chain, notably to produce ATP [174]. The monitoring of $\Delta\Psi_m$ can be used to evaluate the efficacy of SODm to prevent the mitochondrial depolarization induced by mitochondrial oxidative stress and which typically occurs at the early stage of apoptosis [172]. A common assay to examine $\Delta\Psi_m$ is based on the use of a lipophilic cationic fluorescent probe JC-1. In physiological conditions, JC-1 forms aggregates that are characterized by an emission peak at 590 nm. However, the loss of membrane potential observed in oxidative stress conditions favors the monomeric form of JC-1, that is characterized by an emission peak at 525 nm [175]. The ratio of fluorescence intensity JC-1 aggregate/monomer can then be inferred to $\Delta\Psi_m$. The group of Xia performed this assay to demonstrate the ability of MnTMPyP to attenuate the loss of $\Delta\Psi_m$ induced by

H₂O₂ in primary rat cortical neurons (Figure 18) [84]. The further investigation of antiapoptotic protein levels suggested that MnTMPyP inhibited the mitochondrial apoptotic pathway initiated by H₂O₂ treatment. The JC-1 assay was also applied by Carballal *et al.* to the evaluation of the MnTnBuOE-2-PyP⁵⁺ capacity for protecting endothelial cells exposed to peroxynitrite-induced nitro-oxidative stress (Figure 18) [106]. The SODm was able to abrogate the increase in the monomeric JC-1 fraction occurring after SIN-1 treatment and so to prevent the disruption of $\Delta\Psi_m$.

The assessment of $\Delta\Psi_m$ changes can also be achieved by cytofluorometry using the fluorescent molecular probe DiOC6. DiOC6 is a cationic fluorescent carbocyanine dye (3,3'-dihexyloxacarbocyanine iodide) that labels mitochondria and displays only low quenching effects that bias microscopic visualization. However, this probe is highly sensitive to changes in the plasma and ER membranes potential, requiring the dissipation of these two other potentials to exclusively measure the mitochondrial membrane potential $\Delta\Psi_m$. Kain *et al.* treated DiOC6-stained cells with a high glucose concentration and observed a decrease in fluorescence intensity, resulting from the hyperglycemia-induced mitochondrial depolarization (Figure 18) [81]. They then demonstrated the cytoprotective action of a Mn complex designed by Vyas *et al.* by combining thiosemicarbazone and aminoethanethiol as respective primary and ancillary ligands [81,82]. The compound preincubation in hyperglycemia-exposed cells restored the loss of $\Delta\Psi_m$ and attenuated the resulting facilitated mitochondrial release of apoptogenic cytochrome *c*. The subcellular localization and quantification of cytochrome *c* was assessed by double-labelling of cells with a mitochondria tracker and an antibody against cytochrome *c*.

Mitochondrial dysfunction is known to involve defective oxidative phosphorylation, which is compensated by the use of glycolysis as an emergency backup for energy [176]. The

oxidation of NADH generated by glycolysis results in abnormal lactate/pyruvate cellular ratio, that reflects the presence of respiratory chain defects [177,178]. In more details, Robinson *et al* reported several cases where in presence of glucose the amount of pyruvate is decreased while the amount of lactate is increased resulting in a lactate/pyruvate ratio raised above the normal range [177,178]. The group of Day treated HepG2 cells with NRTI stavudine, known to elevate mitochondrial superoxide, alone or in combination with MnTBAP SODm [107]. After addition of glucose, they determined lactate and pyruvate concentrations using commercial kits. In absence of MnTBAP, a 1.5-fold increase in lactate to pyruvate ratio occurred which is consistent with stavudine affecting oxidative phosphorylation during mitochondrial protein synthesis. Simultaneous treatment with MnTBAP avoided this effect.

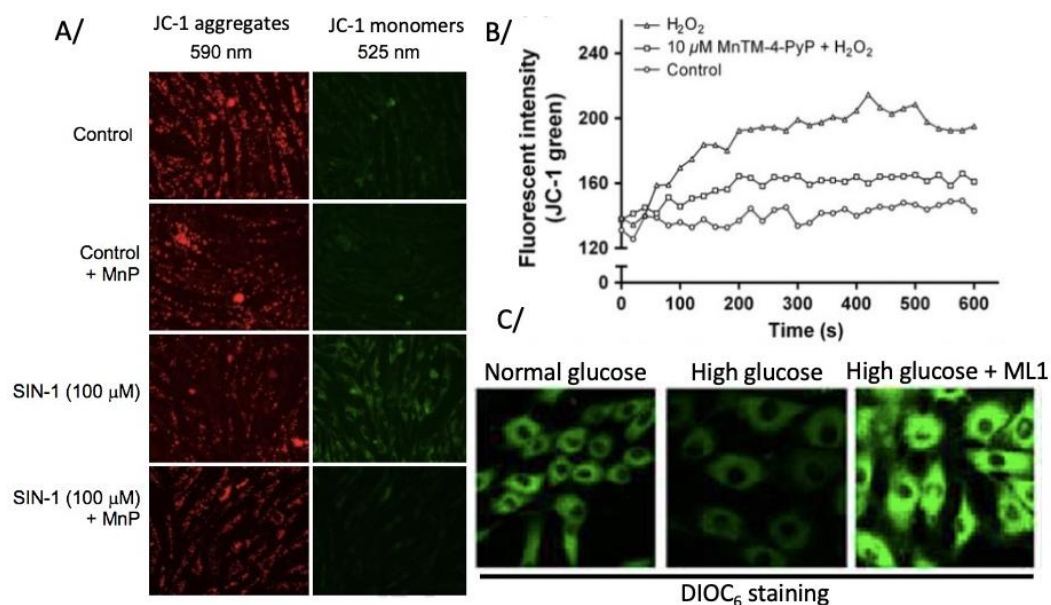


Figure 18. Effect of SODm on the depletion of the mitochondrial membrane potential $\Delta\Psi_m$ resulting from cellular oxidative stress. (A, B) Measurement of $\Delta\Psi_m$ through the use of JC-1 fluorescent dye whose monomer distribution (fluorescent at 590 nm, green) instead of aggregates (fluorescent at 525 nm, red) is indicative of lowered $\Delta\Psi_m$. A/ Figure from [106]. Mn(III)TnBuOE-2-PyP⁵⁺ was able to attenuate the loss in $\Delta\Psi_m$ in bovine aorta endothelial cells exposed to SIN-1. B/ Figure from [84]. MnTMPyP similarly decreased the disaggregation of JC-1 into monomers upon H₂O₂ treatment of primary rat cortical neurons. C/ Figure from [81]. $\Delta\Psi_m$ determination using DiOC₆ probe whose fluorescence intensity is directly proportional to the $\Delta\Psi_m$. The $\Delta\Psi_m$ depletion observed in H9c2 cells subjected to high glucose was rescued by ML1 SODm.

All the above-mentioned mitochondrial dysfunctions result in compromised mitochondrial respiration whose quantification is useful to assess the efficacy of SODm in

preserving healthy mitochondrial function and subsequent respiration. The viability assays presented in section 3.2.3 evaluate efficiently the overall metabolic activity of cells. However, there exists another way to monitor specifically the mitochondrial respiration through the measurement of cellular dioxygen consumption. Recently, the group of Radi determined the dioxygen consumption rates (QO_2) of bovine aortic endothelial cells (BAEC) in real time using an extracellular flux analyzer named Seahorse and designed by Ferrick *et al* [106,179]. They thus provided a representative time course of cell respiration after induction of oxidative stress and in presence or not of a SODm drug. From the measured QO_2 , they calculated several parameters related to mitochondrial function, such as the basal respiration rate, the spare respiratory capacity and the respiratory control ratio (RCR). RCR is especially relevant as it reflects the ability of mitochondria to tightly couple oxygen consumption to oxidative phosphorylation. The RCR was strongly reduced and the other parameters were similarly impaired for cell subjected to peroxynitrite-induced nitro-oxidative stress but were significantly restored when BAEC were pre-incubated with MnTnBuOE-2-PyP⁵⁺, revealing the high protective effect of the MnP on dioxygen consumption profile.

More recently, a new flow cytometry-based method termed SCENITH was developed to functionally profile the cellular energetic metabolism at the single-cell level. SCENITH technology relies on the detection of variations in the expression of multiple proteins involved in different metabolic pathways. The use of SCENITH may be considered to assess the metabolic responses of cells to oxidative stress and SODm treatment [180].

3.2.5.3. Measure of cytosolic calcium fluctuations

The monitoring of calcium influx is informative of ER stress. Indeed, disturbance of Ca²⁺ homeostasis, associated with sustained and excessive influx of cytosolic Ca²⁺ from the

extracellular environment was reported to trigger ER stress and cell apoptosis [181]. Josephson *et al.* demonstrated that ROS can induce cytosolic calcium influx through voltage-gated calcium channels [182].

Huang *et al.* worked on the continuous detection of the changes in cytosolic Ca^{2+} levels in neurons after H_2O_2 treatment using a fluorescence indicator of intracellular calcium, Fluo 3-AM probe. Fluo 3-AM is an ester of Fluo 3 that is easily loaded into cells by incubation. After hydrolysis by intracellular esterases, Fluo 3, which is almost non-fluorescent in its free ligand form, is highly fluorescent when it forms complexes with calcium [85]. The results demonstrated that the addition of MnTMPyP, immediately after the H_2O_2 -induced increase in cellular Ca^{2+} level, leads to the detection of decreased Ca^{2+} concentration in a dose-dependent manner and thus MnTMPyP incubation contributes to the inhibition of early calcium overload state.

To gain further knowledge on the mechanisms of actions of SODm, other organelles would be worthy of studying such as peroxisomes or macrophages extracellular vesicles.

3.3. Indirect effects of SODm on ROS-induced cellular damages

Variations in ROS concentrations are known to induce major changes in the cell physiology. In this way, given their superoxide dismutation activity, the SODm may have significant underlying effects on the cell phenotype. This section aims to review the impacts of SODm treatment on various ROS-induced cell phenotype modifications described in the literature. They include the impacts on the cellular antioxidant defenses, on lipid peroxidation, on DNA damages and on inflammation.

3.3.1. *Effect of SODm on cellular constituents*

3.3.1.1. Effects on abundance and activities of endogenous antioxidant enzymes

Several papers have studied the effects of SODm on the transcription of SOD genes and on the expression and activity of SOD enzymes in cells [82,84].

The effect of SODm on mRNA expression levels of SOD genes is commonly evaluated by Reverse Transcriptase-quantitative Polymerase Chain Reaction (RT-qPCR) on total mRNA extracted from cells using commercial RNA extraction kits [84,183]. This was notably conducted by Homayouni-Tabrizi *et al.* on natural antioxidant peptides extracted from camel milk. The authors showed a strong increase of SOD gene expression levels in HepG2 cells after incubation with these peptides. However, since there is no perfect correlation between mRNA and protein abundance in cells [184], it is important to perform analysis at the protein level as well.

Cu/ZnSOD (SOD1) and MnSOD (SOD2) protein levels are routinely quantified by Western Blot [36,82,84,123]. Contradictory results were reported depending on the tested SODm and the cellular model used (Figure 19). In some cases, the native SOD content was decreased following the generation of certain stress in cells and the presence of SODm reactivated the expression of the enzyme. In other cases, stressed cells displayed native SOD overexpression and the treatment with SODm resulted in contrast to a suppression of the stress-induced overexpression of the native SODs. The SODm was in this case interpreted as an efficient superoxide scavenger, consequently limiting the cellular requirement for SOD enzymes [36,123].

As an example of the first mentioned observation, Cheng *et al.* showed that endogenous SOD2 in primary cortical neurons was decreased following H₂O₂ addition but was maintained at normal levels when incubated with MnP MnTMPyP (Figure 19). The group of Padhye also quantified SOD2 expression in glucose-stressed HEK-293 kidney cells and showed that a SODm made of thiosemicarbazones and bipyridyl/aminoethanethiol ligands enhanced SOD2

expression in mitochondria [82]. Similarly, the group of Papaccio showed that mechanical and chemical stresses were responsible for a decrease of SOD2 content in pancreatic islets. When the commercial SODm AEOL10150 was added to these stressed pancreatic islets, the levels of SOD2 were significantly increased in a dose-dependent manner [121]. Lastly, Kain *et al.* reported the efficiency of a SODm (thiosemicarbazone ligands) to reverse the high glucose-induced decrease in SOD2 expression in H9c2 myoblasts (Figure 19) [81]. In 2017, the group of D. K. St Clair reported the indirect mode of action through which MnTnBuOE-2-PyP⁵⁺ SODm limits the hypoxia-induced SOD2 overexpression in hematopoietic stem/progenitor cells [185]. They evidenced that MnTnBuOE-2-PyP⁵⁺ induces Nrf2 pathway via S-glutathionylation of Keap1 and thus upregulates the enzymes under the control of Nrf2, such as SOD2.

Interestingly, Mathieu *et al.* reported an opposite effect for the SODm named Mn1 [36]. Indeed, they observed that the MnSOD was clearly overexpressed in LPS-stressed HT29-MD2 cells while MnSOD was overexpressed to a weaker extent when LPS was co-incubated with Mn1 (Figure 19). The interpretation of the authors is that Mn1 compensates MnSOD activity, which constitutes an indirect proof that Mn1 possesses a SOD-like activity in cells.

These opposite results on SOD2 expression highlight fundamental differences in the cellular response to the applied stress and most probably to the mode of action of the SODm. However, even when overexpressed, SOD2 may be present in an inactive form, it is thus important to check its activity [186]. After separation of the various SOD according to their molecular weight by native gel electrophoresis, gels are incubated with a superoxide generating system and nitroblue tetrazolium (NBT), that can react with superoxide to form a blue tetrazolium salt [36,187]. A competition then occurs between the SOD and the yellow NBT to react with superoxide leading to a blue species. The presence of achromatic

(clear/yellow) band in the blue gel indicates a SOD activity. This NBT staining method is commonly used to confirm the lack of SOD function in SOD-deleted microorganisms [71,188]. Assays with other tetrazolium salts have been used to investigate the effect of oxidative stress and SODm treatment on SOD activity (WST [84] or INT, commercially available as RanSOD kit [121]).

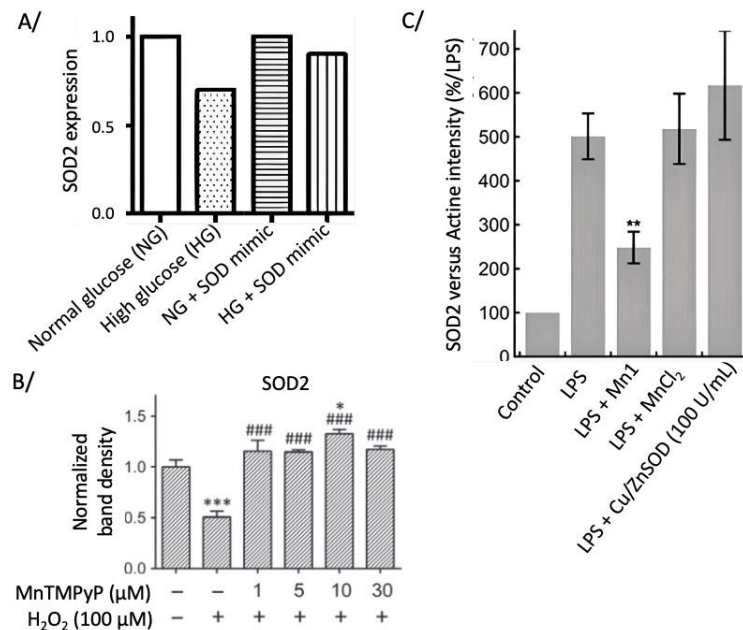


Figure 19. Examination of MnSOD (SOD2) levels by Western blot and quantification of band intensities relative to the unstressed control group. Left: Stress-induced decrease in SOD2 expression. Right: Stress-induced increase in MnSOD expression. (A) Figure from [81]. Basal SOD2 content is conserved for rat cardiac myoblasts exposed to glucose stress but treated with a SODm. (B) Figure from [84]. MnTMPyP is able to reverse the H₂O₂-induced loss in SOD2 levels. (C) Mn1 partially prevents the LPS-induced overexpression of SOD2. Adapted with permission from . Copyright 2017 American Chemical Society.

The activity of a gene promoter is another interesting parameter to measure. The assay relies on the transfection of cells with an expression vector containing the SOD promoter fused with a reporter gene (luciferase). The luciferase activity is measured by luminescence using luciferin as a substrate. This assay was used by Cheng *et al.* to investigate the impact of MnPs on the H₂O₂-induced repression of SOD2 promoter activity. Furthermore, following MnP treatment, they showed that the increased SOD2 activity correlated with a decrease of the SOD2 acetylation level and a concomitant induction of Sirt3. This is entirely consistent with the function of Sirt3, which is a protein lysine deacetylase known to reduce oxidative

stress by deacetylating and activating proteins involved in antioxidation such as SOD2 [190,191]. This result suggests that MnP could exert an indirect antioxidant effect via the induction of Sirt3 expression that regulates SOD2 activity through posttranslational modifications.

To explore the mechanism underlying the antioxidant properties of MnP, the level and activities of other endogenous antioxidant systems were investigated, in particular the catalase enzyme and various redox responsive transcription factors involved in antioxidant response [86,188]. While the expression of catalase was not affected by MnPs treatment in the study conducted by Cheng *et al.* [84], the group of Soltani reported an increase in mRNA levels of catalase in H₂O₂-stressed cells exposed to antioxidant peptides compared to untreated cells [183]. The measurement of glutathione levels in its reduced (GSH) and oxidized (GSSG) states was also used to assess the antioxidant effects of SODm [86,192], the ratio of GSSG to GSH, being a common indicator of oxidative stress [193].

3.3.1.2. Effects on lipid peroxidation

Excess ROS have been shown to result in various oxidative-related damages and notably in cell membranes lipid peroxidation. The three-steps mechanism of lipid peroxidation has been clearly reviewed and illustrated by Ayala *et. al* (Figure 20) [194].

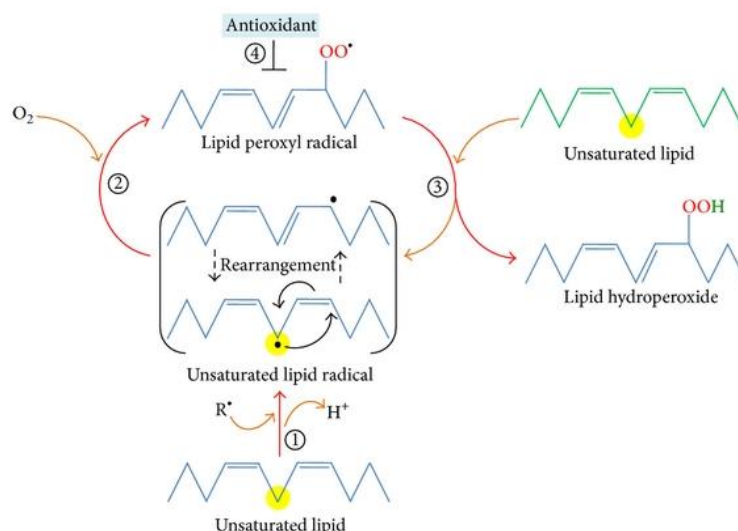


Figure 20. Illustration of the lipid peroxidation process from [194]. Initiation: a prooxidant abstracts the allylic hydrogen to form an unsaturated lipid radical step (1). The carbon radical undergoes stabilizing molecular rearrangement to form a conjugated diene. Propagation phase: the lipid radical rapidly reacts with oxygen to form a lipid peroxy radical (step 2) which then abstracts the allylic hydrogen from another lipid molecule generating a new lipid radical and lipid hydroperoxide (step 3). Termination reaction: antioxidants donate a hydrogen atom to the lipid peroxy radical resulting in the formation of nonradical products (step 4).

Since 1999, the MnPs were described as potent inhibitors of lipid peroxidation by Day *et al.* related to their ability to act as electron acceptor [195]. However, the implication of MnPs in lipid peroxidation proved to be more complex. Indeed, A. Bloodsworth specified that the MnP MnTE-2-PyP⁵⁺ initiates lipid oxidation in the absence of biological reductants by cycling between the +III and +IV redox states. On the contrary, in presence of biological reductants such as ascorbate or GSH, MnTE-2-PyP⁵⁺ can reach the +II redox state and cycles between +II and +III redox states. If lipid oxidation can occur when Mn(II)TE-2-PyP⁵⁺ is oxidized into Mn(III)TE-2-PyP⁵⁺, initiation of lipid peroxidation is readily terminated when Mn(III)TE-2-PyP⁵⁺ is reduced into Mn(II)TE-2-PyP⁵⁺ [196]. In these conditions, Fe mediated-lipid oxidation is inhibited.

Lipid peroxidation by ROS results in the production of various byproducts such as malondialdehyde (MDA), which is considered as a reliable biochemical marker for oxidative-related lipid peroxidation. MDA is easily quantified by a colorimetric assay, the thiobarbituric acid reactive substances (TBARS) assay. For example, the TBARS assay revealed an increase

of MDA levels in cells subjected to heat or oxidative shock [197], in the brain of rats treated with paraquat [198], and in animal tissues injured by tetrachloride intoxication [199]. Although the TBARS assay is widely used for assessing lipid peroxidation, the rate of MDA formation can be very slow and thus requires long incubation periods [200]. In the literature, several papers examined the ability of SODm to protect cells from lipid peroxidation induced by oxidative stress. In 2009, the group of B. Valtancoli conducted TBARS assay and reported the ability of SODm with cyclic polyamine-polycarboxylate ligands to inhibit the superoxide-induced increase in MDA observed in rat aorta smooth muscle cells treated with xanthine/xanthine oxidase [83]. Similar results were obtained in N-formyl-Met-Leu-Phe peptide-challenged RAW264.7 cells. Likewise, Lieb *et al.* tested the effect of amphiphilic pentaazamacrocyclic (PAC1-5, Figure 5) MnSODm on lipid peroxidation induced by paraquat via its superoxide generation in Raji cells [112]. The MDA level was shown to drop to a basal level or even below when cells were incubated with the PAM-based mimics. Interestingly, the efficiency of the tested mimics to counteract the induced lipid peroxidation was well correlated with their ability to decrease superoxide levels, measured using the fluorescent dye hydroethidine. It was also correlated with their lipophilicity and thus with their ability to accumulate in lipid-rich regions. TBARS assay was also useful to evidence the ability of a nitroxide radicals SODm to lower the lipid peroxidation occurring in ram spermatozoa during the cooling process for cryopreservation [201]. Efficiency of SODm against lipid peroxidation caused by chronological aging was also investigated by Ribeiro *et al.* [68]. They observed that three metal-based SODm were able to reduce the levels of lipid peroxidation to half of the levels observed in non-treated aged cells. This result may explain their anti-aging property and their ability to extend yeast life span. Moreover, the authors studied the effect of the

mimics on protein carbonylation, which rises along chronological aging, and noted a great reduction of carbonylation in treated aged cells.

3.3.1.3. Effect on ROS-induced DNA damages

Oxidative stress is responsible for DNA damages that can result in mutations when they are not repaired by cellular mechanisms [202]. This section focuses on the effect of SODm on nuclear DNA fragmentation, including double-strand breaks and single-strand breaks, as well as on mitochondrial DNA (mtDNA) damage.

The TUNEL (terminal deoxynucleotidyl transferase dUTP nick end labeling) assay is a widely used method to detect double-stranded DNA fragmentation in individual cells. Such breaks occur during apoptosis and the assay is based on the end-labelling of the 3-OH termini of DNA double-strand breaks with a marker such as dUTP tagged with a fluorochrome by the terminal deoxynucleotidyl transferase (TdT). Peng *et al.* calculated the percentage of rat dopaminergic neuronal cells displaying TUNEL staining following cell treatment with paraquat (Figure 21) [105]. Data demonstrated that pretreatment with two salen manganese SODm EUK-134 and EUK-189 significantly attenuated the paraquat-mediated DNA fragmentation. Another method to monitor double-stranded DNA fragmentation relies on the detection of the phosphorylation of the Ser-139 residue of the histone variant γ -H2AX. Indeed, this phosphorylation event is known to occur during the early cellular response to double strand DNA breaks induction [203]. This assay was notably used to detect DNA damage in irradiated ataxia telangiectasia lymphoblastoid cells and MnTnHex-2-PyP was significantly able to reduce the intensity of the labelling following irradiation (Figure 21) [95]. To support these results, the authors also used the neutral comet assay as another assessment of DNA damage. This assay consists in electrophoresis of the DNA of single cells embedded on agarose-coated slides and lysed, followed by staining with

a fluorescent DNA binding dye. The fragmented DNA (the comet “tail”) can be visualized under the microscope as it migrates out of the nucleoid body (the comet “head”) in which remains the unfragmented DNA (Figure 21).

The measurement of DNA single-strand breaks is also informative in the context of SODm evaluation as they constitute one of the hallmark of H₂O₂-induced damages [204]. DNA with single-strand breaks are historically measured using the alkaline elution technique of Kohn *et al.* based on the specific flow of DNA with single-strand breaks through a filter while undamaged DNA remains retained [205]. This assay allowed to demonstrate the protection of lens epithelial cells exposed to H₂O₂ by n-propyl gallate, that is able to curtail DNA single-strand breaks in cells [86].

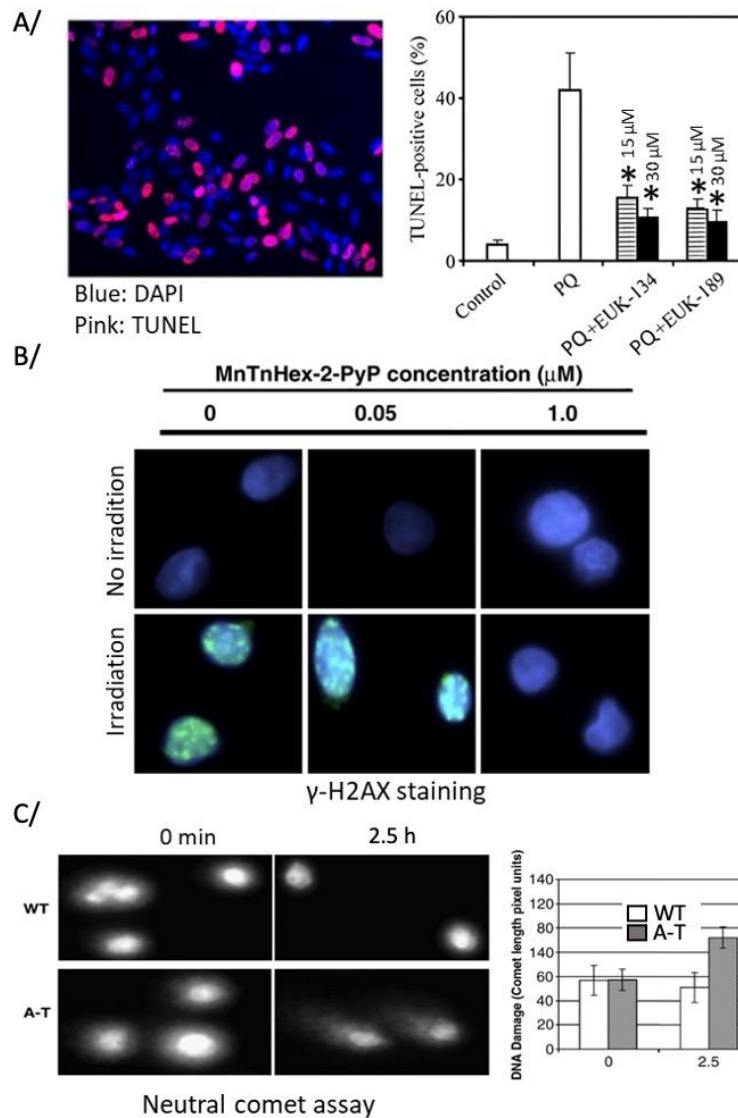


Figure 21. Illustration of the various techniques available to assess DNA double-strand breaks and used for the evaluation of the SODm effects on DNA damages. (A) Figure from [105]. TUNEL staining of paraquat (PQ)-stressed dopaminergic cells. Treatment with EUK-134 and EUK-189 SODm results in a decreased number of TUNEL-positive cells and thus to reduced double-stranded DNA fragmentation. Pink: TUNEL staining, blue: DAPI staining (nuclei). (B) Figure from [95]. γ -H2AX staining of lymphoblastoid cells. A decrease in fluorescence indicative of limited Ser-139 residue phosphorylation when incubated with MnTnHex-2-PyP at 1 μ M evidences the occurrence of less DNA fragmentation events. (C) Figure from [95]. Neutral comet assay: DNA staining with a fluorescent dye and measurement of the comet tail. The length of the tail is directly correlated to the presence of fragmented nuclei DNA.

Oxidative damage to mtDNA is known to be more frequent and persistent than that of nucleus DNA. This is due to (i) the lack of protection provided by histones, (ii) the lack of mtDNA repairing enzymes, and (iii) to mtDNA exposure to a high steady-state level of ROS in the matrix of mitochondria [206]. Milano *et al.* investigated the use of MnTBAP to reduce the effects of H₂O₂ exposure on mtDNA amplification efficiency in mouse lung fibroblasts (MLFs) [207]. They performed direct PCR on whole cells to detect mtDNA and noticed a

decline in the amount of amplified mtDNA in H₂O₂-subjected MLFs. The amplification efficiency could be rescued and returned to control values by pre-treatment with MnTBAP. The same group examined the capacity of MnTBAP to counteract the decrease in mtDNA amplification and the correlative increase in mitochondrial oxidative stress induced by stavudine (d4T), a nucleoside reverse transcriptase inhibitor [107]. The authors used HepG2 cells as a cellular model because of their high abundance of mitochondria. They conducted a standard DNA polymerase-gamma assay based on the use of polymerase-gamma (pol-g), the sole polymerase for mitochondrial DNA replication. Stavudine was shown to alter mtDNA replication via its incorporation into mtDNA, which blocks DNA pol-g and then the subsequent chain elongation. Direct PCR results showed a dose-dependent effect of MnTBAP on reversing the stavudine-induced loss of mtDNA amplification efficiency. Moreover, the authors carried out mtDNA isolation and analysis for 8-hydroxy-2-deoxyguanosine (8OH2dG), one of the major products of DNA oxidation. 8OH2dG abundance was increased in cells treated with stavudine and this 8OH2dG accumulation was diminished by MnTBAP co-treatment.

In brief, the three preceding sections provided an overview of the SODm ability to protect cells from ROS by preventing damages to antioxidant proteins, lipids or DNA. When not resolved, these cumulative injuries can ultimately result in cell death. The impact of SODm on the expression and/or activity of many proteins involved in various physiological processes was investigated by immunoblotting, immunofluorescence and activity measurement. Some examples were mentioned but an exhaustive survey is beyond the scope of this review. To go further, one should consider investigating the effect of SODm on the oxidative damages caused to proteins. Such data would be very informative to decipher their mechanisms of action.

3.3.2. Effect of SODm in a pathological context: focus on inflammation

Oxidative stress has been tightly associated with inflammatory response in various chronic inflammation diseases [208]. It was firstly considered as a consequence of the inflammation, since this latter triggers a high generation of ROS by activated phagocytic immune cells such as polymorphonuclear neutrophils and macrophages [209]. Moreover, some inflammatory pathways, such as the nuclear factor-kappa B (NF- κ B) pathway, are known to control the expression of oxidant and antioxidant enzymes. However, ROS may also contribute to the initiation and the perpetuation of the inflammation. Important pro-inflammatory roles for ROS include endothelial cell damages, increased microvascular permeability [210] and recruitment of the neutrophils at inflammation sites [211]. They were also shown to alter the activation of the nuclear factor NF- κ B pathway [212].

This interweaving between inflammation and oxidative stress suggests that SODm may indirectly impact the progress of the inflammatory cascade by reducing oxidative stress. Several papers focused on the effects of SODm on the activation of inflammatory pathways, such as NF- κ B and mitogen-activated protein kinase (MAPK) pathways, on the release of pro-inflammatory cytokines and on the inflammation-mediated up-regulation of inducible nitric oxide synthase (iNOS) and apoptosis signaling proteins.

3.3.2.1. Inhibition of NF κ B and MAPK activation and signaling by SODm

Given the role of ROS in mediating signaling events in the NF- κ B and MAPK pathways, SODm may be able, through removal of superoxide, to modulate these redox-dependent pathways that initiate the innate pro-inflammatory immune response. The following section provide an overview of SODm effects on NF- κ B transactivation and DNA binding activity as well as on the different MAPK family members activation.

In 2004, the group of J.D. Piganelli published a rich mechanistic analysis of the immunomodulatory effects of two MnPs named AEOL 10113 and AEOL 10150 in LPS-stimulated macrophages isolated from mouse bone marrow [213]. These MnPs were shown to prevent the initiation of the innate immune response as evidenced by the suppression of proinflammatory cytokines secretion. The authors aimed to elucidate the involved mechanism of these inhibitory effects. First, they demonstrated that the MnPs do not act through the impairment of the MAPK pathway. Indeed, according to immunoblotting using phospho-specific antibodies against the phosphorylated forms of p38-MAPK, ERK1/2, and JNK1/2, these three major components of MAPK pathway were phosphorylated and thus activated upon LPS stimulation. However, the phosphorylation kinetics were similar, irrespective of the presence or absence of MnPs. The authors then suspected the MnPs to operate through the blockade of LPS-induced I κ B phosphorylation and degradation, and p65 nuclear translocation. However, immunoblotting of cytoplasmic and nuclear extracts with antibodies against phospho-I κ B, I κ B and p65-revealed that the levels of phosphorylated and degraded I κ B or translocated p65 were not modified by the MnPs. Eventually, they demonstrated that pre-treatment with the two MnPs were efficient to inhibit NF- κ B DNA binding activity by an electrophoretic mobility shift assay (EMSA). They evidenced both the increase in NF- κ B-specific DNA binding 15 minutes after LPS addition as well as the ability of the MnPs to prevent this LPS-induced effect. In addition, they showed that p50 and p65 subunits of NF- κ B were involved in the DNA binding after LPS stimulation. The p50 DNA binding activity was shown to be prevented by the MnPs via a reversible oxidation mechanism since the addition of the reducing agent dithiothreitol was able to restore it. Surprisingly, although the MnPs were primarily used for their antioxidant activity, they

actually suppress the innate proinflammatory immune response via their ability to oxidize the redox-sensitive transcription factor p50 to prevent its DNA binding ability.

One year later, the group of D. Salvemini conducted a similar molecular analysis of signal transduction pathways to characterize the mechanism of action of the SODm M40403 in modulating LPS-induced cytokine production in alveolar macrophages [116]. Removal of superoxide by M40403 was shown to suppress the LPS-induced TNF- α and IL-6 secretion which was associated to the inhibition of upstream redox-sensitive signaling event involving the transcription factor NF- κ B. More precisely, EMSA analysis showed a maximal induction of NF- κ B DNA binding 1h after LPS stimulation which was clearly reduced upon treatment with M40403. They also observed, consistently with the results of J.D. Piganelli, that NF- κ B binding activity mainly involved the p50/p65 heterodimeric form. Interestingly, M40403 significantly counteracted the LPS-induced increase of the p65 subunit in the nuclear extracts according to western blot data. The authors then sought to establish if this SODm effect on DNA-binding activity of NF- κ B and p65 nuclear translocation was related to the inhibition of upstream activation of NF- κ B. Western Blot analysis evidenced only a modest decrease in cytoplasmic I κ B degradation in macrophages treated with M40403 at early time points (a few hours) after their exposition to LPS. In conclusion, M40403-related blockade of cytokines production was shown to be mediated by the decrease of redox-sensitive NF- κ B transactivation. The effect of M40403 was further evaluated and revealed that the mimic was additionally able to attenuate the induced phosphorylation of redox-sensitive p38-MAPK [214]. Another example of SODm effect on inflammatory pathways were described more recently by Y. Fang *et al.* They demonstrated the ability of a new synthetic Cu/Zn SODm to decrease the phosphorylation of p38-MAPK induced by oxidative stress in HeLa

cells treated with Paraquat [103]. These results further highlight the importance in the cell cycle of p38-MAPK activation that plays the role of pathway checkpoint.

NF- κ B and MAPK pathways activation are known to be also a downstream event of EGFR signaling and abnormalities of EGFR signaling were notably observed in various inflammatory and malignant diseases. Since a long time, ROS are known to be important contributors of EGFR activation, particularly UV-induced ROS. In this way, SODm are good candidates to modulate UV-induced and ROS-mediated EGFR activation. In MnSOD knockdown HaCaT human keratinocytes subjected to UV exposition, an increased EGFR activation was observed, as determined by phosphorylation occurring at Tyr1068 [74]. Interestingly, UV-induced phosphorylation of EGFR Tyr1068 was abrogated by treatment with MnTnBuOE-2-PyP⁵⁺. The authors sought to determine whether observed EGFR activation could be related to an increase of EGF content, known to activate EGFR. However, according to ELISA, EGFR activation occurs independently of EGF secretion as no EGF was detected post-irradiation in MnSOD deficient cells.

Another cellular model of inflammation derived from oxidative stress was used to evaluate the anti-inflammatory activity of the SODm MnP MnTM-2-PyP⁵⁺: chondrocytes isolated from mouse articular cartilage exposed to an oxidative burst generated by Fe(II) and ascorbic acid [215]. The ensuing excessive production of ROS was shown to induce the degradation of hyaluronan (HA), a major component of the cartilage extracellular matrix [216]. The resulting HA oligosaccharides are able to activate, among others, the toll-like receptors TLR-4 and TLR-2 and in turn to stimulate the inflammatory NF- κ B response [217]. Interestingly, MnTM-2-PyP⁵⁺, probably by its antioxidant activity, was able to prevent HA degradation and to reverse the HA fragments-induced elevation in mRNA expression and in the related protein synthesis of TLR-4 and TLR-2. Moreover, the authors evaluated the NF- κ B

p50/65 DNA binding activity in nuclear and cytosolic extracts of Fe(II) and ascorbic acid treated chondrocytes. They observed a marked increase in the heterodimer translocation and in the activation of the NF- κ B pathway. Again, a significant reduction of NF- κ B activation was obtained by the treatment of stressed chondrocytes with MnTMPyP⁵⁺ after exposure to oxidants. Lastly, the combined treatment of chondrocytes with MnTMPyP⁵⁺ and a specific HA-blocking peptide yielded to a greater reduction of all the described inflammatory parameters up-regulated by the oxidant stimulation.

Based on the concept that removal of superoxide anion alters the course of NF- κ B and MAPK inflammatory cascade, SODm were assessed for their ability to modulate the downstream transcriptional up- or down-regulation of the various targets mentioned. The effects of SODm on the inhibition of pro-inflammatory cytokines, oxidant enzyme iNOS and FAS apoptosis signaling protein production are reviewed in the following section.

3.3.2.2. Impact on inflammation-related up-regulation of pro-inflammatory cytokines, iNOS and FAS

As detailed in the previous section, the inflammatory response is characterized by the release of various cytokines. The cytokine production is known to be notably mediated at the level of gene expression by the redox-sensitive transcription factors: NF- κ B [218,219] and MAPK [220,221]. The effect of SODm on the release of pro-inflammatory cytokines in cellular models of inflammation were widely investigated.

Since the early 2000s, the cyclic polyamines SODm M40401 and M40403 were assessed for their ability to inhibit the superoxide-regulated release of pro-inflammatory cytokines in animal models of acute and chronic inflammation [222,223]. M40401 and M40403 were notably efficient to mitigate the release of TNF α and IL-1 β respectively in plasma of rats after splanchnic artery occlusion and reperfusion [179], and in pleural exudates of rats with

carrageenan-induced pleurisy [223]. The protective effect observed *in vivo* in these rat models of inflammation may be due at least in part to a decrease in pro-inflammatory cytokines production.

Few years later, the influence and role of SODm on the production of various pro-inflammatory cytokines were evaluated on different cellular models of inflammation [36,66,116,119,122–124]. For that purpose, macrophages are of particular interest as they are key cellular components of the inflammatory process and are widely used for anti-inflammatory drug-screening studies. For instance, the modulation of cytokine production by M40403 treatment was studied in cultured rat alveolar macrophages stimulated with LPS [116]. LPS activation was shown to induce increased TNF α and IL-6 production and increased superoxide production. However, the involvement of ROS generation on subsequent cytokine biosynthesis remains unelucidated. Interestingly, M40403 was found to potently suppress TNF α and IL-6 production and secretion in cell supernatants of LPS-stimulated alveolar macrophages. Shortly after, Jackson *et al.* observed that the production of the cytokines TGF- β and VEGF by hypoxia-stimulated alveolar macrophages was significantly reduced when incubated with MnTE-2-PyP⁵⁺ [119]. The authors proposed that the chronic oxidative stress resulting from hypoxia contributes to increased macrophage cytokine production which can be minimized through the use of SODm. More recently, SOD-active manganese complexes made of tail-tied aza-scorpion ligands were similarly able to hamper the accumulation of TNF- α and IL-6 proinflammatory cytokines in LPS-activated THP-1 human macrophages [66]. Other examples were reported by the group of C. Polcar [36,122–124]. The authors incubated HT29-MD2 cells, previously described in section 2.2.4, with, on the one hand, Mn-complexes bio-inspired from the MnSOD active site and conjugated or not with cell or mitochondria-penetrating peptides, and, on the other hand, a peptidyl copper

complex. They described that the SODm elicit the inhibition of interleukin-8 (IL-8) secretion following HT29-MD2 activation by LPS. The unconjugated manganese complex, when co-incubated with LPS, was also able to limit the LPS-induced increase in cyclooxygenase 2 (COX-2) level, another inflammatory marker. The monitoring of pro-inflammatory cytokines production in cellular models of inflammation constitutes a good way to evaluate the anti-inflammatory effects of SODm.

The ROS-elicited cellular signaling events implicating MAPKs (ERK, p38 and JNK) and the nuclear factor NF- κ B signal transducers result in addition in the activated transcription of inducible nitric oxide synthetase (iNOS) and First Apoptosis Signal (FAS). iNOS is an isoform of NOS enzymes, which catalyzes the production of the reactive species nitric oxide as an immune defense mechanism. FAS ligand belongs to the tumor necrosis factor family and trigger apoptosis when bound to its FAS receptor. iNOS and FAS up-regulation may be susceptible to inhibition by SODm. The MnP AEOL10150 was able to exert protective effects toward mechanically stressed islets β -cells by blocking the transcription of iNOS and FAS [121]. Indeed, real-time PCR data showed that iNOS and FAS mRNA transcripts were clearly expressed in mechanically stressed islets but were suppressed when AEOL10150 was added at a concentration above 54 μ M. The iNOS enzymatic activity can be determined directly by measuring the conversion of [3 H]-L-arginine to [3 H]-L- citrulline in the cell or tissue homogenates. This technique was notably used by D. Salvemini *et al.* in pleural macrophages and lung cells isolated from rats subjected to carrageenan-induced pleurisy [223]. However, the authors did not notice any impact of M40403 SODm on iNOS activity. Lastly, MnTM-2-PyP $^{5+}$ reversed the up-regulation of inflammatory cytokines TNF- α , IL-1 β and other inflammatory mediators such as iNOS and matrix metalloprotease 13 (MMP-13) in chondrocytes stimulated with Fe(II) plus ascorbate (Figure 22) [215]. This effect could be

associated to the ability of the SODm to abrogate the hyaluronan degradation, that we have mentioned above.

To conclude this section, SODm exert beneficial effects in cellular models of ROS-related inflammation. They reduced inflammation by regulating the NF- κ B and MAPK signaling pathways through the dismutation of superoxide, involved in exacerbating the inflammatory response. They may prove valuable as pharmaceutical drug candidates for controlling inflammatory-mediated diseases.

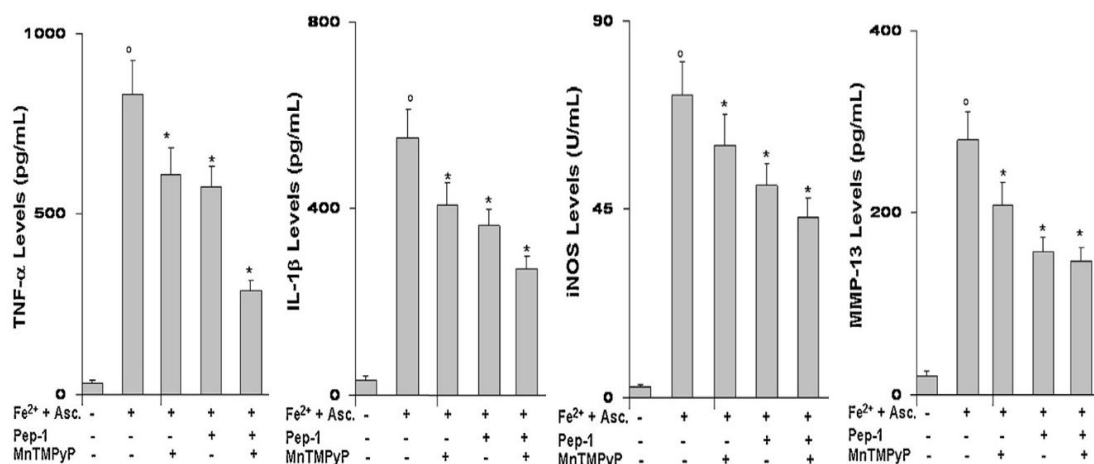


Figure 22. Examples of SODm effects on the expression of inflammatory markers: pro-inflammatory cytokines and oxidant enzyme iNOS. Figure from [215]. The increase in TNF- α , IL-1 β , iNOS and MMP13 protein levels measured in mouse chondrocytes following Fe²⁺ plus ascorbate oxidative stimulation is partially inhibited by Pep-1 and MnTMPyP SODm. Their co-treatment offers synergic effect.

3.3.3. Opening remarks: SODm use in cancer and diabetes

Otherwise, SODm were largely investigated as a therapeutic alternative for cancer therapy. Very interestingly, in this context, their therapeutic action does not result from their anti-superoxide activity. In contrast, their anti-cancer activity was shown to be due to their pro-oxidant activity related to the fast kinetics of superoxide dismutation resulting in an overproduction of H₂O₂. SODm may push the level of H₂O₂ above the threshold of toxicity in cancer cells. Indeed, the level of oxidative stress in cancer cells is higher than in normal cells [224]. So, a strong boost, even transiently, of H₂O₂ induced by SODm can lead to oxidative-stress mediated toxicity. In addition, cancer cells are more sensitive to H₂O₂

because their considerable proliferative property requires a lot of energy and consequently fragilize them [225]. Many anticancer drugs such as oxaliplatin act in this way by increasing intracellular hydrogen peroxide levels and taking advantage of the increased vulnerability of cancer cells toward H_2O_2 [94,226]. A number of studies evidenced the ability of SODm, mostly Mn porphyrins, to act as chemo/radiosensitizers of tumor cells, but as chemo/radioprotectors of normal tissue in preclinic disease models. We will not go further on the use of SODm as anticancer drugs which is beyond the scope of this review. However, interested readers may refer to the book chapter “Redox Therapeutics in Breast Cancer: Role of SODm” published by A Fernandes *et. al* in 2016 as well as the book chapter “Mn Porphyrin-Based Redox-Active Drugs: Differential Effects as Cancer Therapeutics and Protectors of Normal Tissue Against Oxidative Injury” published by I. Batinic-Haberle *et. al* in 2018 [227,228]. They both give an in-depth overview of SODm application in therapeutic purposes as anti- cancer agents.

At last, mitochondrial superoxide has been described for a while as a key contributor to the pathophysiology of diabetes complications such as cardiomyopathy [229,230]. Moreover, streptozotocin-induced diabetes were shown to be associated to a decrease of pancreatic islet endogenous SOD levels. SODm then naturally appear as potent therapeutics to counter the mitochondrial oxidative stress in diabetic cases. In the section 2.2.4, we discussed a cellular model of oxidative stress resulting from high glucose challenge. Some SODm were shown to protect cells from the oxidative damages induced by a high glucose concentration in the cell culture medium [81,128]. Furthermore, SODm were assessed for their ability to restore healthy insulin secretion rates by pancreatic islet cultures exposed to static glucose challenge, mechanical stress or IL-1 β chemical stress [120,121]. Again, we will not go more into detail as this topic is beyond the scope of this review.

4. Conclusion

SODm belong to the emerging family of the catalytic drugs. Because their mode of action relies on catalysis, each molecule of SODm present in cells is able to dismutate several molecules of superoxide. Indeed, this opens up very interesting perspectives since this may allow decreasing the administrated doses and thus may limit toxicity and detrimental side effects.

Efficient SODm described up today are metal complexes, thus involving metal coordination bounds. Such metal complexes are prone to ligand or metal exchanges, in particular in biological environments that are rich in Lewis bases and different metal ions. Such exchanges can lead to the inactivation of the complexes, thus decreasing the concentration of the active principle. In order to use SODm in cells or in living organisms, a particular attention must be paid to design complexes with high thermodynamic stability as well as high kinetic inertness to limit the above-mentioned exchanges [123].

Owing to their very interesting catalytic properties, SODm have been widely used in many different contexts where oxidative stress plays a central role. However, in many cases, it is very tedious to directly correlate the bioactivity measured with the specific catalytic properties of the SODm.

First, this is because no commercially available probe allows to detect superoxide selectively in real time in living cells. As mentioned earlier, HPLC separation of the oxidized products resulting from the reaction of the probe with superoxide is required for reliable quantification. Alternatively, superoxide concentration can be back calculated from the electrochemical detection of others ROS, but it is indeed an indirect method that requires a

non-routine set-up. Efforts to develop direct assays measuring superoxide concentration inside cells must be pursued.

Finally, since superoxide concentration is low in normal cells, its detection requires to increase its concentration and thus to induce an oxidative stress. In this review, we have given an overview of cellular models of oxidative stress that have been used to study SODm for a therapeutic perspective. The tables 1 to 5 summarize these cellular models with drawbacks and advantages for each of them that guide the choice of the model. One of the simplest cellular models allowing to generate the production of a high amount of ROS are macrophages. Interestingly, using these immune cells, ROS are continuously produced in cells or in the extracellular medium, consequently, SODm activity can be easily monitored after penetration or outside cells.

When bioactivities result from intracellular effects of the investigated SODm, the SODm bioactivities measured are composite. They are due to the intrinsic catalytic activity of the mimics and to their ability to enter cells and reach their target without being destroyed. Mitochondria are often targeted since ROS are mainly produced in these organelles. In order to ensure that intact complexes are present in cells or even in mitochondria, specific imaging and/or analytic techniques enabling the detection of the metal and the ligand are required. Among them ionic mobility coupled to mass spectrometry has been particularly efficient to detect and quantify labile manganese complexes such as Mn1 [231].

Acknowledgments

GS thanks the “Interface pour le vivant” doctoral program from Sorbonne Université for PhD fellowship.

Funding sources

This work was supported by Agence Nationale de la Recherche: ANR-15-CE07-0027 project MAGIC; ANR-16-CE07-0025 Project Metallopezyme; ANR 20-CE07-0039-01 project CATMAN; ANR-21-CE18-0053 project MOBIDIC; IFCPAR/CEFIPRA (Indo-French center for the Promotion of Advanced Research project)

References

- [1] C. Policar, Mimicking SOD, Why and How: Bio-Inspired Manganese Complexes as SOD Mimic, in: Redox-Active Therapeutics, Springer, 2016: pp. 125–164.
- [2] A.V. Snezhkina, A.V. Kudryavtseva, O.L. Kardymon, M.V. Savvateeva, N.V. Melnikova, G.S. Krasnov, A.A. Dmitriev, ROS Generation and Antioxidant Defense Systems in Normal and Malignant Cells, *Oxidative Medicine and Cellular Longevity* 2019 (2019) 1–17. <https://doi.org/10.1155/2019/6175804>.
- [3] M.D. Brand, The sites and topology of mitochondrial superoxide production, *Experimental Gerontology* 45 (2010) 466–472. <https://doi.org/10.1016/j.exger.2010.01.003>.
- [4] J.D. Lambeth, NOX enzymes and the biology of reactive oxygen, *Nat Rev Immunol* 4 (2004) 181–189. <https://doi.org/10.1038/nri1312>.
- [5] M.P. Murphy, How mitochondria produce reactive oxygen species, *Biochemical Journal* 417 (2009) 1–13. <https://doi.org/10.1042/BJ20081386>.
- [6] F. Magnani, A. Mattevi, Structure and mechanisms of ROS generation by NADPH oxidases, *Current Opinion in Structural Biology* 59 (2019) 91–97. <https://doi.org/10.1016/j.sbi.2019.03.001>.
- [7] J.P. Kehrer, The Haber–Weiss reaction and mechanisms of toxicity, *Toxicology* 149 (2000) 43–50. [https://doi.org/10.1016/S0300-483X\(00\)00231-6](https://doi.org/10.1016/S0300-483X(00)00231-6).
- [8] C.P. Rubio, J.J. Cerón, Spectrophotometric assays for evaluation of Reactive Oxygen Species (ROS) in serum: general concepts and applications in dogs and humans, *BMC Vet Res* 17 (2021) 226. <https://doi.org/10.1186/s12917-021-02924-8>.
- [9] J. Cadet, T. Delatour, T. Douki, D. Gasparutto, J.-P. Pouget, J.-L. Ravanat, S. Sauvaigo, Hydroxyl radicals and DNA base damage, *Mutation Research/Fundamental and Molecular Mechanisms of Mutagenesis* 424 (1999) 9–21. [https://doi.org/10.1016/S0027-5107\(99\)00004-4](https://doi.org/10.1016/S0027-5107(99)00004-4).
- [10] I. Fridovich, Superoxide Anion Radical (O_2^-), Superoxide Dismutases, and Related Matters, *Journal of Biological Chemistry* 272 (1997) 18515–18517. <https://doi.org/10.1074/jbc.272.30.18515>.
- [11] E. Birben, U.M. Sahiner, C. Sackesen, S. Erzurum, O. Kalayci, Oxidative Stress and Antioxidant Defense, *World Allergy Organization Journal* 5 (2012) 9–19. <https://doi.org/10.1097/WOX.0b013e3182439613>.
- [12] C.E. Cross, Oxygen Radicals and Human Disease, *Ann Intern Med* 107 (1987) 526. <https://doi.org/10.7326/0003-4819-107-4-526>.
- [13] T. Finkel, Signal transduction by reactive oxygen species, *Journal of Cell Biology* 194 (2011) 7–15. <https://doi.org/10.1083/jcb.201102095>.
- [14] A. Panday, M.K. Sahoo, D. Osorio, S. Batra, NADPH oxidases: an overview from structure to innate immunity-associated pathologies, *Cell Mol Immunol* 12 (2015) 5–23. <https://doi.org/10.1038/cmi.2014.89>.
- [15] C.C. Winterbourn, Reconciling the chemistry and biology of reactive oxygen species, *Nat Chem Biol* 4 (2008) 278–286. <https://doi.org/10.1038/nchembio.85>.

- [16] C. Espinosa-Diez, V. Miguel, D. Mennerich, T. Kietzmann, P. Sánchez-Pérez, S. Cadenas, S. Lamas, Antioxidant responses and cellular adjustments to oxidative stress, *Redox Biology* 6 (2015) 183–197. <https://doi.org/10.1016/j.redox.2015.07.008>.
- [17] M. Valko, D. Leibfritz, J. Moncol, M.T.D. Cronin, M. Mazur, J. Telser, Free radicals and antioxidants in normal physiological functions and human disease, *The International Journal of Biochemistry & Cell Biology* 39 (2007) 44–84. <https://doi.org/10.1016/j.biocel.2006.07.001>.
- [18] A. Meister, Glutathione metabolism and its selective modification., *Journal of Biological Chemistry* 263 (1988) 17205–17208. [https://doi.org/10.1016/S0021-9258\(19\)77815-6](https://doi.org/10.1016/S0021-9258(19)77815-6).
- [19] V. Nivière, M. Fontecave, Discovery of superoxide reductase: an historical perspective, *J Biol Inorg Chem* 9 (2004) 119–123. <https://doi.org/10.1007/s00775-003-0519-7>.
- [20] Y. Sheng, I.A. Abreu, D.E. Cabelli, M.J. Maroney, A.-F. Miller, M. Teixeira, J.S. Valentine, Superoxide Dismutases and Superoxide Reductases, *Chem. Rev.* 114 (2014) 3854–3918. <https://doi.org/10.1021/cr4005296>.
- [21] I.A. Abreu, D.E. Cabelli, Superoxide dismutases—a review of the metal-associated mechanistic variations, *Biochimica et Biophysica Acta (BBA) - Proteins and Proteomics* 1804 (2010) 263–274. <https://doi.org/10.1016/j.bbapap.2009.11.005>.
- [22] W.H. Koppenol, D.M. Stanbury, P.L. Bounds, Electrode potentials of partially reduced oxygen species, from dioxygen to water, *Free Radical Biology and Medicine* 49 (2010) 317–322. <https://doi.org/10.1016/j.freeradbiomed.2010.04.011>.
- [23] J.A. Imlay, I. Fridovich, Assay of metabolic superoxide production in *Escherichia coli*., *Journal of Biological Chemistry* 266 (1991) 6957–6965. [https://doi.org/10.1016/S0021-9258\(20\)89596-9](https://doi.org/10.1016/S0021-9258(20)89596-9).
- [24] P.R. Gardner, I. Raineri, L.B. Epstein, C.W. White, Superoxide Radical and Iron Modulate Aconitase Activity in Mammalian Cells, *Journal of Biological Chemistry* 270 (1995) 13399–13405. <https://doi.org/10.1074/jbc.270.22.13399>.
- [25] I. Batinic-Haberle, A. Tovmasyan, E.R.H. Roberts, Z. Vujaskovic, K.W. Leong, I. Spasojevic, SOD Therapeutics: Latest Insights into Their Structure-Activity Relationships and Impact on the Cellular Redox-Based Signaling Pathways, *Antioxidants & Redox Signaling* 20 (2014) 2372–2415. <https://doi.org/10.1089/ars.2012.5147>.
- [26] D. Salvemini, C. Muscoli, D.P. Riley, S. Cuzzocrea, Superoxide Dismutase Mimetics, *Pulmonary Pharmacology & Therapeutics* 15 (2002) 439–447. <https://doi.org/10.1006/pupt.2002.0374>.
- [27] O. Iranzo, Manganese complexes displaying superoxide dismutase activity: A balance between different factors, *Bioorganic Chemistry* 39 (2011) 73–87. <https://doi.org/10.1016/j.bioorg.2011.02.001>.
- [28] S. Miriyala, I. Spasojevic, A. Tovmasyan, D. Salvemini, Z. Vujaskovic, D. St. Clair, I. Batinic-Haberle, Manganese superoxide dismutase, MnSOD and its mimics, *Biochimica et Biophysica Acta (BBA) - Molecular Basis of Disease* 1822 (2012) 794–814. <https://doi.org/10.1016/j.bbadis.2011.12.002>.
- [29] C. Policar, J. Bouvet, H.C. Bertrand, N. Delsuc, SOD mimics: From the tool box of the chemists to cellular studies, *Curr. Opin. Chem. Biol.* 67 (2022) 102109. <https://doi.org/10.1016/j.cbpa.2021.102109>.
- [30] S. Signorella, C. Palopoli, G. Ledesma, Rationally designed mimics of antioxidant manganese enzymes: Role of structural features in the quest for catalysts with catalase and superoxide dismutase activity, *Coordination Chemistry Reviews* 365 (2018) 75–102. <https://doi.org/10.1016/j.ccr.2018.03.005>.
- [31] D. Salvemini, Z.-Q. Wang, J.L. Zweier, A. Samouilov, H. Macarthur, T.P. Misko, M.G. Currie, S.

Cuzzocrea, J.A. Sikorski, D.P. Riley, A Nonpeptidyl Mimic of Superoxide Dismutase with Therapeutic Activity in Rats, *Science* 286 (1999) 304–306. <https://doi.org/10.1126/science.286.5438.304>.

[32] S.R. Doctrow, K. Huffman, C.B. Marcus, G. Tocco, E. Malfroy, C.A. Adinolfi, H. Kruk, K. Baker, N. Lazarowych, J. Mascarenhas, B. Malfroy, Salen–Manganese Complexes as Catalytic Scavengers of Hydrogen Peroxide and Cytoprotective Agents: Structure–Activity Relationship Studies, *Journal of Medicinal Chemistry* 45 (2002) 4549–4558. <https://doi.org/10.1021/jm020207y>.

[33] H. Sheng, J.J. Enghild, R. Bowler, M. Patel, I. Batinić-Haberle, C.L. Calvi, B.J. Day, R.D. Pearlstein, J.D. Crapo, D.S. Warner, Effects of metalloporphyrin catalytic antioxidants in experimental brain ischemia, *Free Radical Biology and Medicine* 33 (2002) 947–961. [https://doi.org/10.1016/S0891-5849\(02\)00979-6](https://doi.org/10.1016/S0891-5849(02)00979-6).

[34] T. Celic, J. Španjol, M. Bobinac, A. Tovmasyan, I. Vukelic, J.S. Reboucas, I. Batinic-Haberle, D. Bobinac, Mn porphyrin-based SOD mimic, MnTnHex-2-PyP⁵⁺, and non-SOD mimic, MnTBAP³⁻, suppressed rat spinal cord ischemia/reperfusion injury *via* NF- κ B pathways, *Free Radical Research* 48 (2014) 1426–1442. <https://doi.org/10.3109/10715762.2014.960865>.

[35] S. Cuzzocrea, E. Mazzon, L. Dugo, A.P. Caputi, D.P. Riley, D. Salvemini, Protective effects of M40403, a superoxide dismutase mimetic, in a rodent model of colitis, *European Journal of Pharmacology* 432 (2001) 79–89. [https://doi.org/10.1016/S0014-2999\(01\)01427-3](https://doi.org/10.1016/S0014-2999(01)01427-3).

[36] E. Mathieu, A.-S. Bernard, N. Delsuc, E. Quévrain, G. Gazzah, B. Lai, F. Chain, P. Langella, M. Bachelet, J. Masliah, P. Seksik, C. Policar, A Cell-Penetrant Manganese Superoxide Dismutase (MnSOD) Mimic Is Able To Complement MnSOD and Exerts an Antiinflammatory Effect on Cellular and Animal Models of Inflammatory Bowel Diseases, *Inorg. Chem.* 56 (2017) 2545–2555. <https://doi.org/10.1021/acs.inorgchem.6b02695>.

[37] B. Gauter-Fleckenstein, K. Fleckenstein, K. Owzar, C. Jian, I. Batinic-Haberle, Z. Vujaskovic, Comparison of two Mn porphyrin-based mimics of superoxide dismutase (SOD) in pulmonary radioprotection, *Free Radic Biol Med* 44 (2008) 982–989. <https://doi.org/10.1016/j.freeradbiomed.2007.10.058>.

[38] B. Gauter-Fleckenstein, K. Fleckenstein, K. Owzar, C. Jiang, J.S. Rebouças, I. Batinic-Haberle, Z. Vujaskovic, Early and late administration of MnTE-2-PyP⁵⁺ in mitigation and treatment of radiation-induced lung damage, *Free Radical Biology and Medicine* 48 (2010) 1034–1043. <https://doi.org/10.1016/j.freeradbiomed.2010.01.020>.

[39] S.R. Doctrow, A. Lopez, A.M. Schock, N.E. Duncan, M.M. Jourdan, E.B. Olsz, J.E. Moulder, B.L. Fish, M. Mäder, J. Lazar, Z. Lazarova, A Synthetic Superoxide Dismutase/Catalase Mimetic EUK-207 Mitigates Radiation Dermatitis and Promotes Wound Healing in Irradiated Rat Skin, *Journal of Investigative Dermatology* 133 (2013) 1088–1096. <https://doi.org/10.1038/jid.2012.410>.

[40] I. Batinic-Haberle, L.T. Benov, An SOD mimic protects NADP⁺-dependent isocitrate dehydrogenase against oxidative inactivation, *Free Radical Research* 42 (2008) 618–624. <https://doi.org/10.1080/10715760802209639>.

[41] Y. Rong, S.R. Doctrow, G. Tocco, M. Baudry, EUK-134, a synthetic superoxide dismutase and catalase mimetic, prevents oxidative stress and attenuates kainate-induced neuropathology, *PNAS* 96 (1999) 9897–9902. <https://doi.org/10.1073/pnas.96.17.9897>.

[42] S. Miriyala, I. Spasojevic, A. Tovmasyan, D. Salvemini, Z. Vujaskovic, D. St. Clair, I. Batinic-Haberle, Manganese superoxide dismutase, MnSOD and its mimics, *Biochim. Biophys. Acta Mol. Basis Dis.* 1822 (2012) 794–814. <https://doi.org/10.1016/j.bbadis.2011.12.002>.

[43] A. Haber, Z. Gross, Catalytic antioxidant therapy by metallodrugs: lessons from metallocorrols, *Chem. Commun.* 51 (2015) 5812–5827. <https://doi.org/10.1039/C4CC08715A>.

[44] C. Muscoli, S. Cuzzocrea, D.P. Riley, J.L. Zweier, C. Thiemermann, Z.-Q. Wang, D. Salvemini,

On the selectivity of superoxide dismutase mimetics and its importance in pharmacological studies, *British Journal of Pharmacology* 140 (2003) 445–460. <https://doi.org/10.1038/sj.bjp.0705430>.

[45] J. Alexandre, C. Nicco, C. Chéreau, A. Laurent, B. Weill, F. Goldwasser, F. Batteux, Improvement of the Therapeutic Index of Anticancer Drugs by the Superoxide Dismutase Mimic Mangafodipir, *J Natl Cancer Inst* 98 (2006) 236–244. <https://doi.org/10.1093/jnci/djj049>.

[46] M.C. McDonald, R. d’Emmanuele di Villa Bianca, N.S. Wayman, A. Pinto, M.A. Sharpe, S. Cuzzocrea, P.K. Chatterjee, C. Thiemermann, A superoxide dismutase mimetic with catalase activity (EUK-8) reduces the organ injury in endotoxic shock, *European Journal of Pharmacology* 466 (2003) 181–189. [https://doi.org/10.1016/S0014-2999\(03\)01538-3](https://doi.org/10.1016/S0014-2999(03)01538-3).

[47] E. Masini, D. Bani, A. Vannacci, S. Pierpaoli, P.F. Mannaioni, S.A.A. Comhair, W. Xu, C. Muscoli, S.C. Erzurum, D. Salvemini, Reduction of antigen-induced respiratory abnormalities and airway inflammation in sensitized guinea pigs by a superoxide dismutase mimetic, *Free Radical Biology and Medicine* 39 (2005) 520–531. <https://doi.org/10.1016/j.freeradbiomed.2005.04.006>.

[48] D. Tsiapalis, D.I. Zeugolis, It is time to crowd your cell culture media – Physicochemical considerations with biological consequences, *Biomaterials* 275 (2021) 120943. <https://doi.org/10.1016/j.biomaterials.2021.120943>.

[49] A. Tovmasyan, J.S. Reboucas, L. Benov, Simple Biological Systems for Assessing the Activity of Superoxide Dismutase Mimics, *Antioxidants & Redox Signaling* 20 (2014) 2416–2436. <https://doi.org/10.1089/ars.2013.5576>.

[50] H. Nikaido, Preventing drug access to targets: cell surface permeability barriers and active efflux in bacteria, *Seminars in Cell & Developmental Biology* 12 (2001) 215–223. <https://doi.org/10.1006/scdb.2000.0247>.

[51] D. Benedetto Tiz, D. Kikelj, N. Zidar, Overcoming problems of poor drug penetration into bacteria: challenges and strategies for medicinal chemists, *Expert Opinion on Drug Discovery* 13 (2018) 497–507. <https://doi.org/10.1080/17460441.2018.1455660>.

[52] M. Fasnacht, N. Polacek, Oxidative Stress in Bacteria and the Central Dogma of Molecular Biology, *Front. Mol. Biosci.* 8 (2021) 671037. <https://doi.org/10.3389/fmolb.2021.671037>.

[53] L. Benov, N.M. Kredich, I. Fridovich, The Mechanism of the Auxotrophy for Sulfur-containing Amino Acids Imposed upon *Escherichia coli* by Superoxide, *J. Biol. Chem.* 271 (1996) 21037–21040. <https://doi.org/10.1074/jbc.271.35.21037>.

[54] I. Batinić-Haberle, S. Cuzzocrea, J.S. Rebouças, G. Ferrer-Sueta, E. Mazzon, R. Di Paola, R. Radi, I. Spasojević, L. Benov, D. Salvemini, Pure MnTBAP selectively scavenges peroxyxynitrite over superoxide: Comparison of pure and commercial MnTBAP samples to MnTE-2-PyP in two models of oxidative stress injury, an SOD-specific *Escherichia coli* model and carrageenan-induced pleurisy, *Free Radical Biology and Medicine* 46 (2009) 192–201. <https://doi.org/10.1016/j.freeradbiomed.2008.09.042>.

[55] I. Kos, L. Benov, I. Spasojević, J.S. Rebouças, I. Batinić-Haberle, High Lipophilicity of meta Mn(III) *N*-Alkylpyridylporphyrin-Based Superoxide Dismutase Mimics Compensates for Their Lower Antioxidant Potency and Makes Them as Effective as Ortho Analogues in Protecting Superoxide Dismutase-Deficient *Escherichia coli*, *J. Med. Chem.* 52 (2009) 7868–7872. <https://doi.org/10.1021/jm900576g>.

[56] I. Batinić-Haberle, I. Spasojević, P. Hambright, L. Benov, A.L. Crumbliss, I. Fridovich, Relationship among Redox Potentials, Proton Dissociation Constants of Pyrrolic Nitrogens, and in Vivo and in Vitro Superoxide Dismutating Activities of Manganese(III) and Iron(III) Water-Soluble Porphyrins, *Inorg. Chem.* 38 (1999) 4011–4022. <https://doi.org/10.1021/ic990118k>.

[57] A. Okado-Matsumoto, I. Batinić-Haberle, I. Fridovich, Complementation of SOD-deficient

Escherichia coli by manganese porphyrin mimics of superoxide dismutase activity, *Free Radical Biology and Medicine* 37 (2004) 401–410. <https://doi.org/10.1016/j.freeradbiomed.2004.04.040>.

[58] W. Munroe, C. Kingsley, A. Durazo, E. Butler Gralla, J.A. Imlay, C. Srinivasan, J. Selverstone Valentine, Only one of a wide assortment of manganese-containing SOD mimicking compounds rescues the slow aerobic growth phenotypes of both *Escherichia coli* and *Saccharomyces cerevisiae* strains lacking superoxide dismutase enzymes, *Journal of Inorganic Biochemistry* 101 (2007) 1875–1882. <https://doi.org/10.1016/j.jinorgbio.2007.07.008>.

[59] A. Carlioz, D. Touati, Isolation of superoxide dismutase mutants in *Escherichia coli*: is superoxide dismutase necessary for aerobic life? *The EMBO Journal* 5 (1986) 623–630. <https://doi.org/10.1002/j.1460-2075.1986.tb04256.x>.

[60] E.B. Gralla, J.S. Valentine, Null mutants of *Saccharomyces cerevisiae* Cu,Zn superoxide dismutase: characterization and spontaneous mutation rates., *Journal of Bacteriology* 173 (1991) 5918–5920. <https://doi.org/10.1128/JB.173.18.5918-5920.1991>.

[61] V.D. Longo, E.B. Gralla, J.S. Valentine, Superoxide Dismutase Activity Is Essential for Stationary Phase Survival in *Saccharomyces cerevisiae*: MITOCHONDRIAL PRODUCTION OF TOXIC OXYGEN SPECIES *IN VIVO*, *J. Biol. Chem.* 271 (1996) 12275–12280. <https://doi.org/10.1074/jbc.271.21.12275>.

[62] E.C. CHANGt, D.J. Kosman, O₂-Dependent Methionine Auxotrophy in Cu,Zn Superoxide Dismutase-Deficient Mutants of *Saccharomyces cerevisiae*, *J. BACTERIOL.* 172 (1990) 6.

[63] K.M. Faulkner, S.I. Liochev, I. Fridovich, Stable Mn(II) Porphyrins Mimic Superoxide Dismutase *In Vitro* and Substitute for It *In Vivo*, *The Journal of Biological Chemistry* 269 (1994) 23471–23476.

[64] L. Benov, I. Fridovich, Why Superoxide Imposes an Aromatic Amino Acid Auxotrophy on *Escherichia coli*: the transketolase connection, *J. Biol. Chem.* 274 (1999) 4202–4206. <https://doi.org/10.1074/jbc.274.7.4202>.

[65] M.P. Clares, C. Serena, S. Blasco, A. Nebot, L. del Castillo, C. Soriano, A. Domènech, A.V. Sánchez-Sánchez, L. Soler-Calero, J.L. Mullor, A. García-España, E. García-España, Mn(II) complexes of scorpiand-like ligands. A model for the MnSOD active centre with high *in vitro* and *in vivo* activity, *Journal of Inorganic Biochemistry* 143 (2015) 1–8. <https://doi.org/10.1016/j.jinorgbio.2014.11.001>.

[66] J. González-García, À. Martínez-Camarena, B. Verdejo, M.P. Clares, C. Soriano, E. García-España, H.R. Jiménez, A. Doménech-Carbó, R. Tejero, E. Calvo, L. Briansó-Llort, C. Serena, S. Trefler, A. Garcia-España, Oxidative stress protection by manganese complexes of tail-tied aza-scorpiand ligands, *Journal of Inorganic Biochemistry* 163 (2016) 230–239. <https://doi.org/10.1016/j.jinorgbio.2016.04.020>.

[67] L. Guijarro, M. Inclán, J. Pitarch-Jarque, A. Doménech-Carbó, J.U. Chicote, S. Trefler, E. García-España, A. García-España, B. Verdejo, Homo- and Heterobinuclear Cu²⁺ and Zn²⁺ Complexes of Ditopic Aza Scorpiand Ligands as Superoxide Dismutase Mimics, *Inorg. Chem.* 56 (2017) 13748–13758. <https://doi.org/10.1021/acs.inorgchem.7b01756>.

[68] T. de P. Ribeiro, F.L. Fonseca, M.D.C. de Carvalho, R.M. da C. Godinho, F.P. de Almeida, T.D. Saint’Pierre, N.A. Rey, C. Fernandes, A. Horn, M.D. Pereira, Metal-based superoxide dismutase and catalase mimics reduce oxidative stress biomarkers and extend life span of *Saccharomyces cerevisiae*, *Biochemical Journal* 474 (2017) 301–315. <https://doi.org/10.1042/BCJ20160480>.

[69] J.S. Rebouças, I. Spasojević, I. Batinić-Haberle, Pure manganese(III) 5,10,15,20-tetrakis(4-benzoic acid)porphyrin (MnTBAP) is not a superoxide dismutase mimic in aqueous systems: a case of structure–activity relationship as a watchdog mechanism in experimental therapeutics and biology, *J Biol Inorg Chem* 13 (2008) 289–302. <https://doi.org/10.1007/s00775-007-0324-9>.

[70] S. Clède, F. Lambert, R. Saint-Fort, M.-A. Plamont, H. Bertrand, A. Vessières, C. Policar,

Influence of the Side-Chain Length on the Cellular Uptake and the Cytotoxicity of Rhenium Triscarbonyl Derivatives: A Bimodal Infrared and Luminescence Quantitative Study, *Chem. Eur. J.* 20 (2014) 8714–8722. <https://doi.org/10.1002/chem.201402471>.

[71] S.S. Giles, I. Batinić-Haberle, J.R. Perfect, G.M. Cox, *Cryptococcus neoformans* Mitochondrial Superoxide Dismutase: an Essential Link between Antioxidant Function and High-Temperature Growth, *Eukaryotic Cell* 4 (2005) 46–54. <https://doi.org/10.1128/EC.4.1.46-54.2005>.

[72] M.N. Patel, Metalloporphyrins improve the survival of Sod2-deficient neurons, *Aging Cell* 2 (2003) 219–222. <https://doi.org/10.1046/j.1474-9728.2003.00055.x>.

[73] J.A. Imlay, S. Linn, Mutagenesis and stress responses induced in *Escherichia coli* by hydrogen peroxide, *J Bacteriol* 169 (1987) 2967–2976. <https://doi.org/10.1128/jb.169.7.2967-2976.1987>.

[74] A.K. Holley, Y. Xu, T. Noel, V. Bakthavatchalu, I. Batinic-Haberle, D.K. St. Clair, Manganese Superoxide Dismutase-Mediated Inside-Out Signaling in HaCaT Human Keratinocytes and SKH-1 Mouse Skin, *Antioxidants & Redox Signaling* 20 (2014) 2347–2360. <https://doi.org/10.1089/ars.2013.5204>.

[75] K. Cramer-Morales, C.D. Heer, K.A. Mapuskar, F.E. Domann, SOD2 targeted gene editing by CRISPR/Cas9 yields Human cells devoid of MnSOD, *Free Radical Biology and Medicine* 89 (2015) 379–386. <https://doi.org/10.1016/j.freeradbiomed.2015.07.017>.

[76] J. Baumber, B.A. Ball, C.G. Gravance, V. Medina, M.C.G. Davies-Morel, The Effect of Reactive Oxygen Species on Equine Sperm Motility, Viability, Acrosomal Integrity, Mitochondrial Membrane Potential, and Membrane Lipid Peroxidation, *Journal of Andrology*, 21 (2000) 895-902, doi:10.1002/j.1939-4640.2000.tb03420.x.

[77] T. Satoh, T. Numakawa, Y. Abiru, T. Yamagata, Y. Ishikawa, Y. Enokido, H. Hatanaka, Production of Reactive Oxygen Species and Release of l-Glutamate During Superoxide Anion-Induced Cell Death of Cerebellar Granule Neurons, *Journal of Neurochemistry* 70 (2002) 316–324. <https://doi.org/10.1046/j.1471-4159.1998.70010316.x>.

[78] A.B. Fisher, Redox Signaling Across Cell Membranes, *Antioxidants & Redox Signaling* 11 (2009) 1349–1356. <https://doi.org/10.1089/ars.2008.2378>.

[79] C. Moriscot, S. Candel, V. Sauret, J. Kerr-Conte, M.J. Richard, M.C. Favrot, P.Y. Benhamou, MnTMPyP, a metalloporphyrin-based superoxide dismutase/catalase mimetic, protects INS-1 cells and human pancreatic islets from an in vitro oxidative challenge, *Diabetes & Metabolism* 33 (2007) 44–53. <https://doi.org/10.1016/j.diabet.2006.09.004>.

[80] X. Zou, Y. Ji, G. Gao, X. Zhu, S. Lv, F. Yan, S. Han, X. Chen, C. Gao, J. Liu, G. Luo, A Novel Selenium and Copper-containing Peptide with Both Superoxide Dismutase and Glutathione Peroxidase Activities, *Journal of Microbiology and Biotechnology* 20 (2010) 88–93. <https://doi.org/10.4014/jmb.0907.07014>.

[81] V. Kain, M.A. Sawant, A. Dasgupta, G. Jaiswal, A. Vyas, S. Padhye, S.L. Sitasawad, A novel SOD mimic with a redox-modulating mn (II) complex, ML1 attenuates high glucose-induced abnormalities in intracellular Ca²⁺ transients and prevents cardiac cell death through restoration of mitochondrial function, *Biochemistry and Biophysics Reports* 5 (2016) 296–304. <https://doi.org/10.1016/j.bbrep.2016.01.003>.

[82] A. Vyas, V. Kain, Z. Afrasiabi, S. Sitasawad, M. Khetmalas, V. Nivière, S. Padhye, Novel Mn-SOD Mimetics Offer Superior Protection Against Oxidative Damages in Hek293 Kidney Cells, *J Pharmaceut Sci Pharmacol* 1 (2014) 146–153. <https://doi.org/10.1166/jpsp.2014.1011>.

[83] P. Failli, D. Bani, A. Bencini, M. Cantore, L. Di Cesare Mannelli, C. Ghelardini, C. Giorgi, M. Innocenti, F. Rugi, A. Spepi, R. Udisti, B. Valtancoli, A Novel Manganese Complex Effective as Superoxide Anion Scavenger and Therapeutic Agent against Cell and Tissue Oxidative Injury, *J. Med.*

Chem. 52 (2009) 7273–7283. <https://doi.org/10.1021/jm901298x>.

[84] K.-Y. Cheng, F. Guo, J.-Q. Lu, Y.-Z. Cao, T.-C. Wang, Q. Yang, Q. Xia, MnTM-4-PyP Modulates Endogenous Antioxidant Responses and Protects Primary Cortical Neurons against Oxidative Stress, *CNS Neurosci Ther* 21 (2015) 435–445. <https://doi.org/10.1111/cns.12373>.

[85] H.-F. Huang, F. Guo, Y.-Z. Cao, W. Shi, Q. Xia, Neuroprotection by Manganese Superoxide Dismutase (MnSOD) Mimics: Antioxidant Effect and Oxidative Stress Regulation in Acute Experimental Stroke, *CNS Neurosci Ther* 18 (2012) 811–818. <https://doi.org/10.1111/j.1755-5949.2012.00380.x>.

[86] J.R. Reddan, F.J. Giblin, M. Sevilla, V. Padgaonkar, D.C. Dziedzic, V.R. Leverenz, I.C. Misra, J.S. Chang, J.T. Pena, Propyl gallate is a superoxide dismutase mimic and protects cultured lens epithelial cells from H₂O₂ insult, *Experimental Eye Research* 76 (2003) 49–59. [https://doi.org/10.1016/S0014-4835\(02\)00256-7](https://doi.org/10.1016/S0014-4835(02)00256-7).

[87] I. Anderson, C. Adinolfi, S.R. Doctrow, K. Huffman, K. Joy, B. Malfroy, P. Soden, H. Rupniak, J. Barnes, Oxidative signalling and inflammatory pathways in Alzheimer's disease., *Biochem Soc Symp* 67 (2001) 141–149.

[89] B.J. Day, I. Fridovich, J.D. Crapo, Manganic Porphyrins Possess Catalase Activity and Protect Endothelial Cells against Hydrogen Peroxide-Mediated Injury, *Archives of Biochemistry and Biophysics* 347 (1997) 256–262. <https://doi.org/10.1006/abbi.1997.0341>.

[90] K. Coulibaly, M. Thauvin, A. Melenbacher, C. Testard, E. Trigoni, A. Vincent, M.J. Stillman, S. Vríz, C. Policar, N. Delsuc, A di-Copper Peptidyl Complex Mimics the Activity of Catalase, a Key Antioxidant Metalloenzyme, *Inorg. Chem.* 60 (2021) 9309–9319. <https://doi.org/10.1021/acs.inorgchem.0c03718>.

[91] A. Vincent, M. Thauvin, E. Quévrain, E. Mathieu, S. Layani, P. Seksik, I. Batinic-Haberle, S. Vríz, C. Policar, N. Delsuc, Evaluation of the compounds commonly known as superoxide dismutase and catalase mimics in cellular models, *Journal of Inorganic Biochemistry* 219 (2021) 111431. <https://doi.org/10.1016/j.jinorgbio.2021.111431>.

[92] C.H. Coyle, Mechanisms of H₂O₂-induced oxidative stress in endothelial cells, Doctor of Philosophy, University of Iowa, 2004. <https://doi.org/10.17077/etd.lqmo7cxy>.

[93] V.V. Belousov, A.F. Fradkov, K.A. Lukyanov, D.B. Staroverov, K.S. Shakhbazov, A.V. Terskikh, S. Lukyanov, Genetically encoded fluorescent indicator for intracellular hydrogen peroxide, *Nat Methods* 3 (2006) 281–286. <https://doi.org/10.1038/nmeth866>.

[94] M.-A. Guillaumot, O. Cerles, H.C. Bertrand, E. Benoit, C. Nicco, S. Chouzenoux, A. Schmitt, F. Batteux, C. Policar, R. Coriat, Oxaliplatin-induced neuropathy: the preventive effect of a new superoxide dismutase modulator, *Oncotarget* 10 (2019). <https://doi.org/10.18632/oncotarget.27248>.

[95] J.M. Pollard, J.S. Reboucas, A. Durazo, I. Kos, F. Fike, M. Panni, E.B. Gralla, J.S. Valentine, I. Batinic-Haberle, R.A. Gatti, Radioprotective effects of manganese-containing superoxide dismutase mimics on ataxia–telangiectasia cells, *Free Radical Biology and Medicine* 47 (2009) 250–260. <https://doi.org/10.1016/j.freeradbiomed.2009.04.018>.

[96] J. Alexandre, C. Nicco, C. Chéreau, A. Laurent, B. Weill, F. Goldwasser, F. Batteux, Improvement of the Therapeutic Index of Anticancer Drugs by the Superoxide Dismutase Mimic Mangafodipir, *JNCI: Journal of the National Cancer Institute* 98 (2006) 236–244. <https://doi.org/10.1093/jnci/djj049>.

[97] C. Prieux-Klotz, H. Chédotal, M. Zoumpoulaki, S. Chouzenoux, C. Chêne, A. Lopez-Sanchez, M. Thomas, P. Ranjan Sahoo, C. Policar, F. Batteux, H.C. Bertrand, C. Nicco, R. Coriat, A New Manganese Superoxide Dismutase Mimetic Improves Oxaliplatin-Induced Neuropathy and Global Tolerance in Mice, *IJMS* 23 (2022) 12938. <https://doi.org/10.3390/ijms232112938>.

- [98] E.I. Azzam, J.-P. Jay-Gerin, D. Pain, Ionizing radiation-induced metabolic oxidative stress and prolonged cell injury, *Cancer Letters* 327 (2012) 48–60. <https://doi.org/10.1016/j.canlet.2011.12.012>.
- [99] R. Liu, Y. Bian, L. Liu, L. Liu, X. Liu, S. Ma, Molecular pathways associated with oxidative stress and their potential applications in radiotherapy (Review), *Int J Mol Med* 49 (2022) 65. <https://doi.org/10.3892/ijmm.2022.5121>.
- [100] Kim, Lee, Seo, Kim, Kim, Kim, Kang, Seong, Youn, Youn, Cellular Stress Responses in Radiotherapy, *Cells* 8 (2019) 1105. <https://doi.org/10.3390/cells8091105>.
- [101] M. Ambrose, J.V. Goldstine, R.A. Gatti, Intrinsic mitochondrial dysfunction in ATM-deficient lymphoblastoid cells, *Human Molecular Genetics* 16 (2007) 2154–2164. <https://doi.org/10.1093/hmg/ddm166>.
- [102] H. Zhao, J. Joseph, H.M. Fales, E.A. Sokoloski, R.L. Levine, J. Vasquez-Vivar, B. Kalyanaraman, Detection and characterization of the product of hydroethidine and intracellular superoxide by HPLC and limitations of fluorescence, *Proceedings of the National Academy of Sciences* 102 (2005) 5727–5732. <https://doi.org/10.1073/pnas.0501719102>.
- [103] Y.-C. Fang, Y.-P. Chen, C.-T. Chen, T.-S. Lin, C.-Y. Mou, Protection of HeLa cells against ROS stress by CuZnSOD mimic system, *J. Mater. Chem. B* 1 (2013) 6042. <https://doi.org/10.1039/c3tb21052a>.
- [104] M. Patel, Inhibition of Neuronal Apoptosis by a Metalloporphyrin Superoxide Dismutase Mimic, *Journal of Neurochemistry* 71 (2002) 1068–1074. <https://doi.org/10.1046/j.1471-4159.1998.71031068.x>.
- [105] J. Peng, F.F. Stevenson, S.R. Doctrow, J.K. Andersen, Superoxide Dismutase/Catalase Mimetics Are Neuroprotective against Selective Paraquat-mediated Dopaminergic Neuron Death in the Substantia Nigra: IMPLICATIONS FOR PARKINSON DISEASE, *J. Biol. Chem.* 280 (2005) 29194–29198. <https://doi.org/10.1074/jbc.M500984200>.
- [106] S. Carballal, V. Valez, D. Alvarez-Paggi, A. Tovmasyan, I. Batinic-Haberle, G. Ferrer-Sueta, D.H. Murgida, R. Radi, Manganese porphyrin redox state in endothelial cells: Resonance Raman studies and implications for antioxidant protection towards peroxynitrite, *Free Radical Biology and Medicine* 126 (2018) 379–392. <https://doi.org/10.1016/j.freeradbiomed.2018.08.023>.
- [107] L.W. Velsor, M. Kovacevic, M. Goldstein, H.M. Leitner, W. Lewis, B.J. Day, Mitochondrial oxidative stress in human hepatoma cells exposed to stavudine, *Toxicology and Applied Pharmacology* 199 (2004) 10–19. <https://doi.org/10.1016/j.taap.2004.03.005>.
- [108] D.N. Criddle, S. Gillies, H.K. Baumgartner-Wilson, M. Jaffar, E.C. Chinje, S. Passmore, M. Chvanov, S. Barrow, O.V. Gerasimenko, A.V. Tepikin, R. Sutton, O.H. Petersen, Menadione-induced Reactive Oxygen Species Generation via Redox Cycling Promotes Apoptosis of Murine Pancreatic Acinar Cells, *Journal of Biological Chemistry* 281 (2006) 40485–40492. <https://doi.org/10.1074/jbc.M607704200>.
- [109] R. Lascano, N. Munoz, G. Robert, M. Rodriguez, M. Melchiorre, V. Trippi, G. Quero, Paraquat: An Oxidative Stress Inducer, in: M.N. Hasaneen (Ed.), *Herbicides - Properties, Synthesis and Control of Weeds*, InTech, 2012. <https://doi.org/10.5772/32590>.
- [110] M. Jimenez-Del-Rio, G. Suarez-Cedeño, C. Velez-Pardo, Using paraquat to generate anion free radicals and hydrogen peroxide in *in vitro*: Antioxidant effect of vitamin E: A procedure to teach theoretical and experimental principles of reactive oxygen species biochemistry, *Biochem. Mol. Biol. Educ.* 38 (2010) 104–109. <https://doi.org/10.1002/bmb.20349>.
- [111] N. Hogg, V.M. Darley-Usmar, M.T. Wilson, S. Moncada, Production of hydroxyl radicals from the simultaneous generation of superoxide and nitric oxide, *Biochemical Journal* 281 (1992) 419–424. <https://doi.org/10.1042/bj2810419>.

- [112] D. Lieb, I. Kenkell, J.Lj. Miljković, D. Moldenhauer, N. Weber, M.R. Filipović, F. Gröhn, I. Ivanović-Burmazović, Amphiphilic Pentaazamacrocyclic Manganese Superoxide Dismutase Mimetics, *Inorg. Chem.* 53 (2014) 1009–1020. <https://doi.org/10.1021/ic402469t>.
- [113] A.-S. Bernard, C. Giroud, H.Y.V. Ching, A. Meunier, V. Ambike, C. Amatore, M.G. Collignon, F. Lemaître, C. Policar, Evaluation of the anti-oxidant properties of a SOD-mimic Mn-complex in activated macrophages, *Dalton Trans.* 41 (2012) 6399. <https://doi.org/10.1039/c2dt12479c>.
- [114] S. Asayama, E. Kawamura, S. Nagaoka, H. Kawakami, Design of Manganese Porphyrin Modified with Mitochondrial Signal Peptide for a New Antioxidant, *Mol. Pharmaceutics* 3 (2006) 468–470. <https://doi.org/10.1021/mp0500667>.
- [115] I.L. Jackson, I.L. Jackson, I. Batinic-Haberle, P. Sonveaux, M.W. Dewhirst, Z. Vujaskovic, ROS production and angiogenic regulation by macrophages in response to heat therapy, *International Journal of Hyperthermia* 22 (2006) 263–273. <https://doi.org/10.1080/02656730600594027>.
- [116] M.M. Ndengele, C. Muscoli, Z.Q. Wang, T.M. Doyle, G.M. Matuschak, D. Salvemini, Superoxide potentiates NF- κ B activation and modulates endotoxin-induced cytokine production in alveolar macrophages., *Shock* 23 (2005) 186–193. <https://doi.org/10.1097/01.shk.0000144130.36771.d6>.
- [117] F. Matemadombo, M. Durmus, V. Escriou, S. Griveau, D. Scherman, F. Bedioui, T. Nyokong, Evaluation of the Performance of Manganese Phthalocyanines as Superoxide Dismutase Mimics, *CAC* 5 (2009) 330–338. <https://doi.org/10.2174/157341109789077731>.
- [118] H.M. Peshavariya, G.J. Dusting, S. Selemidis, Analysis of dihydroethidium fluorescence for the detection of intracellular and extracellular superoxide produced by NADPH oxidase, *Free Radical Research* 41 (2007) 699–712. <https://doi.org/10.1080/10715760701297354>.
- [119] I.L. Jackson, L. Chen, I. Batinic-Haberle, Z. Vujaskovic, Superoxide dismutase mimetic reduces hypoxia-induced , TGF- β , and VEGF production by macrophages, *Free Radical Research* 41 (2007) 8–14. <https://doi.org/10.1080/10715760600913150>.
- [120] R. Bottino, A.N. Balamurugan, S. Bertera, M. Pietropaolo, M. Trucco, J.D. Piganelli, Preservation of Human Islet Cell Functional Mass by Anti-Oxidative Action of a Novel SOD Mimic Compound, *Diabetes* 51 (2002) 2561–2567. <https://doi.org/10.2337/diabetes.51.8.2561>.
- [121] M. Pedullà, R. d’Aquino, V. Desiderio, F. de Francesco, A. Puca, G. Papaccio, MnSOD mimic compounds can counteract mechanical stress and islet β cell apoptosis, although at appropriate concentration ranges, *J. Cell. Physiol.* 212 (2007) 432–438. <https://doi.org/10.1002/jcp.21034>.
- [122] E. Mathieu, A.-S. Bernard, H.Y.V. Ching, A. Somogyi, K. Medjoubi, J.R. Fores, H.C. Bertrand, A. Vincent, S. Trépout, J.-L. Guerquin-Kern, A. Scheitler, I. Ivanović-Burmazović, P. Seksik, N. Delsuc, C. Policar, Anti-inflammatory activity of superoxide dismutase mimics functionalized with cell-penetrating peptides, *Dalton Trans.* 49 (2020) 2323–2330. <https://doi.org/10.1039/C9DT04619D>.
- [123] G. Schanne, M. Zoumpoulaki, G. Gazzah, A. Vincent, H. Preud’homme, R. Lobinski, S. Demignot, P. Seksik, N. Delsuc, C. Policar, Inertness of Superoxide Dismutase Mimics Mn(II) Complexes Based on an Open-Chain Ligand, Bioactivity, and Detection in Intestinal Epithelial Cells, *Oxidative Medicine and Cellular Longevity* 2022 (2022) 3858122. <https://doi.org/10.1155/2022/3858122>.
- [124] A. Vincent, J.R. Fores, E. Tauziet, E. Quévrain, Á. Dancs, A. Conte-Daban, A.-S. Bernard, P. Pelupessy, K. Coulibaly, P. Seksik, C. Hureau, K. Selmecci, C. Policar, N. Delsuc, An easy-to-implement combinatorial approach involving an activity-based assay for the discovery of a peptidyl copper complex mimicking superoxide dismutase, *Chem. Commun.* 56 (2020) 399–402. <https://doi.org/10.1039/C9CC07920C>.
- [125] C. Bogdan, M. Röllinghoff, A. Diefenbach, Reactive oxygen and reactive nitrogen

intermediates in innate and specific immunity, *Current Opinion in Immunology* 12 (2000) 64–76. [https://doi.org/10.1016/S0952-7915\(99\)00052-7](https://doi.org/10.1016/S0952-7915(99)00052-7).

[126] C. Amatore, S. Arbault, M. Guille, F. Lemaitre, Electrochemical Monitoring of Single Cell Secretion: Vesicular Exocytosis and Oxidative Stress, *Chem. Rev.* 108 (2008) 2585–2621, doi:10.1021/cr068062g.

[127] M.R. Filipović, A.C.W. Koh, S. Arbault, V. Niketić, A. Debus, U. Schleicher, C. Bogdan, M. Guille, F. Lemaître, C. Amatore, I. Ivanović-Burmazović, Striking Inflammation from Both Sides: Manganese(II) Pentaazamacrocyclic SOD Mimics Act Also as Nitric Oxide Dismutases: A Single-Cell Study, *Angewandte Chemie International Edition* 49 (2010) 4228–4232. <https://doi.org/10.1002/anie.200905936>.

[128] S. Kumar, V. Kain, S.L. Sitasawad, High glucose-induced Ca²⁺ overload and oxidative stress contribute to apoptosis of cardiac cells through mitochondrial dependent and independent pathways, *Biochimica et Biophysica Acta (BBA) - General Subjects* 1820 (2012) 907–920. <https://doi.org/10.1016/j.bbagen.2012.02.010>.

[129] R.B. Stevens, J.D. Ansite, C.D. Mills, A. Lokeh, T.J. Rossini, M. Saxena, R.R. Brown, D.E.R. Sutherland, Nitric oxide mediates early dysfunction of rat and mouse islets after transplantation, *Transplantation* 61 (1996) 1740–1749.

[130] C. Lenoir, C. Sapin, A.H. Broquet, A.-M. Jouniaux, S. Bardin, I. Gasnereau, G. Thomas, P. Seksik, G. Trugnan, J. Masliah, M. Bachelet, MD-2 controls bacterial lipopolysaccharide hyporesponsiveness in human intestinal epithelial cells, *Life Sciences* 82 (2008) 519–528. <https://doi.org/10.1016/j.lfs.2007.12.007>.

[131] T. Guzik, R. Korbut, T. Adamek-Guzik, Nitric oxide and superoxide in inflammation and immune regulation, *J Physiol Pharmacol.* 54 (2003) 469–487.

[132] M. Patel, B.J. Day, J.D. Crapo, I. Fridovich, J.O. McNamara, Requirement for Superoxide in Excitotoxic Cell Death, *Neuron* 16 (1996) 345–355. [https://doi.org/10.1016/S0896-6273\(00\)80052-5](https://doi.org/10.1016/S0896-6273(00)80052-5).

[133] P.M. Gallop, M.A. Paz, E. Henson, S.A. Latt, Dynamic approaches to the delivery of reporter reagents into living cells., 1 (1984) 32–36.

[134] G. Rothe, G. Valet, Flow Cytometric Analysis of Respiratory Burst Activity in Phagocytes With Hydroethidine and 2',7'-Dichlorofluorescein, *J Leukoc Biol* 47 (1990) 440–448. <https://doi.org/10.1002/jlb.47.5.440>.

[135] L. Benov, L. Szejnberg, I. Fridovich, Critical evaluation of the use of hydroethidine as a measure of superoxide anion radical, *Free Radical Biology and Medicine* 25 (1998) 826–831. [https://doi.org/10.1016/S0891-5849\(98\)00163-4](https://doi.org/10.1016/S0891-5849(98)00163-4).

[136] C. Bucana, I. Saiki, R. Nayar, Uptake and accumulation of the vital dye hydroethidine in neoplastic cells., *J Histochem Cytochem.* 34 (1986) 1109–1115. <https://doi.org/10.1177/34.9.2426339>.

[137] H. Zhao, S. Kalivendi, H. Zhang, J. Joseph, K. Nithipatikom, J. Vásquez-Vivar, B. Kalyanaram, Superoxide reacts with hydroethidine but forms a fluorescent product that is distinctly different from ethidium: potential implications in intracellular fluorescence detection of superoxide, *Free Radical Biology and Medicine* 34 (2003) 1359–1368. [https://doi.org/10.1016/S0891-5849\(03\)00142-4](https://doi.org/10.1016/S0891-5849(03)00142-4).

[138] J. Zielonka, J. Vasquez-Vivar, B. Kalyanaram, Detection of 2-hydroxyethidium in cellular systems: a unique marker product of superoxide and hydroethidine, *Nat Protoc* 3 (2008) 8–21. <https://doi.org/10.1038/nprot.2007.473>.

[139] V. Bindokas, J. Jordan, C. Lee, R. Miller, Superoxide production in rat hippocampal neurons: selective imaging with hydroethidine, *J. Neurosci.* 16 (1996) 1324–1336.

<https://doi.org/10.1523/JNEUROSCI.16-04-01324.1996>.

[140] B. Fink, K. Laude, L. McCann, A. Doughan, D.G. Harrison, S. Dikalov, Detection of intracellular superoxide formation in endothelial cells and intact tissues using dihydroethidium and an HPLC-based assay, *American Journal of Physiology-Cell Physiology* 287 (2004) C895–C902. <https://doi.org/10.1152/ajpcell.00028.2004>.

[141] J. Zielonka, B. Kalyanaraman, Hydroethidine- and MitoSOX-derived red fluorescence is not a reliable indicator of intracellular superoxide formation: Another inconvenient truth, *Free Radical Biology and Medicine* 48 (2010) 983–1001. <https://doi.org/10.1016/j.freeradbiomed.2010.01.028>.

[142] M. Kauffman, M. Kauffman, K. Traore, H. Zhu, M. Trush, Z. Jia, Y. Li, MitoSOX-Based Flow Cytometry for Detecting Mitochondrial ROS, *ROS* (2016). <https://doi.org/10.20455/ros.2016.865>.

[143] S. Melov, P. Coskun, M. Patel, R. Tuinstra, B. Cottrell, A.S. Jun, T.H. Zastawny, M. Dizdaroglu, S.I. Goodman, T.-T. Huang, H. Mizioroko, C.J. Epstein, D.C. Wallace, Mitochondrial disease in superoxide dismutase 2 mutant mice, *Proc. Natl. Acad. Sci. U.S.A.* 96 (1999) 846–851. <https://doi.org/10.1073/pnas.96.3.846>.

[144] K.M. Robinson, M.S. Janes, M. Pehar, J.S. Monette, M.F. Ross, T.M. Hagen, M.P. Murphy, J.S. Beckman, Selective fluorescent imaging of superoxide in vivo using ethidium-based probes, *Proceedings of the National Academy of Sciences* 103 (2006) 15038–15043. <https://doi.org/10.1073/pnas.0601945103>.

[145] M.F. Ross, G.F. Kelso, F.H. Blaikie, A.M. James, H.M. Cochemé, A. Filipovska, T. Da Ros, T.R. Hurd, R.A.J. Smith, M.P. Murphy, Lipophilic triphenylphosphonium cations as tools in mitochondrial bioenergetics and free radical biology, *Biochemistry (Moscow)* 70 (2005) 222–230. <https://doi.org/10.1007/s10541-005-0104-5>.

[146] P. Mukhopadhyay, M. Rajesh, G. Haskó, B.J. Hawkins, M. Madesh, P. Pacher, Simultaneous detection of apoptosis and mitochondrial superoxide production in live cells by flow cytometry and confocal microscopy, *Nat Protoc* 2 (2007) 2295–2301. <https://doi.org/10.1038/nprot.2007.327>.

[147] P. Mukhopadhyay, M. Rajesh, K. Yoshihiro, G. Haskó, P. Pacher, Simple quantitative detection of mitochondrial superoxide production in live cells, *Biochemical and Biophysical Research Communications* 358 (2007) 203–208. <https://doi.org/10.1016/j.bbrc.2007.04.106>.

[148] B. Halliwell, M. Whiteman, Measuring reactive species and oxidative damage *in vivo* and in cell culture: how should you do it and what do the results mean? *British Journal of Pharmacology* 142 (2004) 231–255. <https://doi.org/10.1038/sj.bjp.0705776>.

[149] I. Minkenberg, E. Ferber, Lucigenin-dependent chemiluminescence as a new assay for NAD(P)H-oxidase activity in particulate fractions of human polymorphonuclear leukocytes, *Journal of Immunological Methods* 71 (1984) 61–67. [https://doi.org/10.1016/0022-1759\(84\)90206-0](https://doi.org/10.1016/0022-1759(84)90206-0).

[150] R. Sharma, M.K. Panner Selvam, A. Agarwal, Reactive Oxygen Species Methodology Using Chemiluminescence Assay, in: *Oxidants, Antioxidants and Impact of the Oxidative Status in Male Reproduction*, Elsevier, 2019: pp. 183–193. <https://doi.org/10.1016/B978-0-12-812501-4.00017-1>.

[151] S.I. Liochev, I. Fridovich, Lucigenin as mediator of superoxide production: revisited, *Free Radical Biology and Medicine* 25 (1998) 926–928. [https://doi.org/10.1016/S0891-5849\(98\)00121-X](https://doi.org/10.1016/S0891-5849(98)00121-X).

[152] J. McCord, I. Fridovich, Superoxide dismutase. An enzymic function for erythrocuprein (hemocuprein), *The Journal of Biological Chemistry* 244 (1969) 6045–6055.

[153] H. Ukeda, S. Maeda, T. Ishii, M. Sawamura, Spectrophotometric Assay for Superoxide Dismutase Based on Tetrazolium Salt 3'-{1-[(Phenylamino)-carbonyl]-3,4-tetrazolium}-bis(4-methoxy-6-nitro)benzenesulfonic Acid Hydrate Reduction by Xanthine–Xanthine Oxidase, *Analytical Biochemistry* 251 (1997) 206–209. <https://doi.org/10.1006/abio.1997.2273>.

- [154] M.V. Berridge, P.M. Herst, A.S. Tan, Tetrazolium dyes as tools in cell biology: New insights into their cellular reduction, in: *Biotechnology Annual Review*, Elsevier, 2005: pp. 127–152. [https://doi.org/10.1016/S1387-2656\(05\)11004-7](https://doi.org/10.1016/S1387-2656(05)11004-7).
- [155] J.J. Hu, N.-K. Wong, S. Ye, X. Chen, M.-Y. Lu, A.Q. Zhao, Y. Guo, A.C.-H. Ma, A.Y.-H. Leung, J. Shen, D. Yang, Fluorescent Probe HKSOX-1 for Imaging and Detection of Endogenous Superoxide in Live Cells and In Vivo, *J. Am. Chem. Soc.* 137 (2015) 6837–6843. <https://doi.org/10.1021/jacs.5b01881>.
- [156] L. Wu, A.C. Sedgwick, X. Sun, S.D. Bull, X.-P. He, T.D. James, Reaction-Based Fluorescent Probes for the Detection and Imaging of Reactive Oxygen, Nitrogen, and Sulfur Species, *Acc. Chem. Res.* 52 (2019) 2582–2597. <https://doi.org/10.1021/acs.accounts.9b00302>.
- [157] D. Flint, E. Smyk-Randall, F. Tuminello, B. Draczynska-lusiak, O. Brown, The Inactivation of Dihydroxy-acid Dehydratase in *Escherichia coli* Treated with Hyperbaric Oxygen Occurs Because of the Destruction of Its Fe-S Cluster, but the Enzyme Remains in the Cell in a Form That Can Be Reactivated, *The Journal of Biological Chemistry* 268 (1993) 25547–25552.
- [158] A. Hausladen, I. Fridovich, Superoxide and Peroxynitrite Inactivate Aconitases, but Nitric Oxide Does Not, *J. Biol. Chem.* 269 (1994) 29405–29408. doi:10.1016/S0021-9258(18)43893-8.
- [159] P. Gardner, I. Rainer, L. Epstein, C. White, Superoxide Radical and Iron Modulate Aconitase Activity in Mammalian Cells, (1995) 13399–13405. <https://doi.org/10.1074/jbc.270.22.13399>.
- [160] P.R. Gardner, Aconitase: Sensitive target and measure of superoxide, in: *Methods in Enzymology*, Academic Press, 2002: pp. 9–23. [https://doi.org/10.1016/S0076-6879\(02\)49317-2](https://doi.org/10.1016/S0076-6879(02)49317-2).
- [161] L. Castro, M. Rodriguez, R. Radif, Aconitase Is Readily Inactivated by Peroxynitrite, but Not by Its Precursor, Nitric Oxide, (*J. Biol. Chem.* 269 (1994) 29409–29415. doi:10.1016/S0021-9258(18)43894-X.
- [162] G.F. Kelso, A. Maroz, H.M. Cochemé, A. Logan, T.A. Prime, A.V. Peskin, C.C. Winterbourn, A.M. James, M.F. Ross, S. Brooker, C.M. Porteous, R.F. Anderson, M.P. Murphy, R.A.J. Smith, A Mitochondria-Targeted Macrocyclic Mn(II) Superoxide Dismutase Mimetic, *Chemistry & Biology* 19 (2012) 1237–1246. <https://doi.org/10.1016/j.chembiol.2012.08.005>.
- [163] C. Amatore, S. Arbault, M. Guille, F. Lemaître, Electrochemical Monitoring of Single Cell Secretion: Vesicular Exocytosis and Oxidative Stress, *Chem. Rev.* 108 (2008) 2585–2621. <https://doi.org/10.1021/cr068062g>.
- [164] C. Amatore, S. Arbault, C. Bouton, J.-C. Drapier, H. Ghandour, A.C.W. Koh, Real-Time Amperometric Analysis of Reactive Oxygen and Nitrogen Species Released by Single Immunostimulated Macrophages, *ChemBioChem* 9 (2008) 1472–1480. <https://doi.org/10.1002/cbic.200700746>.
- [165] Y. Xu, Y. Zhou, R. Yin, C. Wang, H. Chu, J. Wang, A novel 76-mer peptide mimic with the synergism of superoxide dismutase and glutathione peroxidase, *In Vitro Cell.Dev.Biol.-Animal* 54 (2018) 335–345. <https://doi.org/10.1007/s11626-018-0240-z>.
- [166] M.C. Jaramillo, M.M. Briehl, J.D. Crapo, I. Batinic-Haberle, M.E. Tome, Manganese Porphyrin, MnTE-2-PyP5+, Acts as a Pro-Oxidant to Potentiate Glucocorticoid-Induced Apoptosis in Lymphoma Cells, *Free Radical Biology and Medicine* 52 (2012) 1272–1284. <https://doi.org/10.1016/j.freeradbiomed.2012.02.001>.
- [167] J. Peng, X.O. Mao, F.F. Stevenson, M. Hsu, J.K. Andersen, The Herbicide Paraquat Induces Dopaminergic Nigral Apoptosis through Sustained Activation of the JNK Pathway, *J. Biol. Chem.* 279 (2004) 32626–32632. <https://doi.org/10.1074/jbc.M404596200>.
- [168] Y.D. Ladner, M. Alini, A.R. Armiento, The Dimethylmethylene Blue Assay (DMMB) for the

Quantification of Sulfated Glycosaminoglycans, in: M.J. Stoddart, E. Della Bella, A.R. Armiento (Eds.), *Cartilage Tissue Engineering*, Springer US, New York, NY, 2023: pp. 115–121. https://doi.org/10.1007/978-1-0716-2839-3_9.

[169] S. Kamiloglu, G. Sari, T. Ozdal, E. Capanoglu, Guidelines for cell viability assays, *Food Frontiers* 1 (2020) 332–349. <https://doi.org/10.1002/fft2.44>.

[170] K.T. Brunner, J. Mael, Quantitative Assay of the Lytic Action of Immune Lymphoid Cells on ⁵¹Cr-Labelled Allogeneic Target Cells In vitro; Inhibition by Isoantibody and by Drugs, *Immunology* 14 (1968) 181-196.

[171] N.A. Thornberry, Caspases: Enemies Within, *Science* 281 (1998) 1312–1316. <https://doi.org/10.1126/science.281.5381.1312>.

[172] T.R. Figueira, M.H. Barros, A.A. Camargo, R.F. Castilho, J.C.B. Ferreira, A.J. Kowaltowski, F.E. Sluse, N.C. Souza-Pinto, A.E. Vercesi, Mitochondria as a Source of Reactive Oxygen and Nitrogen Species: From Molecular Mechanisms to Human Health, *Antioxidants & Redox Signaling* 18 (2013) 2029–2074. <https://doi.org/10.1089/ars.2012.4729>.

[173] M. Csala, É. Margittai, G. Bánhegyi, Redox Control of Endoplasmic Reticulum Function, *Antioxidants & Redox Signaling* 13 (2010) 77–108. <https://doi.org/10.1089/ars.2009.2529>.

[174] L.D. Zorova, V.A. Popkov, E.Y. Plotnikov, D.N. Silachev, I.B. Pevzner, S.S. Jankauskas, V.A. Babenko, S.D. Zorov, A.V. Balakireva, M. Juhaszova, S.J. Sollott, D.B. Zorov, Mitochondrial membrane potential, *Analytical Biochemistry* 552 (2018) 50–59. <https://doi.org/10.1016/j.ab.2017.07.009>.

[175] M. Reers, T.W. Smith, L.B. Chen, J-aggregate formation of a carbocyanine as a quantitative fluorescent indicator of membrane potential, *Biochemistry* 30 (1991) 4480–4486. <https://doi.org/10.1021/bi00232a015>.

[176] R. Chaudhry, V. Matthew, *Biochemistry, Glycolysis*, StatPearls (2020).

[177] B.H. Robinson, Use of fibroblast and lymphoblast cultures for detection of respiratory chain defects, in: *Methods in Enzymology*, Elsevier, 1996: pp. 454–464. [https://doi.org/10.1016/S0076-6879\(96\)64041-5](https://doi.org/10.1016/S0076-6879(96)64041-5).

[178] B.H. Robinson, J. Ward, P. Goodyer, A. Baudet, Respiratory chain defects in the mitochondria of cultured skin fibroblasts from three patients with lacticacidemia., *J. Clin. Invest.* 77 (1986) 1422–1427. <https://doi.org/10.1172/JCI112453>.

[179] D.A. Ferrick, A. Neilson, C. Beeson, Advances in measuring cellular bioenergetics using extracellular flux, *Drug Discovery Today* 13 (2008) 268–274. <https://doi.org/10.1016/j.drudis.2007.12.008>.

[180] R.J. Argüello, A.J. Combes, R. Char, J.-P. Gigan, A.I. Baaziz, E. Bousiquot, V. Camosseto, B. Samad, J. Tsui, P. Yan, S. Boissonneau, D. Figarella-Branger, E. Gatti, E. Tabouret, M.F. Krummel, P. Pierre, SCENITH: A Flow Cytometry-Based Method to Functionally Profile Energy Metabolism with Single-Cell Resolution, *Cell Metabolism* 32 (2020) 1063-1075.e7. <https://doi.org/10.1016/j.cmet.2020.11.007>.

[181] E. Bahar, H. Kim, H. Yoon, ER Stress-Mediated Signaling: Action Potential and Ca²⁺ as Key Players, *IJMS* 17 (2016) 1558. <https://doi.org/10.3390/ijms17091558>.

[182] R.A. Josephson, J.L. Zweier, Study of the Mechanisms of Hydrogen Peroxide and Hydroxyl Free Radical-induced Cellular Injury and Calcium Overload in Cardiac Myocytes, *The Journal of Biological Chemistry* 266 (1991) 2354–2361.

[183] M. Homayouni-Tabrizi, A. Asoodeh, M. Soltani, Cytotoxic and antioxidant capacity of camel milk peptides: Effects of isolated peptide on superoxide dismutase and catalase gene expression, *Journal of Food and Drug Analysis* 25 (2017) 567–575. <https://doi.org/10.1016/j.jfda.2016.10.014>.

- [184] C. Vogel, E.M. Marcotte, Insights into the regulation of protein abundance from proteomic and transcriptomic analyses, *Nat Rev Genet* 13 (2012) 227–232. <https://doi.org/10.1038/nrg3185>.
- [185] Y. Zhao, D.W. Carroll, Y. You, L. Chaiswing, R. Wen, I. Batinic-Haberle, S. Bondada, Y. Liang, D.K. St. Clair, A novel redox regulator, MnTnBuOE-2-PyP5+, enhances normal hematopoietic stem/progenitor cell function, *Redox Biology* 12 (2017) 129–138. <https://doi.org/10.1016/j.redox.2017.02.005>.
- [186] L. Kruidenier, I. Kuiper, W. van Duijn, S.L. Marklund, R.A. van Hogezaand, C.B. Lamers, H.W. Verspaget, Differential mucosal expression of three superoxide dismutase isoforms in inflammatory bowel disease, *J. Pathol.* 201 (2003) 7–16. <https://doi.org/10.1002/path.1407>.
- [187] C.J. Weydert, J.J. Cullen, Measurement of superoxide dismutase, catalase and glutathione peroxidase in cultured cells and tissue, *Nat Protoc* 5 (2010) 51–66. <https://doi.org/10.1038/nprot.2009.197>.
- [188] J. Fan, W. Hsu, H. Hung, W. Zhang, Y. Lee, K. Chen, C. Chu, T. Ko, M. Lee, C. Lin, C. Cheng, Reduction in MnSOD promotes the migration and invasion of squamous carcinoma cells, *Int J Oncol* (2019). <https://doi.org/10.3892/ijo.2019.4750>.
- [190] A.S. Bause, M.C. Haigis, SIRT3 regulation of mitochondrial oxidative stress, *Experimental Gerontology* 48 (2013) 634–639. <https://doi.org/10.1016/j.exger.2012.08.007>.
- [191] Y. Chen, J. Zhang, Y. Lin, Q. Lei, K. Guan, S. Zhao, Y. Xiong, Tumour suppressor SIRT3 deacetylates and activates manganese superoxide dismutase to scavenge ROS, *EMBO Rep* 12 (2011) 534–541. <https://doi.org/10.1038/embor.2011.65>.
- [192] P.P. Jumbo-Lucioni, E.L. Ryan, M.L. Hopson, H.M. Bishop, T. Weitner, A. Tovmasyan, I. Spasojevic, I. Batinic-Haberle, Y. Liang, D.P. Jones, J.L. Fridovich-Keil, Manganese-Based Superoxide Dismutase Mimics Modify Both Acute and Long-Term Outcome Severity in a *Drosophila melanogaster* Model of Classic Galactosemia, *Antioxidants & Redox Signaling* 20 (2014) 2361–2371. <https://doi.org/10.1089/ars.2012.5122>.
- [193] F.J. Giblin, J.P. McCready, J.R. Reddan, D.C. Dziedzic, V.N. Reddy, Detoxification of H₂O₂ by cultured rabbit lens epithelial cells: Participation of the glutathione redox cycle, *Experimental Eye Research* 40 (1985) 827–840. [https://doi.org/10.1016/0014-4835\(85\)90128-9](https://doi.org/10.1016/0014-4835(85)90128-9).
- [194] A. Ayala, M.F. Muñoz, S. Argüelles, Lipid Peroxidation: Production, Metabolism, and Signaling Mechanisms of Malondialdehyde and 4-Hydroxy-2-Nonenal, *Oxidative Medicine and Cellular Longevity* 2014 (2014) 1–31. <https://doi.org/10.1155/2014/360438>.
- [195] B.J. Day, I. Batinic-Haberle, J.D. Crapo, Metalloporphyrins are potent inhibitors of lipid peroxidation, *Free Radical Biology and Medicine* 26 (1999) 730–736. [https://doi.org/10.1016/S0891-5849\(98\)00261-5](https://doi.org/10.1016/S0891-5849(98)00261-5).
- [196] A. Bloodworth, Manganese-porphyrin reactions with lipids and lipoproteins, *Free Radical Biology and Medicine* 28 (2000) 1017–1029. [https://doi.org/10.1016/S0891-5849\(00\)00194-5](https://doi.org/10.1016/S0891-5849(00)00194-5).
- [197] E.L. Steels, R.P. Learmonth, K. Watson, Stress tolerance and membrane lipid unsaturation in *Saccharomyces cerevisiae* grown aerobically or anaerobically, *Microbiology* 140 (1994) 569–576. <https://doi.org/10.1099/00221287-140-3-569>.
- [198] V. Mollace, M. Iannone, C. Muscoli, E. Palma, T. Granato, V. Rispoli, R. Nisticò, D. Rotiroti, D. Salvemini, The role of oxidative stress in paraquat-induced neurotoxicity in rats: protection by non peptidyl superoxide dismutase mimetic, *Neuroscience Letters* 335 (2003) 163–166. [https://doi.org/10.1016/S0304-3940\(02\)01168-0](https://doi.org/10.1016/S0304-3940(02)01168-0).
- [199] H. Ohkawa, N. Ohishi, K. Yagi, Assay for lipid peroxides in animal tissues by thiobarbituric acid reaction, *Analytical Biochemistry* 95 (1979) 351–358. [https://doi.org/10.1016/0003-2697\(79\)90738-](https://doi.org/10.1016/0003-2697(79)90738-)

3.

- [200] J. Aitken, J. Clarkson, S. Fishel, Generation of Reactive Oxygen Species, Lipid Peroxidation, and Human Sperm Function, *Biology of Reproduction* 40 (1989) 183–197.
- [201] A. Santiani, S. Evangelista, N. Sepúlveda, J. Risopatrón, J. Villegas, R. Sánchez, Addition of superoxide dismutase mimics during cooling process prevents oxidative stress and improves semen quality parameters in frozen/thawed ram spermatozoa, *Theriogenology* 82 (2014) 884–889. <https://doi.org/10.1016/j.theriogenology.2014.07.002>.
- [202] E. Cadenas, Biochemistry of oxygen toxicity, *Annu. Rev. Biochem.* 58 (1989) 79-110. doi: 10.1146/annurev.bi.58.070189.000455.
- [203] L.-J. Mah, A. El-Osta, T. Karagiannis, cH2AX: a sensitive molecular marker of DNA damage and repair, *Leukemia* 24 (2010) 679–86. <https://doi.org/10.1038/leu.2010.6>.
- [204] N.J. Kleiman, R.-R. Wang, A. Spector, Hydrogen peroxide-induced DNA damage in bovine lens epithelial cells, *Mutation Research/Genetic Toxicology* 240 (1990) 35–45. [https://doi.org/10.1016/0165-1218\(90\)90006-N](https://doi.org/10.1016/0165-1218(90)90006-N).
- [205] K.W. Kohn, L.C. Erickson, R.A.G. Ewig, C.A. Friedman, Fractionation of DNA from mammalian cells by alkaline elution, *Biochemistry* 15 (1976) 4629–4637. <https://doi.org/10.1021/bi00666a013>.
- [206] Y.-H. Wei, Oxidative Stress and Mitochondrial DNA Mutations in Human Aging, *Experimental Biology and Medicine* 217 (1998) 53–63. <https://doi.org/10.3181/00379727-217-44205>.
- [207] J. Milano, B. Day, A catalytic antioxidant metalloporphyrin blocks hydrogen peroxide-induced mitochondrial DNA damage, *Nucleic Acids Research* 28 (2000) 968–973. <https://doi.org/10.1093/nar/28.4.968>.
- [208] C. Pereira, D. Grácio, J.P. Teixeira, F. Magro, Oxidative Stress and DNA Damage: Implications in Inflammatory Bowel Disease, *Inflammatory Bowel Diseases* (2015) 1. <https://doi.org/10.1097/MIB.0000000000000506>.
- [209] M. Mittal, M.R. Siddiqui, K. Tran, S.P. Reddy, A.B. Malik, Reactive Oxygen Species in Inflammation and Tissue Injury, *Antioxidants & Redox Signaling* 20 (2014) 1126–1167. <https://doi.org/10.1089/ars.2012.5149>.
- [210] M.T. Droy-Lefaix, Y. Drouet, G. Geraud, D. Hosford, P. Braquet, Superoxide dismutase (sod) and the paf- antagonist (bn 52021) reduce small intestinal damage induced by ischemia- reperfusion, *Free Radic. Res. Commun.* 13 (1991) 725-735. doi: 10.3109/10715769109145852.
- [211] D. Salvemini, D.P. Riley, P.J. Lennon, Z.-Q. Wang, M.G. Currie, H. Macarthur, T.P. Misko, Protective effects of a superoxide dismutase mimetic and peroxynitrite decomposition catalysts in endotoxin-induced intestinal damage, *Br. J. Pharmacol.* 127 (1999) 685-692. doi: 10.1038/sj.bjp.0702604.
- [212] M.J. Morgan, Z. Liu, Crosstalk of reactive oxygen species and NF-κB signaling, *Cell Res* 21 (2011) 103–115. <https://doi.org/10.1038/cr.2010.178>.
- [213] H. Tse, J. Martha, J. Milton, J.D. Piganelli, Mechanistic analysis of the immunomodulatory effects of a catalytic antioxidant on antigen-presenting cells: implication for their use in targeting oxidation–reduction reactions in innate immunity, *Free Radical Biology and Medicine* 36 (2004) 233–247. <https://doi.org/10.1016/j.freeradbiomed.2003.10.029>.
- [214] M.M. Ndengele, Z.-Q. Wang, T.M. Doyle, G.M. Matuschak, D. Salvemini, Superoxide-mediated regulation of NF-κB and p38 kinase activation critically modulates E. coli endotoxin-induced TNF-α, IL-1, IL-6 and IL-10 production in alveolar macrophages, *Am J Respir Crit Care Med* 165 (2002).
- [215] G.M. Campo, A. Avenoso, A. D’Ascola, M. Scuruchi, G. Nastasi, A. Micali, D. Puzzolo, A. Pisani,

A. Calatroni, S. Campo, The SOD mimic MnTM-2-PyP(5+) reduces hyaluronan degradation-induced inflammation in mouse articular chondrocytes stimulated with Fe (II) plus ascorbate, *The International Journal of Biochemistry & Cell Biology* 45 (2013) 1610–1619. <https://doi.org/10.1016/j.biocel.2013.05.007>.

[216] M.E. Monzon, N. Fregien, N. Schmid, N.S. Falcon, M. Campos, S.M. Casalino-Matsuda, R.M. Forteza, Reactive Oxygen Species and Hyaluronidase 2 Regulate Airway Epithelial Hyaluronan Fragmentation, *J. Biol. Chem.* 285 (2010) 26126–26134. <https://doi.org/10.1074/jbc.M110.135194>.

[217] G.M. Campo, A. Avenoso, S. Campo, A. D'Ascola, G. Nastasi, A. Calatroni, Small hyaluronan oligosaccharides induce inflammation by engaging both toll-like-4 and CD44 receptors in human chondrocytes, *Biochemical Pharmacology* 80 (2010) 480–490. <https://doi.org/10.1016/j.bcp.2010.04.024>.

[218] T. Liu, L. Zhang, D. Joo, S.-C. Sun, NF- κ B signaling in inflammation, *Sig Transduct Target Ther* 2 (2017) 17023. <https://doi.org/10.1038/sigtrans.2017.23>.

[219] T. Lawrence, *The Nuclear Factor NF- κ B Pathway in Inflammation*, Cold Spring Harbor Perspectives in Biology 1 (2009) a001651–a001651. <https://doi.org/10.1101/cshperspect.a001651>.

[220] A.P. de Souza, V.L.C. Vale, M. da C. Silva, I.B. de Oliveira Araújo, S.C. Trindade, L.F. de Moura-Costa, G.C. Rodrigues, T.S. Sales, H.A. dos Santos, P.C. de Carvalho-Filho, M.G. de Oliveira-Neto, R.E. Schaer, R. Meyer, MAPK involvement in cytokine production in response to *Corynebacterium pseudotuberculosis* infection, *BMC Microbiol* 14 (2014) 230. <https://doi.org/10.1186/s12866-014-0230-6>.

[221] C. Klemm, C. Bruchhagen, A. van Krüchten, S. Niemann, B. Löffler, G. Peters, S. Ludwig, C. Ehrhardt, Mitogen-activated protein kinases (MAPKs) regulate IL-6 over-production during concomitant influenza virus and *Staphylococcus aureus* infection, *Sci Rep* 7 (2017) 42473. <https://doi.org/10.1038/srep42473>.

[222] S. Cuzzocrea, E. Mazzon, L. Dugo, A.P. Caputi, K. Aston, D.P. Riley, D. Salvemini, Protective effects of a new stable, highly active SOD mimetic, M40401 in splanchnic artery occlusion and reperfusion, *Br. J. Pharmacol.* 132 (2001) 19–29. doi: 10.1038/sj.bjp.0703775.

[223] D. Salvemini, E. Mazzon, L. Dugo, D.P. Riley, I. Serraino, A.P. Caputi, S. Cuzzocrea, Pharmacological manipulation of the inflammatory cascade by the superoxide dismutase mimetic, M40403, *Br. J. Pharmacol.* 132 (2001) 815–827. doi: 10.1038/sj.bjp.0703841.

[224] J.D. Hayes, A.T. Dinkova-Kostova, K.D. Tew, Oxidative Stress in Cancer, *Cancer Cell* 38 (2020) 167–197. <https://doi.org/10.1016/j.ccell.2020.06.001>.

[225] D. Erudaitius, J. Mantooh, A. Huang, J. Soliman, C.M. Doskey, G.R. Buettner, V.G.J. Rodgers, Calculated cell-specific intracellular hydrogen peroxide concentration: Relevance in cancer cell susceptibility during ascorbate therapy, *Free Radical Biology and Medicine* 120 (2018) 356–367. <https://doi.org/10.1016/j.freeradbiomed.2018.03.044>.

[226] J. Liu, Z. Wang, Increased Oxidative Stress as a Selective Anticancer Therapy, *Oxidative Medicine and Cellular Longevity* 2015 (2015) 1–12. <https://doi.org/10.1155/2015/294303>.

[227] A.S. Fernandes, N. Saraiva, N.G. Oliveira, Redox Therapeutics in Breast Cancer: Role of SOD Mimics, in: I. Batinić-Haberle, J.S. Rebouças, I. Spasojević (Eds.), *Redox-Active Therapeutics*, Springer International Publishing, Cham, 2016: pp. 451–467. https://doi.org/10.1007/978-3-319-30705-3_18.

[228] I. Batinić-Haberle, A. Tovmasyan, I. Spasojević, Mn Porphyrin-Based Redox-Active Drugs: Differential Effects as Cancer Therapeutics and Protectors of Normal Tissue Against Oxidative Injury, *Antioxidants & Redox Signaling* 29 (2018) 1691–1724. <https://doi.org/10.1089/ars.2017.7453>.

[229] L. Piconi, L. Quagliaro, A. Ceriello, Oxidative Stress in Diabetes, *Clinical Chemistry and*

Laboratory Medicine 41 (2003). <https://doi.org/10.1515/CCLM.2003.177>.

[230] F. Giacco, M. Brownlee, Oxidative Stress and Diabetic Complications, *Circ Res* 107 (2010) 1058–1070. <https://doi.org/10.1161/CIRCRESAHA.110.223545>.

[231] M. Zoumpoulaki, G. Schanne, N. Delsuc, H. Preud'homme, E. Quévrain, N. Eskenazi, G. Gazzah, R. Guillot, P. Seksik, J. Vinh, R. Lobinski, C. Polcar, Deciphering the Metal Speciation in Low-Molecular-Weight Complexes by IMS-MS: Application to the Detection of Manganese Superoxide Dismutase Mimics in Cell Lysates, *Angewandte Chemie International Edition* n/a (n.d.) e202203066. <https://doi.org/10.1002/anie.202203066>.